Nonlinear dynamics

Axelle Amon

Université de Rennes 1

Axelle AMON

NONLINEAR DYNAMICS

This course has been given from 2007 to 2017 in the 2d year of the Master *Systèmes Complexes Naturels et Industriels* at Université Rennes 1.

Part of it was based on slides that are not provided in the following notes. In particular the course used to begin by a general historical introduction. Such an introduction is very classical and can be find in numerous books.

The course is largely based on two books in particular :

- **Nonlinear dynamics and chaos**, S. Strogatz,
- **L'ordre dans le chaos**, P. Bergé, Y. Pomeau, C. Vidal.

[...] and people stopped patiently building their little houses of rational sticks in the chaos of the universe and started getting interested in the chaos itself – partly because it was a lot easier to be an expert on chaos, but mostly because it made really good patterns that you could put on a t-shirt.

Terry Pratchett, *Witches Abroad*

Contents

Introduction

During this course, I will mostly provide you mathematical tools to understand the qualitative behavior of dynamical systems. Now that it is easy and cheap to integrate numerically differential equations, it might seem to you a waste of time to learn all those mathematics. In fact, I hope to convince you during this course that on the contrary, determining the general feature of the response of a dynamical system without a systematic integration is very powerful and provides a true understanding of those systems.

All the systems we are going to study are *deterministic*. This mean that the future of the system is entirely determined by the initial conditions. We will discuss in the second part of the course why for some nonlinear systems such prediction is still very difficult because of the sensitivity to initial conditions.

[For an historical introduction to chaos and dynamical systems, read chapters of the book *Le chaos dans la nature* of C. Letellier.]

Chapter 1

Introduction to dynamical systems

In this course we will be interested in the study of the evolution with time of an ensemble of quantities describing a system.

From a scientific point of view, when studying the evolution of a phenomena, the main task is the modeling part, i.e. evidenced the significant quantities or the ones which can be truely measured and find the mathematical description of their temporal evolution. When this task is done, we obtain a set of mathematical expressions which are differential equations. In the case of a dependance on several variables (usually space and time), we obtain partial differential equations (PDEs). In this course we will only study *ordinary differential equations* (ODEs), for which the derivatives are only as a function of a unique variable, which will always be considered to be the time t in the following.

The goal of this first chapter is to provide the basic mathematical tools for the study of those ODEs. The specificity of the dynamical point of view is the way to deal with such mathematical problems. We will not try to find exact analytical solutions, which usually do not exist at all for the systems we will consider, but we will learn general tools which give insights on the evolution of such systems as the possible long-term behaviors or the evolution of the system near some particular points.

1.1 Definitions

1.1.1 Dynamical systems

We will consider systems described by a finite set of n real quantities: X_1, X_2,...,X_n, whose temporal evolutions are given by ordinary differential equations of the first order:

$$\left\{ \begin{array}{rcl} \frac{dX_1}{dt} & = & f_1(X_1, X_2, \ldots, X_n, t) \\ \frac{dX_2}{dt} & = & f_2(X_1, X_2, \ldots, X_n, t) \\ & \vdots & \\ \frac{dX_n}{dt} & = & f_n(X_1, X_2, \ldots, X_n, t) \end{array} \right. \tag{1.1}$$

All the functions f_i will always be sufficiently regular on $\mathbb{R}^{n+1}$.

We will use the notation $\frac{dX_i}{dt} = \dot{X}_i$. We will also use a vectorial formulation for the set of quantities, so that the system (1.1) can be written:

$$\frac{d\mathbf{X}}{dt} = \vec{F}(\mathbf{X}, t) \tag{1.2}$$

with

$$\mathbf{X} = \begin{pmatrix} X_1 \\ X_2 \\ \vdots \\ X_n \end{pmatrix} \text{ and } \vec{F}(\mathbf{X}, t) = \begin{pmatrix} f_1(X_1, X_2, \ldots, X_n, t) \\ f_2(X_1, X_2, \ldots, X_n, t) \\ \vdots \\ f_n(X_1, X_2, \ldots, X_n, t) \end{pmatrix}.$$

$\vec{F}$ is a vector field, function of $\mathbb{R}^{n+1}$ in $\mathbb{R}^n$.

The quantities designated by X_1, X_2,...,X_n can be for example:

- positions and velocities of bodies submitted to mutual gravitational interaction and conservation of momentum,
- the currents and voltages in an electrical network linked by the eletrical laws,
- the number of individuals in interacting populations in an ecosystem,
- the concentrations of reactants in a chemical reaction scheme described by reaction kinetics,
- ...

Remarks:

- the differential equations are **ordinary**, there are no partial derivatives.
- they are of the first order. If higher order derivatives appear during the model derivation, it is always possible to reformulate the model as a first-order one of higher dimension (see examples).
- existence and unicity of the solution of the system: a mathematical theorem (Cauchy-Lipschitz) tells us that for the initial value problem

$$\begin{cases} \frac{d\mathbf{X}}{dt} & = & \vec{F}(\mathbf{X}, t) \\ \mathbf{X}(0) & = & \mathbf{x_0} \end{cases}$$

with $\mathbf{X} \in \mathbb{R}^n$ and all the f_i continuous as well as all their partial derivatives $\frac{\partial f_i}{\partial X_j}$ in an open ensemble Ω such that $\mathbf{x_0} \in \Omega$, then the problem as a unique solution $\mathbf{x}(t)$ defined on a time interval around 0 $]t_-(x_0); t_+(x_0)[$ which can be finite or infinite.

From a practical point of view, the unicity of the solution is the mathematical formulation of what we call **determinism**. For a given initial condition, there is only one possible future.

- When $\frac{d\mathbf{X}}{dt} = \vec{F}(\mathbf{X})$, i.e. when $\vec{F}$ has no explicit dependence on t, the system is called **autonomous**. Otherwise, when $\frac{d\mathbf{X}}{dt} = \vec{F}(\mathbf{X}, t)$, the system is called **non-autonomous**. A non-autonomous system can be transformed in an autonomous one by increasing the dimension of the system of one (see examples).
- We will also study in the following discrete dynamics. In that case, the problems will be of the form:
$$\mathbf{X}_{k+1} = \vec{F}(\mathbf{X}_k).$$
Instead of a continuous dependence on a variable t, we have an iterative map which gives the value of $\mathbf{X}$ at the step $k+1$ as a function of the previous step.

1.1.2 Phase space

The vector $\mathbf{X}$ belongs to the space $\mathbb{R}^n$, called **phase space**. The dimension of the space, n, is the number of **degrees of freedom** of the system.

For any initial state $\mathbf{x_0} = \mathbf{X}(0)$, a solution $\mathbf{x}(t)$ exists which can be obtained for example by numerical integration. The path followed by the system in the phase space during time is called the **trajectory** or **orbit** of the system.

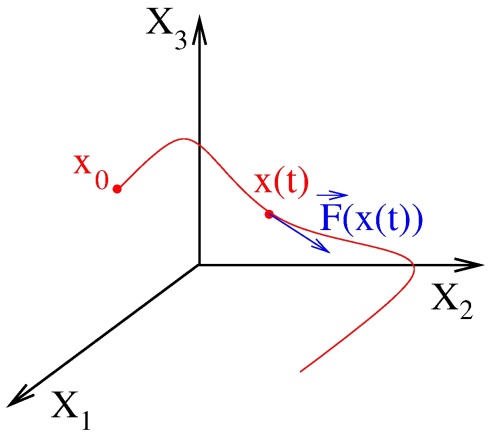

Figure 1.1: A trajectory in the phase space.

At each points $\mathbf{x}(t)$, $\frac{d\mathbf{x}}{dt} = \vec{F}(\mathbf{x})$, so that the vector field $\vec{F}$ gives the tangent to the trajectory at that point, i.e. the instantaneous direction followed by the system. Consequently, for a step δt small enough, we have[1]:

$$\mathbf{x}(t + \delta t) \simeq \mathbf{x}(t) + \vec{F}(\mathbf{x}(t))\delta t,$$

We see that there is a direct analogy with hydrodynamics: $\vec{F}$ can be considered as the velocity field of a fluid. The map ϕ associating to each initial condition $\mathbf{x_0}$ the subsequent trajectory $\mathbf{x}(t)$ is called the **flow** of the field vector:

$$\phi : (\mathbf{x_0}, t) \mapsto \mathbf{x}(t) = \phi_t(\mathbf{x_0})$$

[1]This approximation is the basis of the Euler method of integration of differential equations.

Trajectories in the phase space **never intersect**. Indeed, if such intersection point would exist, taking it as an initial condition would lead to the existence of two distinct trajectories starting from the same point, i.e. two futures possible from the same initial condition, which would be a violation of the determinism (or of the unicity of the solution from a mathematical point of view). Nevertheless, we will meet some singular points in phase space where particular orbits cross. Those points correspond in fact to asymptotic limits for the system: they can only be reach after an infinite time.

1.1.3 Examples

1.1.3.a The simple gravity pendulum

Let's consider a mass m hanging to a pivot O. The cord that hold the mass is rigid and massless. The length of the cord is l.

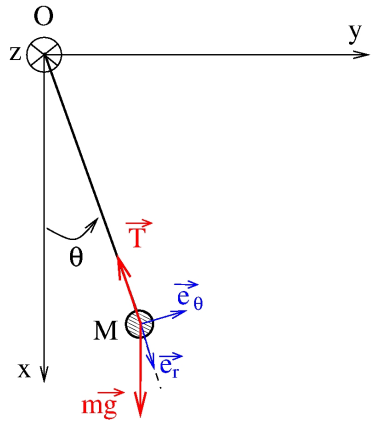

Figure 1.2: Simple gravity pendulum.

The equation describing the movement can be obtained in different ways. Let's use the angular momentum conservation:

$$\frac{d}{dt}(\text{angular momentum}) = \sum(\text{torques})$$

Let's calculate the angular momentum:

$$\begin{aligned} \overrightarrow{OM} \times (m\vec{v}) &= (l\vec{e}_r) \times (ml\dot{\theta}\vec{e}_\theta) \\ &= ml^2\dot{\theta}\vec{e}_z \end{aligned}$$

and the torques associated to the forces:

$$\begin{aligned} \overrightarrow{OM} \times \overrightarrow{T} &= \vec{0} \\ \overrightarrow{OM} \times (m\vec{g}) &= -mgl\sin\theta\vec{e}_z \end{aligned}$$

We obtain:

$$\frac{d}{dt}(ml^2\dot{\theta}) = -mgl\sin\theta$$

$$\boxed{\ddot{\theta} + \frac{g}{l}\sin\theta = 0}$$

You have learned how to solve this problem: you need to consider only small oscillations, so that you can approximate $\sin\theta \simeq \theta$. The differential equation you obtain by doing this approximation is the harmonic oscillator equation:

$$\ddot{\theta} + \frac{g}{l}\theta = 0$$

for which we know the general form of the solution:

$$\theta(t) = A\sin\left(\sqrt{\frac{g}{l}}\ t\right) + B\cos\left(\sqrt{\frac{g}{l}}\ t\right),$$

where the constants A and B are determined by the initial conditions. You can note that you have two unknowns (A and B) so that you need to know two initial conditions to entirely solve the problem: the initial angle θ_0 and the initial angular velocity of the pendulum. This fact gives you a hint of the number of degrees of freedom of the system[2]: it is the number of initial conditions you need, i.e. the number of coordinates of the vector that will describe the system in the phase space.

Note that the analytical solution is valid only in the case of small oscillations. Now, we want to have a global knowledge of the possible trajectories of the system for all the possible initial conditions, which mean that the amplitude of the oscillations may not be small at all.

Let's come back to the nonlinear equation:

$$\ddot{\theta} + \frac{g}{l}\sin\theta = 0.$$

First we will transform this second-order equation in a larger system of first-order derivatives. Let's define $X_1 = \theta$ and $X_2 = \dot{\theta}$. We have:

$$\begin{array}{rcccl} \dot{X}_1 & = & \dot{\theta} & = & X_2 \\ \dot{X}_2 & = & \ddot{\theta} & = & -\frac{g}{l}\sin\theta = -\frac{g}{l}\sin X_1 \end{array}$$

The system can be expressed in the following way:

$$\left\{ \begin{array}{rcl} \dot{X}_1 & = & X_2 \\ \dot{X}_2 & = & -\frac{g}{l}\sin X_1 \end{array} \right.$$

[2]The definition is given from a dynamical system point of view, and may differ from the definition you had in your mechanics class.

which is an autonomous system of the form $\frac{d\mathbf{X}}{dt} = \vec{F}(\mathbf{X})$, with

$$\mathbf{X} = \begin{pmatrix} \theta \\ \dot{\theta} \end{pmatrix} \text{ and } \vec{F} : \begin{pmatrix} X_1 \\ X_2 \end{pmatrix} \mapsto \begin{pmatrix} X_2 \\ -\frac{g}{l} \sin X_1 \end{pmatrix}$$

The phase space is of dimension 2.

To represent the possible trajectories in the phase space, we need to calculate the values of the field vector F at different points. As the trajectories are tangent to those vectors, we can progressively have a picture of the flow by the drawing of those vectors [3]. For complicated expression of the vector field, we will see during the exercises session on Matlab that a function[4] will give directly the vector field over a grid of your choice.

In the case of the example

$$F\begin{pmatrix} \pi/2 \\ 0 \end{pmatrix} = \begin{pmatrix} 0 \\ -g/l \end{pmatrix} \qquad F\begin{pmatrix} -\pi/2 \\ 0 \end{pmatrix} = \begin{pmatrix} 0 \\ g/l \end{pmatrix}$$

$$F\begin{pmatrix} 0 \\ \omega \end{pmatrix} = \begin{pmatrix} \omega \\ 0 \end{pmatrix} \qquad F\begin{pmatrix} \pm\pi \\ \omega \end{pmatrix} = \begin{pmatrix} \omega \\ 0 \end{pmatrix}$$

Such calculation gives coordinates of vectors which are drown as red solid arrows in Figure 1.3. You can note that without an exact calculation you can also draw the general trend of the flow in some areas of the phase space, only by considering the signs of the coordinates of F. We have drawn such trends with red dashed arrows in Figure 1.3. The

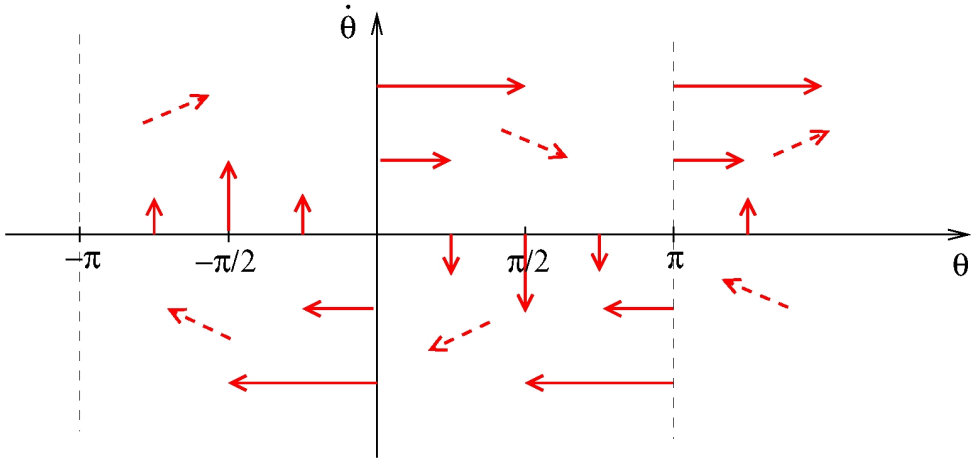

Figure 1.3: Vector field representation. The red arrows represent the vector field F at the considered points.

global picture of the trajectories emerges gradually from the accumulation of the tangents: around the origin, the vectors are going round, drawing curves which look like ellipses.

[3] If you have studied continuum mechanics, you have proceed in the same way to figure out the appearance of a velocity field or a deformation field from some mathematical expressions.

[4] The *quiver* function.

It is in agreement with our analytical solution for the small amplitudes condition. We obtained then the trajectories corresponding to oscillations, they appear as closed orbits in the phase space. Those trajectotries are the closed loops around the origin drawn in blue in Figure 1.5. Far from the origin, for large initial $\dot{\theta}_0$, we see that the trajectory will never cross the θ-axis, which mean that the angular velocity never vanished during the movement. The pendulum does not oscillate back and forth around the vertical axis but rotates continuously over the top. Examples of those trajectories are drawn in blue in Figure 1.5.

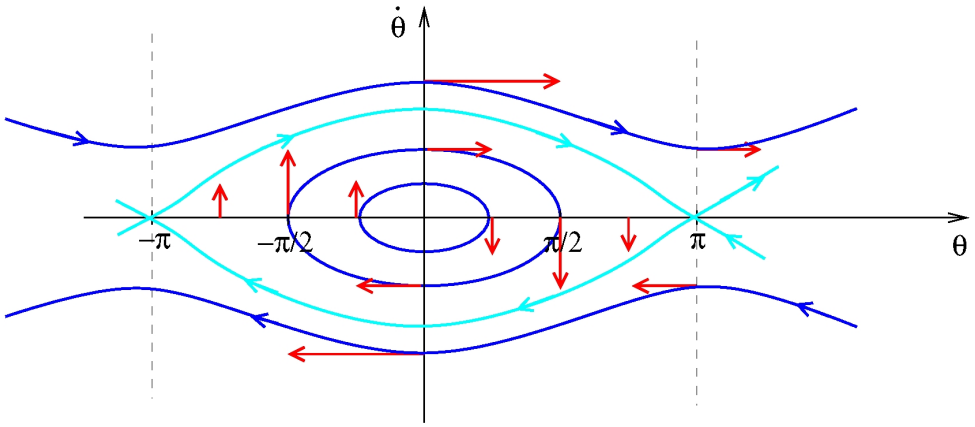

Figure 1.4: Trajectories of a pendulum in the phase space.

Finally, we see in Figure 1.3 that around the points $(\pi, 0)$ and $(-\pi, 0)$ (which are in fact the same due to the 2π-periodicity of the angle coordinate), trajectories behave strangely: a pair of dashed arrows are going towards the point while the other pair moves away from it. We are at the separation between the two types of trajectories, oscillations and rotations. The trajectory that delimits those two behavior is called a **separatrix**. It is drawn in light blue in Figure 1.5. You observe that at the point $(\pi, 0)$, two trajectories cross each other although we said it was forbidden. We are typically in one of those special case we were talking about: if you use as initial condition any point from the separatrix, it will take an infinite time for the system to reach the point $(\pi, 0)$. And if you take that exact point as initial condition it will stay here in the absence of any perturbation. The point is an unstable equilibrium and we will come back to the characterization of the trajectories around it later.

1.1.3.b The damped pendulum

In the previous example, the energy was conserved with time. In fact, we will be mainly interested in the following in **dissipative** systems. In the case of the pendulum, it will lead to the introduction of a damping term in the equation. We will describe this damping through a viscous torque, proportional to the angular velocity and opposed to the move-

ment $-\gamma\dot{\theta}$, which will lead to an exponential decrease of the amplitude of the oscillations.

$$\ddot{\theta} = -\gamma\dot{\theta} - \frac{g}{l}\sin\theta$$

Let's proceed to the re-writting of the system using $X_1 = \theta$ and $X_2 = \dot{\theta}$

$$\left\{ \begin{array}{rcl} \dot{X}_1 & = & X_2 \\ \dot{X}_2 & = & -\frac{g}{l}\sin X_1 - \gamma X_2 \end{array} \right.$$

We can again draw the vector field in several points to determine the appearance of the trajectories.

$$\begin{pmatrix} \theta_0 \\ 0 \end{pmatrix} \mapsto \begin{pmatrix} 0 \\ -g/l\sin\theta_0 \end{pmatrix} \qquad \begin{pmatrix} 0 \\ \omega_0 \end{pmatrix} \mapsto \begin{pmatrix} \omega_0 \\ -\gamma\omega_0 \end{pmatrix}$$

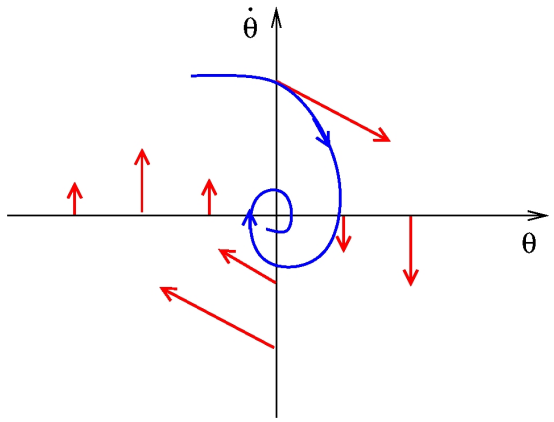

Figure 1.5: An example of trajectory of a damped pendulum in the phase space in a case where the damping is "small" (we will come back later to this example and give a rigourous condition). For "large" damping, the system goes straightly to the origin without spiraling. Those two cases correspond respectively to the underdamped and overdamped regimes.

A big difference with the conservative case is the fact that all the trajectories converge towards the point $(0, 0)$. This feature, the existence of **attractors** in the phase space for dissipative systems, is of central importance in the following of the course. Such feature is totally absent in conservative systems: an infinite number of closed orbits were existing around the origin, each corresponding to a different value of the energy.

That simple example evidences also the fact that if no energy is injected in a dissipative system to compensate the loss of energy by the damping, no exciting dynamics will arise. The system will just converge to a position corresponding to a null energy.

1.1.3.c The driven pendulum

To maintain the movement of the pendulum, one needs to drive it, generally by exerting a periodic torque at a fixed frequency ω: $M\sin(\omega t)$.

$$\ddot{\theta} + \gamma\dot{\theta} + \frac{g}{l}\sin\theta = M\sin(\omega t)$$

With $X_1 = \theta$ and $X_2 = \dot{\theta}$, we obtain the system

$$\left\{ \begin{array}{rcl} \dot{X}_1 & = & X_2 \\ \dot{X}_2 & = & -\frac{g}{l}\sin X_1 - \gamma X_2 + M\sin(\omega t) \end{array} \right.$$

This is our first example of a non-autonomous system. The variable t appears explicitely in the vector field. If we introduce a new variable $X_3 = \omega t$, we obtain the system:

$$\left\{ \begin{array}{rcl} \dot{X}_1 & = & X_2 \\ \dot{X}_2 & = & -\frac{g}{l}\sin X_1 - \gamma X_2 + M\sin X_3 \\ \dot{X}_3 & = & \omega \end{array} \right.$$

which is an autonomous system of dimension 3.[5]

Now, are we able to draw the global features of the flow as we have done for the previous example by determining the vector field in a few points ? Yes, in principle, but the task has become much harder. The phase space is in 3 dimensions, so we will draw projections of the phase space in a plane. Moreover, note that we have now four parameters[6]: $\frac{g}{l}$, γ, M and ω. We mentioned very briefly in the case of the damped pendulum the fact that the transient behavior of the system was not the same depending on the values of the parameters ($\frac{g}{l}$ and γ), but now we have two new parameters to deal with. For example, we can expect that the system will not respond in the same way if ω is close to the natural frequency of the system or very far from it.

Figure 1.6) shows the result of numerical integrations of the system for different values of the parameters. The trajectories that have been drawn correspond to a permanent regime: we show only the behavior after that a time of integration long enough compared to the transient of the system has elapsed. Figure 1.6(a) corresponds well to what we expect for a linear response: the pendulum oscillates at the imposed frequency ω and its periodic motion corresponds to a closed orbit in the phase space. Figure 1.6(c) corresponds also to a periodic orbit but it is a very weird one. The trajectory seems to cross itself but it is only due to the projection in a plane. What is surprising is that the

[5] In this example X_3 is in fact an angle, so that it is 2π-periodic and lives on a circle. In such systems, it is common to measure the values of X_1 and X_2 at discrete time steps fixed by the period of the driving, as in a stromboscopic measurement. Then the dynamics obtained is discrete. We will see examples of that kind later.

[6] Nondimensionalizing the equations would reduce this number to three, but it is still a lot.

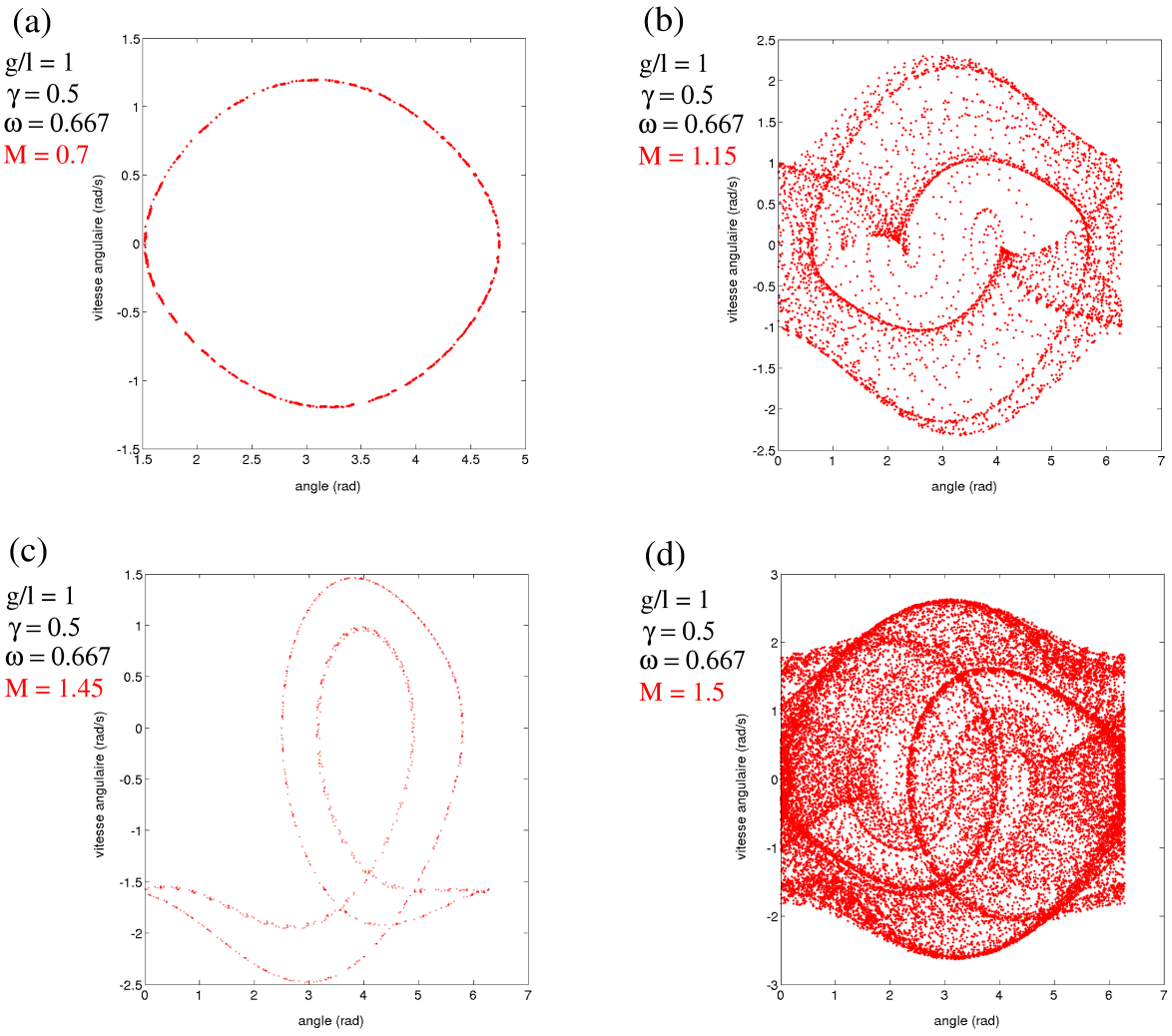

Figure 1.6: Trajectories in the phase space of the driven damped pendulum for different value of the driving force. See also for example `http://www.myphysicslab.com/pendulum2.html`

oscillation is not at the same frequency as the driving one but a sub-harmonic of it. The two last figures 1.6(b) and (d) are totally confusing because the system does not seem to settle on a closed trajectory. You could think that it is due to the fact that a part of the transient is pictured on the figure but it is not the case. You can let the system integrate for a very long time, it will still present such behavior, which is not a mere random motion in the phase space (you can see that the trajectory is confined in a finite part of the phase space) but which is not periodic. Such kind of behavior is precisely what is called **chaos** and the strange structures in the phase space are examples of **strange attractors**.

As you see, even a "simple" example as a driven damped pendulum exhibits a very complex behavior. You are perhaps surprised by this result because you have extensively studied this example before and never encounter such strange behaviors. It is because

you have always studied the **linearized** system, when oscillations are small. A linear system will never present a chaotic behavior or even oscillations at a frequency different from the one you imposed. In a linear system all you can observe is a response at the driven frequency such as the one of Figure 1.6(a). The necessary ingredient to observe exotic behavior as in Figures 1.6(b), (c) or (d) is the nonlinearity, which is in our example the terms "$\sin X_1$" and "$\sin X_3$" in the equations. Note that the nonlinearity is not a sufficient condition to observe chaos: there exist nonlinear differential equations which behave themselves for all the values of the parameters.

At this stage, we realize that even a goal as modest as a rough description of all the possible asymptotic behaviors of the system depending on the value of the parameters is not easy to realize. Considering the complexity of what await us we need some method to deal with such systems: we cannot find all the possible behavior easily as in the two first examples and we cannot just run numerical integration for all the possible values of the parameters. We need a method to address the problem, which is exactly what the two first chapters of this course are about.

Parametric pendulum

There are several ways to drive a system. In the previous example we directly applied a periodic torque to the system. Another method is to drive one of the parameters of the system periodically.

A famous example of those two kinds of excitation is given by the swing (the children's play). You have two manners to make it oscillate: either you sit on it and periodically bend and stretch your legs. You will oscillate at the same frequency as the one of your impulsion. You can also stand on the swing and bend your knees periodically. The swing will then oscillante at half the frequency of the driving one.

The second type of driving is a parametric one because it is formally equivalent to a modulation of the gravity value and can be modeled in the following way:

$$g(t) = g_0 + g_1 \cos(2\omega t)$$

$$\ddot{\theta} + \gamma\dot{\theta} + \left[\frac{g_0}{l} + \frac{g_1}{l}\cos(2\omega t)\right]\sin\theta = 0$$

1.1.4 Hamiltonian vs. dissipative systems

We have seen through the pendulum example that the behavior of a system where there is some damping is very different from the one of a system with no dissipation.

1.1.4.a Hamiltonian systems

From a physicist point of view, a **conservative system** designates a system where the total energy is conserved. From a dynamical system point of view it will mean that the

volumes in the phase space are conserved under the action of the flow. Such systems are also called **hamiltonian systems**.

Consider an initial set Ω_0 in the phase space and let it evolve under the action of the flow. At time t, it has became Ω_t. Quantitatively, the volume of Ω_t is

$$\mathcal{V}(\Omega) = \int_\Omega dX_1 dX_2 \dots dX_n$$

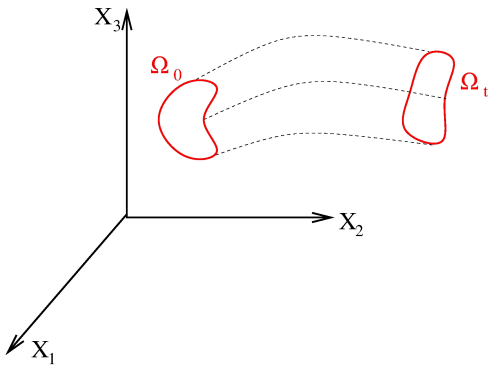

Now consider the small variation of Ω between t and $t+\delta t$, the volume variation is given by:

$$\delta\mathcal{V} = \int_{\partial\Omega} (\delta\mathbf{X}).d\vec{\sigma},$$

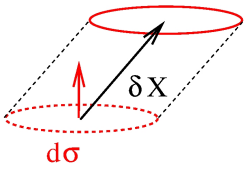

where $\partial\Omega$ is the frontier of the set Ω and $d\vec{\sigma}$ is the vector associated to a surface element of the frontier.

As $\delta\mathbf{X} = \vec{F}(\mathbf{X})\delta t$,

$$\begin{aligned} \delta\mathcal{V} &= \delta t \int_{\partial\Omega} \vec{F}(\mathbf{X}).d\vec{\sigma} \\ \frac{\delta\mathcal{V}}{\delta t} &= \int_\Omega (\vec{\nabla}.\vec{F}) dv, \end{aligned}$$

where we have applied the Ostrogradski relationship and

$$\vec{\nabla}.\vec{F} = \frac{\partial f_1}{\partial X_1} + \frac{\partial f_2}{\partial X_2} + \dots + \frac{\partial f_n}{\partial X_n}$$

If the volume is conserved, $\frac{\delta\mathcal{V}}{\delta t} = 0$, and

$$\boxed{\vec{\nabla}.\vec{F} = 0}$$

This relationship is the mathematical definition of an hamiltonian system.

Example: the simple gravity pendulum

$$\left\{ \begin{array}{rcl} \dot{X}_1 &=& X_2 \\ \dot{X}_2 &=& -\frac{g}{l}\sin X_1 \end{array} \right.$$

We have,

$$\begin{aligned}\vec{\nabla}.\vec{F} &= \frac{\partial f_1}{\partial X_1} + \frac{\partial f_2}{\partial X_2} \\ &= \frac{\partial}{\partial X_1}(X_2) + \frac{\partial}{\partial X_2}\left(-\frac{g}{l}\sin X_1\right) = 0\end{aligned}$$

The system is indeed conservative.

1.1.4.b Dissipative systems and attractors

We said before that we will be interested only in dissipative systems in this course. For these dissipative systems there is **volume contraction** in the phase space under the action of the flow[7]: on average, we have $\vec{\nabla}.\vec{F} < 0$.

Example: The damped pendulum

$$\left\{\begin{array}{lcl}\dot{X}_1 &=& X_2 \\ \dot{X}_2 &=& -\frac{g}{l}\sin X_1 - \gamma X_2\end{array}\right.$$

Then,

$$\begin{aligned}\vec{\nabla}.\vec{F} &= \frac{\partial}{\partial X_1}(X_2) + \frac{\partial}{\partial X_2}\left(-\frac{g}{l}\sin X_1 - \gamma X_2\right) \\ &= -\gamma\end{aligned}$$

as $\gamma > 0$ in the damping case, we have $\vec{\nabla}.\vec{F} < 0$.

Attractors

For dissipative system, as we have seen in the damped pendulum examples, there are **attractors** in the phase space, i.e. sets of the phase space where nearby trajectories all tend to go during the transient regime. On a long time perspective all those trajectories settle on the attractor and never leave it. In the case of the damped oscillator (without driving, Fig. 1.5), the attractor is the point $(0, 0)$ of the phase space. In the simpliest response of the driven, damped oscillator, i.e. the periodic response at the driven frequency of Figure 1.6(a), the closed orbit is an attractor.

The existence of such attractors is closely related to the volume contraction in the phase space. A more rigourous definition of an attractor is the following: an attractor is a set of the phase space invariant under the action of the flow. This means that if you choose as an initial condition a point of the attractor the trajectory of your system will follow the attractor and stay on it forever. An attractor has always a **null volume** because of the volume contraction. Indeed, if it had a volume different from 0, the action of the flow would reduce this volume and the attractor would not be *invariant*

[7] We can also speak of *area* contraction (or area conservation for the hamiltonian case) as the discussion is also true for areas and not only volumes.

under the action of the flow. Each attractor has a **basin of attraction** which contains all the initial conditions which will generate trajectories joining asymptotically this attractor.

When studying a nonlinear dynamical system, if we are only interested in the long-time behaviors, we will only study the attractors of the system and determine their basin of attractions.

The "simpliest" attractors are:

- the point: it is then a **fixed point**, i.e. verifying $\vec{F}(\mathbf{x}^*) = 0$. The corresponding solution of the dynamical system does not depend on time, it is a **stationary state**.
- the **limit cycle**: i.e. a closed trajectory in the phase space. It needs a phase space of dimension at least 2 to exist. This attractor corresponds to a periodic solution: the quantities all take again the same values after the same time, the period of the system.

To observe other attractors than those two types, the dimension of the phase space has to be larger than 2. The two next sections are devoted to the study of fixed points and limit cycles and the characterization of their stability.

1.2 Stability of fixed points

1.2.1 Fixed points

Fixed points are the particular points of the phase space verifying

$$\left.\frac{d\mathbf{X}}{dt}\right|_{\mathbf{x}^*} = 0, \text{ or } \vec{F}(\mathbf{x}^*) = 0.$$

Such a point, if taken as an initial condition, will not move under the action of the flow.

Fixed points can be stables or unstables (compare for example the points $(0, 0)$ and $(\pi, 0)$ in the simple pendulum example of Fig. 1.5). **Only stables fixed points are attractors.**

1.2.2 Linear stability analysis: principle

To have an idea of what the trajectories look like in the vicinity of a fixed point $\mathbf{x}^*$, we linearize the equations around that point. Considering $\mathbf{x}$ near $\mathbf{x}^*$: $\mathbf{x} = \mathbf{x}^* + \delta\mathbf{x}$ with $\delta\mathbf{x}$ small, we have:

$$\begin{aligned} \frac{d\mathbf{x}}{dt} &= \vec{F}(\mathbf{x}) \\ \frac{d\mathbf{x}^*}{dt} + \frac{d(\delta\mathbf{x})}{dt} &= \vec{F}(\mathbf{x}^* + \delta\mathbf{x}) \end{aligned}$$

Let's go back to a detailed writting for the equation, using equation 1.1:

$$\left\{\begin{array}{rcl} \frac{d\delta X_1}{dt} & = & f_1(X_1^*+\delta X_1, X_2^*+\delta X_2, \ldots, X_n^*+\delta X_n) \\ \frac{d\delta X_2}{dt} & = & f_2(X_1^*+\delta X_1, X_2^*+\delta X_2, \ldots, X_n^*+\delta X_n) \\ & \vdots & \\ \frac{d\delta X_n}{dt} & = & f_n(X_1^*+\delta X_1, X_2^*+\delta X_2, \ldots, X_n^*+\delta X_n) \end{array}\right. \tag{1.3}$$

Computing the Taylor expansion of each function, we obtain:

$$\left\{\begin{array}{rcl} \frac{d\delta X_1}{dt} & = & f_1(\mathbf{x}^*) + \left.\frac{\partial f_1}{\partial X_1}\right|_{\mathbf{x}^*}.\delta X_1 + \left.\frac{\partial f_1}{\partial X_2}\right|_{\mathbf{x}^*}.\delta X_2 + \cdots + \left.\frac{\partial f_1}{\partial X_n}\right|_{\mathbf{x}^*}.\delta X_n \\ & \vdots & \\ \frac{d\delta X_n}{dt} & = & f_n(\mathbf{x}^*) + \left.\frac{\partial f_n}{\partial X_1}\right|_{\mathbf{x}^*}.\delta X_1 + \left.\frac{\partial f_n}{\partial X_2}\right|_{\mathbf{x}^*}.\delta X_2 + \cdots + \left.\frac{\partial f_n}{\partial X_n}\right|_{\mathbf{x}^*}.\delta X_n \end{array}\right. \tag{1.4}$$

A condensed way to write this system is to use the *jacobian matrix* of $\vec{F}$:

$$\mathcal{L}_{ij} = \frac{\partial f_i}{\partial X_j}.$$

Then equation 1.4 can be written:

$$\frac{d(\delta\mathbf{x})}{dt} \simeq \vec{F}(\mathbf{x}^*) + \mathcal{L}|_{\mathbf{x}^*}.\delta\mathbf{x},$$

as $\vec{F}(\mathbf{x}^*) = 0$, we obtain

$$\boxed{\frac{d(\delta\mathbf{x})}{dt} = \mathcal{L}|_{\mathbf{x}^*}.\delta\mathbf{x}} \tag{1.5}$$

As $\mathcal{L}|_{\mathbf{x}^*}$ is a matrix with constant coefficients, equation (1.5) is a linear ordinary differential equation which can be explicitely integrated as will be briefly explained in the next part.

1.2.3 Linear differential equations

Consider a system of linear differential equations of the first order with constant coefficients:

$$\frac{d\mathbf{X}}{dt} = M\mathbf{X},$$

with M a matrix of size $n \times n$ with constant coefficients in $\mathbb{R}$ and $\mathbf{X} \in \mathbb{R}^n$. The solutions of this equation are:

$$\mathbf{X} = e^{tM}\mathbf{X}(0),$$

where the matrix exponential e^A is defined for all matrix A by the convergent serie:

$$e^A = \mathbb{1} + A + \frac{A^2}{2!} + \frac{A^3}{3!} + \cdots + \frac{A^p}{p!} + \ldots$$

The matrices e^{tM} verify:

$$e^{t_1 M} e^{t_2 M} = e^{(t_1+t_2)M}$$
$$\frac{d}{dt} e^{tM} = M e^{tM}$$
$$Det(e^{tM}) = e^{tTr(M)}$$

Case of a diagonal matrix

Even if it is mathematically a particular case, you will have a good intuition of what is this matrix exponential by considering that M is a diagonal matrix:

$$M = \begin{pmatrix} \lambda_1 & & 0 \\ & \ddots & \\ 0 & & \lambda_n \end{pmatrix}$$

All the λ_i are in $\mathbb{R}$, they are eigenvalues [8] of M. Then the exponential matrix e^{tM} is:

$$e^{tM} = \begin{pmatrix} e^{\lambda_1 t} & & 0 \\ & \ddots & \\ 0 & & e^{\lambda_n t} \end{pmatrix}$$

Then, choosing as an initial condition the eigenvector of M associated to the eigenvalue λ_i:

$$\mathbf{x_0} = \begin{pmatrix} 0 \\ \vdots \\ 0 \\ 1 \cdots i^{th} \\ 0 \\ \vdots \\ 0 \end{pmatrix}$$

the trajectory is given by[9]:

$$\mathbf{x}(t) = e^{tM}\mathbf{x_0} = e^{\lambda_i t}\mathbf{x_0} = \begin{pmatrix} 0 \\ \vdots \\ e^{\lambda_i t} \\ \vdots \\ 0 \end{pmatrix}$$

We have then three different asymptotic behaviors possible. If $\lambda_i < 0$, $\lim_{t\to+\infty} e^{\lambda_i t} = 0$ and $\mathbf{x}(t)$ will converge to the origin, if $\lambda_i = 0$, $\mathbf{x}(t)$ will stay in $\mathbf{x_0}$ and finally if $\lambda_i > 0$, the i^{th} coordinate of $\mathbf{x}(t)$ will increase exponentially so that $\mathbf{x}(t)$ goes to infinity.

[8] The set of those eigenvalues is called the spectrum of the matrix

[9] Note that e^{tM} is a matrix while $e^{t\lambda_i}$ is a scalar.

Considering any initial condition $\mathbf{x_0}$ and not specifically an aigenvector of M, the vector $\mathbf{x_0}$ can be written as a linear superposition of the eigenvectors $\{\mathbf{v_i}\}$:

$$\mathbf{x_0} = \sum_i \alpha_i \mathbf{v_i},$$

and the evolution of $\mathbf{x}(t)$ is given by :

$$\mathbf{x}(t) = \sum_i \alpha_i e^{\lambda_i t} \mathbf{v_i}.$$

When M is not diagonal, it can be either diagonalizable or not. When it is a diagonalizable, it means that by a change of basis (i.e. a change of coordinates), we are back to the diagonal case. Note that those eigenvalues can be complex even if M is real but then their complex conjugate is also necessarily in the spectrum. Then the real part of the eigenvalue still gives the long-term behavior (exponentially incresing or decreasing depending on its sign) while a non-null imaginary part will lead to an oscillating behavior which superimposed on the trend given by the real part. When M is not diagonalizable, the problem is more tricky but the behavior of e^{tM} is still given by the sign of the real part of the eigenvalues of M. We will see examples on those different cases (complex conjugates eignevalues, non-diagonalizable matrix) among the 2D cases studied in subsection 1.2.5.

Exercises

- Consider the system
$$\begin{cases} \dot{x} &= 2x - y \\ \dot{y} &= 2y - x \end{cases}$$
with initial conditions $x(0) = 1$ and $y(0) = 3$. Show that the solution of the system is :
$$x(t) = 2e^t - e^{3t}$$
$$y(t) = 2e^t + e^{3t}$$
The system can also be written:
$$\begin{pmatrix} \dot{x} \\ \dot{y} \end{pmatrix} = \begin{pmatrix} 2 & -1 \\ -1 & 2 \end{pmatrix} \begin{pmatrix} x \\ y \end{pmatrix}$$
Show that the eigenvalues of the system are 1 and 3.

- Consider the system
$$\begin{cases} \dot{x} &= \omega y \\ \dot{y} &= -\omega x \end{cases}$$
with initial conditions $x(0) = 1$ and $y(0) = 7$. Show that the solution is:
$$x(t) = \cos \omega t + 7 \sin \omega t$$
$$y(t) = 7 \cos \omega t - \sin \omega t$$

The system can also be written:

$$\begin{pmatrix} \dot{x} \\ \dot{y} \end{pmatrix} = \begin{pmatrix} 0 & \omega \\ -\omega & 0 \end{pmatrix} \begin{pmatrix} x \\ y \end{pmatrix}$$

Show that the eigenvalues of the system are the complex conjugates $i\omega$ and $-i\omega$.

1.2.4 Back to the linear stability analysis

In subsection 1.2.2, we were considering the linearization of the system around a fixed point $\mathbf{x}^*$, so that we had to solve the linear equation (1.5):

$$\frac{d(\delta\mathbf{x})}{dt} = \mathcal{L}|_{\mathbf{x}^*} . \delta\mathbf{x}.$$

We know now that the solutions of this equation are of the form $\delta\mathbf{x}(t) = e^{\left(t\,\mathcal{L}|_{\mathbf{x}^*}\right)}\delta\mathbf{x}(0)$. We have then the following properties:

- if we use as an initial condition $\delta\mathbf{x}(0)$ which position compare to $\mathbf{x}^*$ is given by an eigenvector of $\mathcal{L}|_{\mathbf{x}^*}$ associated to an eigenvalue of **strictly positive real part**, λ_+ : $\delta\mathbf{x}(0) = \mathbf{v}_{\lambda_+}$, then $\|\delta\mathbf{x}(t)\|$ increases along the direction given by $\mathbf{v}_{\lambda_+}$ and the system goes away from $\mathbf{x_0}$. Those eigenvectors give the **unstable or dilatant directions**.
- if we use as an initial condition a point which position compare to $\mathbf{x}^*$ is given by an eigenvector of $\mathcal{L}|_{\mathbf{x}^*}$ associated to an eigenvalue of **strictly negative real part**, λ_- : $\delta\mathbf{x}(0) = \mathbf{v}_{\lambda_-}$, then $\|\delta\mathbf{x}(t)\|$ decreases along the direction given by $\mathbf{v}_{\lambda_-}$ and the system goes to $\mathbf{x_0}$. Those eigenvectors give the **stable or contractant directions**.
- the eigenvalues of null real part are problematic, we will discuss briefly this case in the following.

To illustrate those properties, we now study in details all the possible cases in a two-dimensional phase space.

1.2.5 2D case

In the bidimensional case a dynamical system is of the form:

$$\left\{ \begin{array}{rcl} \dot{X}_1 & = & f_1(X_1, X_2) \\ \dot{X}_2 & = & f_2(X_1, X_2) \end{array} \right. \tag{1.6}$$

If we consider a small perturbation in the vicinity of a fixed point $\mathbf{x}^* = \begin{pmatrix} x_1^* \\ x_2^* \end{pmatrix}$:

$$\mathbf{x} = \mathbf{x}^* + \delta\mathbf{x} = \begin{pmatrix} x_1^* + \delta x_1 \\ x_2^* + \delta x_2 \end{pmatrix},$$

we can linearize the system (1.6) around $\mathbf{x}^*$:

$$\left\{ \begin{array}{rcl} \dot{\delta x_1} & = & f_1(x_1^* + \delta x_1, x_2^* + \delta x_2) \\ \dot{\delta x_2} & = & f_2(x_1^* + \delta x_1, x_2^* + \delta x_2) \end{array} \right.$$

$$\left\{ \begin{array}{rcl} \dot{\delta x_1} & = & f_1(x_1^*, x_2^*) + \left.\frac{\partial f_1}{\partial X_1}\right|_{\mathbf{x}^*} \delta x_1 + \left.\frac{\partial f_1}{\partial X_2}\right|_{\mathbf{x}^*} \delta x_2 \\ \dot{\delta x_2} & = & f_2(x_1^*, x_2^*) + \left.\frac{\partial f_2}{\partial X_1}\right|_{\mathbf{x}^*} \delta x_1 + \left.\frac{\partial f_2}{\partial X_2}\right|_{\mathbf{x}^*} \delta x_2 \end{array} \right.$$

Using $L_{ij} = \left.\frac{\partial f_i}{\partial X_j}\right|_{\mathbf{x}^*}$, we have:

$$\left\{ \begin{array}{rcl} \dot{\delta x_1} & = & L_{11}\delta x_1 + L_{12}\delta x_2 \\ \dot{\delta x_2} & = & L_{21}\delta x_1 + L_{22}\delta x_2 \end{array} \right.$$

which is exactly the same as:

$$\frac{d}{dt}\begin{pmatrix} \delta x_1 \\ \delta x_2 \end{pmatrix} = \begin{pmatrix} L_{11} & L_{12} \\ L_{21} & L_{22} \end{pmatrix}\begin{pmatrix} \delta x_1 \\ \delta x_2 \end{pmatrix}$$

To determine the spectrum of L, we compute the characteristic polynomial $P(\lambda)$:

$$\begin{array}{rcl} \mathrm{Det}(L - \lambda\mathbb{1}) & = & \begin{vmatrix} L_{11} - \lambda & L_{12} \\ L_{21} & L_{22} - \lambda \end{vmatrix} \\ & = & (L_{11} - \lambda)(L_{22} - \lambda) - L_{12}L_{21} \\ & = & \lambda^2 - (L_{11} + L_{22})\lambda + L_{11}L_{22} - L_{12}L_{21} \end{array}$$

Which gives:

$$P(\lambda) = \lambda^2 - \mathrm{Tr}(L)\lambda + \mathrm{Det}(L) \tag{1.7}$$

We can now consider all the possible cases for the roots of that polynomial.

1.2.5.a Two real roots distincts and non null

The characteristic polynom can be factorized in the form: $P(\lambda) = (\lambda - \lambda_1)(\lambda - \lambda_2)$. The matrix is then diagonalizable. Any initial condition $\delta\mathbf{x}(0)$ can be decomposed in a basis formed by the eigenvectors $\mathbf{v_1}$ and $\mathbf{v_2}$ associated respectively to the eignevalues λ_1 and λ_2: $\delta\mathbf{x}(0) = \alpha_1\mathbf{v_1} + \alpha_2\mathbf{v_2}$, where α_1 and α_2 are two real constants. The linear behavior with time of $\delta\mathbf{x}(t)$ is then given by: $\delta\mathbf{x}(t) = \alpha_1 e^{\lambda_1}\mathbf{v_1} + \alpha_2 e^{\lambda_2}\mathbf{v_2}$.

Depending of the signs of λ_1 and λ_2 we can have the following behaviors:

• The two roots λ_1 and λ_2 have the same sign. Then the fixed point is called a **node**. The node is **stable** when the two roots are negative, it is **unstable** when they are positive.

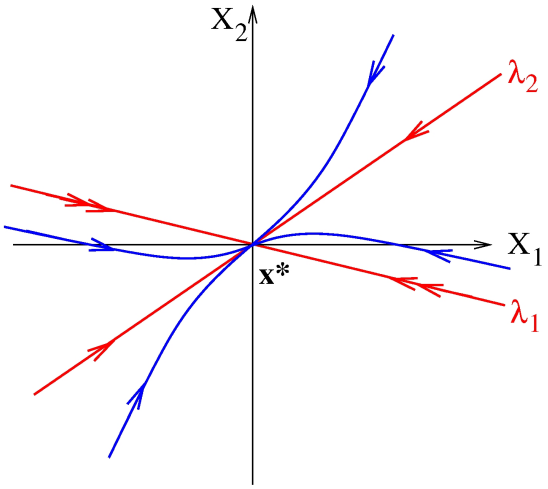

Figure 1.7: Example of a stable node. The red lines are the directions given by the eigenvectors. The blue curves are examples of trajectories in the phase space.

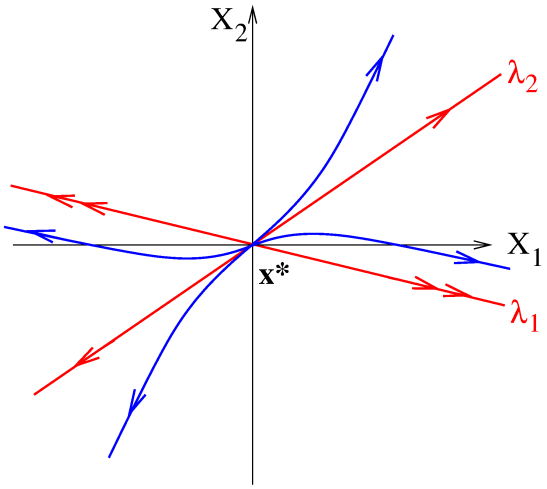

Figure 1.8: Example of an unstable node. As the eigenvalues are of opposite sign compare to the stable case, the figure is similar but with reverse arrows.

• The two roots λ_1 and λ_2 are of opposite signs. The fixed point is called a **saddle point**. It is always **unstable**.

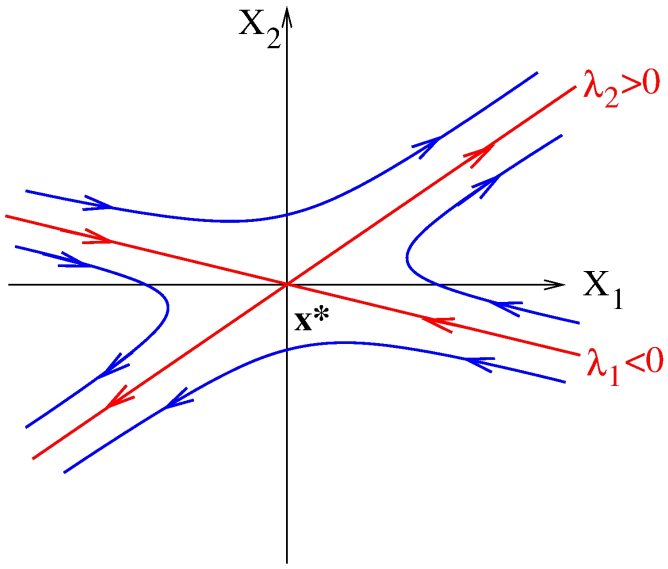

Figure 1.9: Example of a saddle point. The red lines are the directions given by the eigenvectors. The blue curves are examples of trajectories in the phase space.

1.2.5.b Two complex conjugates roots

The characteristic polynom cannot be factorized in $\mathbb{R}$. The complex conjugate eigenvalues can be written: $\lambda_1 = \sigma + i\omega$ and $\lambda_2 = \lambda_1^* = \sigma - i\omega$ with σ and ω reals.

There is a change of coordinates $\begin{pmatrix} x_1 \\ x_2 \end{pmatrix} \rightarrow \begin{pmatrix} y_1 \\ y_2 \end{pmatrix}$ which allows to rewrite the system in the following way:

$$\begin{cases} \dot{y}_1 &= \sigma y_1 + \omega y_2 \\ \dot{y}_2 &= -\omega y_1 + \sigma y_2 \end{cases}$$

The solutions of the system for an initial condition $\begin{pmatrix} y_1^0 \\ y_2^0 \end{pmatrix}$ are then:

$$\begin{cases} y_1(t) &= e^{\sigma t}(y_1^0 \cos\omega t + y_2^0 \sin\omega t) \\ y_2(t) &= e^{\sigma t}(-y_1^0 \sin\omega t + y_2^0 \cos\omega t) \end{cases}$$

The $\cos\omega t$ and $\sin\omega t$ parts of the solution lead to oscillations with time. Such oscillations exist only when the imaginary part of the eignevalues, ω, is different from 0. Concerning the stability of the fixed point, it is determined by the $e^{\sigma t}$ function which is in factor of the two coordinates: the real part of the complex conjugates eignevalues, σ, determine the stability of the fixed point.

We have then the following cases :

When $\sigma \neq 0$, the fixed point is called a **spiral**. It is stable for $\sigma < 0$ and unstable for $\sigma > 0$.

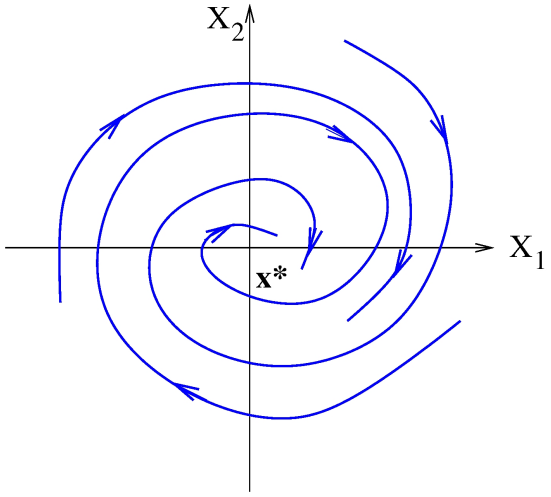

Figure 1.10: Example of a stable spiral. The blue curves are examples of trajectories in the phase space. The unstable spiral is a similar figure with reverse arrows.

When $\sigma = 0$, the fixed point is called a **center**. The stability of the fixed point cannot be determined by a linear analysis: the nonlinearities will determine if the point is finally stable or unstable. Such points are called **neutrally stable**.

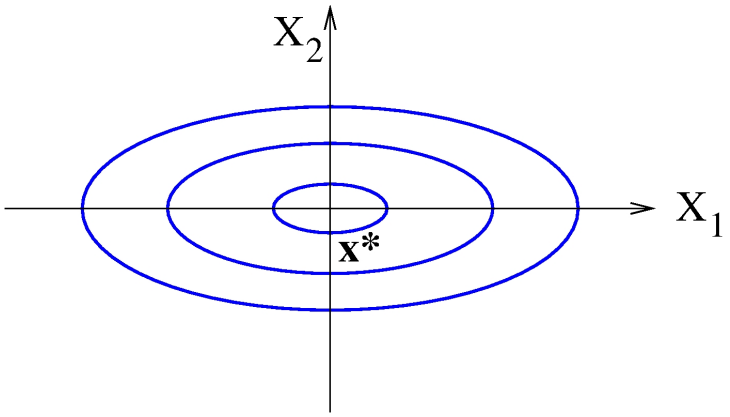

Figure 1.11: Example of a center.

1.2.6 Double root different from zero

A double root means that $\lambda_1 = \lambda_2$. The characteristic polynom is of the form: $P(\lambda) = (\lambda - \lambda_0)^2$, where we have noted λ_0 the double root. In this case the matrix is not always diagonalizable.

• If the matrix is diagonalizable, the matrix is in fact necessarily equal to $\lambda_0 \mathbb{1}$. The fixed point is then a **star node**. It can be stable or unstable depending on the sign of the root.

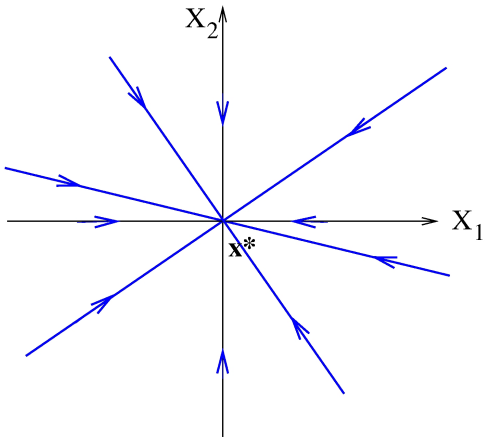

Figure 1.12: Example of a stable star node. All the lines going to the origin are trajectories. The figure of the unstable node is obtained by reversing the arrows.

• If the matrix is not diagonalizable, it can nevertheless be transformed in what is called its *Jordan form*, which means in the following form:

$$\begin{bmatrix} \lambda_0 & 1 \\ 0 & \lambda_0 \end{bmatrix}$$

Then, with the change of coordinates where the matrix is in the above form, the system can be integrated, giving:

$$\begin{cases} y_1(t) &= (y_1^0 + y_2^0 t)e^{\lambda_0 t} \\ y_2(t) &= y_2^0 e^{\lambda_0 t} \end{cases}$$

The fixed point is then a **degenerate node**. Depending on the sign of λ_0, it can be stable or unstable.

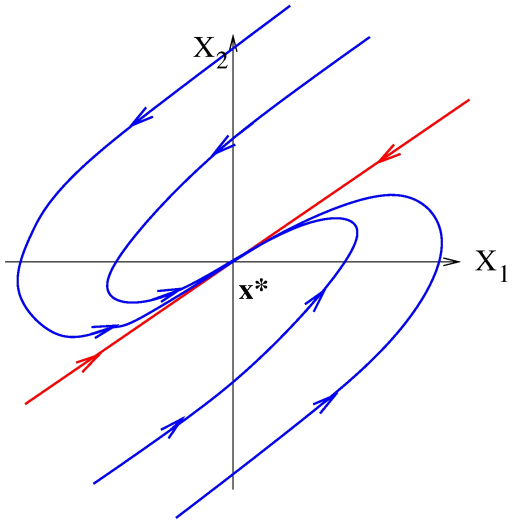

Figure 1.13: Example of a stable degenrate node. The blue curves are examples of trajectories in the phase space. The figure of the unstable node is obtained by reversing the arrows.

1.2.6.a Summary of the 2D case

In the two-dimendional case, the eigenvalues of the matrix can be deduced from the trace (T) and the determinant (Δ) of the matrix. As the characteristic polynomial of the jacobian matrix is (see eq. 1.7):

$$P(\lambda) = \lambda^2 - T\lambda + \Delta$$

the roots of the polynomials are given by:

$$\begin{aligned} \lambda_\pm &= \tfrac{T}{2} \pm \sqrt{\tfrac{T^2}{4} - \Delta} \quad \text{when } \tfrac{T^2}{4} > \Delta \\ \lambda_\pm &= \tfrac{T}{2} \pm i\sqrt{\Delta - \tfrac{T^2}{4}} \quad \text{when } \tfrac{T^2}{4} < \Delta \end{aligned}$$

We can then gathered all the previous cases in the following figure:

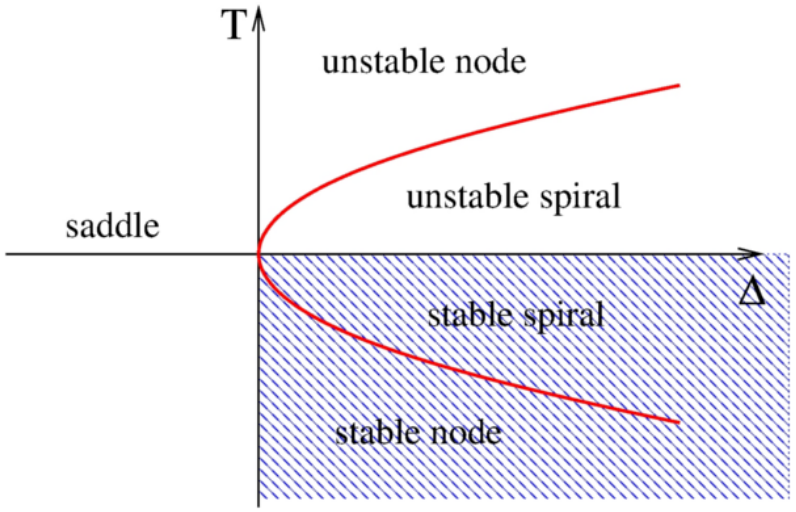

Figure 1.14: Summary of all the possible cases in 2 dimensions in function of the values of the determinant and of the trace of the matrix. The red curve is the curve: $T = \pm 2\sqrt{\Delta}$. The hatched part of the plane corresponds to the stable fixed points.

In **two dimension**, for the fixed point to be stable, you need $T < 0$ and $\Delta > 0$.

1.2.7 Higher dimensions case

The summary given on Figure 1.14 is only valid for the two dimensional case, when the eigenvalues of the matrix can be entirely determined by the trace and the determinant of the jacobian matrix. In the case of a higher dimension n, the eigenvalues are still roots of the characteristic polynomial and we need to determine the sign of the real part of **all** the eigenvalues λ_i to determine the stability of the fixed point.

If **all the eigenvalues** verify $Re(\lambda_i) \neq 0$, the fixed point is called **hyperbolic**. The dynamics deduced from the linearization is an accurate representation of the true (nonlinear) dynamics. We say that those cases are *robust* because their dynamics is not modified by a small perturbation of the model.

Hyperbolic fixed point or not, the general rule is the following:

- If **one** (or more) eigenvalue has **a real part strictly positive**, then the fixed point is **unstable**.
- If **all** the eigenvalues are of **real part strictly negative**, then the fixed point is **stable**.
- If all the eignevalues are of real part ≤ 0 but that **at least one** eigenvalue is of **real part null**, one has to be careful: the linearization of the system does not allow to deduce the dynamics around the fixed point. The nonlinearities determine the stability of the system.

1.2.8 Examples

1.2.8.a The damped pendulum

The dynamical system describing the damped pendulum is (see section 1.1.3.b):

$$\left\{ \begin{array}{rcl} \dot{X}_1 & = & X_2 \\ \dot{X}_2 & = & -\frac{g}{l}\sin X_1 - \gamma X_2 \end{array} \right.$$

To find the fixed points, we search the points $\mathbf{x}^*$ which are solutions of:

$$\left\{ \begin{array}{rcl} 0 & = & x_2 \\ 0 & = & -\frac{g}{l}\sin x_1 - \gamma x_2 \end{array} \right.$$

We deduce that the points $\begin{pmatrix} 0 \\ 0 \end{pmatrix}$ and $\begin{pmatrix} \pi \\ 0 \end{pmatrix}$ are fixed points as well as all the equivalents points deduced from the $2\pi-$periodicity.

To study the stability of those two points, we need the jacobian matrix of the system:

$$\mathcal{L} = \begin{pmatrix} 0 & 1 \\ -\frac{g}{l}\cos X_1 & -\gamma \end{pmatrix}$$

- Stability of $\begin{pmatrix} 0 \\ 0 \end{pmatrix}$

$$\mathcal{L}|_{(0,0)} = \begin{pmatrix} 0 & 1 \\ -\frac{g}{l} & -\gamma \end{pmatrix}$$

$T = -\gamma < 0$ for a realistic damping, $\Delta = \frac{g}{l}$. Consequently the fixed point $\begin{pmatrix} 0 \\ 0 \end{pmatrix}$ is stable. To determine if it is a node or a spiral, we have to calculate explicitely the eignevalues to know if they are real or imaginary.

  - If $\frac{\gamma^2}{4} > \frac{g}{l}$, then the fixed point is a node (overdamped case)

– If $\frac{\gamma^2}{4} < \frac{g}{l}$, then the fixed point is a spiral (underdamped case)

The particular case $\gamma = 0$, without damping, corresponds indeed to a center.

- Stability of $\begin{pmatrix} \pi \\ 0 \end{pmatrix}$

$$\mathcal{L}|_{(\pi,0)} = \begin{pmatrix} 0 & 1 \\ \frac{g}{l} & -\gamma \end{pmatrix}$$

$T = -\gamma < 0$ and $\Delta = -\frac{g}{l}$. Consequently the fixed point $\begin{pmatrix} \pi \\ 0 \end{pmatrix}$ is a saddle point, which is always unstable.

1.2.8.b Non hyperbolic example

Consider the following system, where $a \in \mathbb{R}^*$

$$\begin{cases} \dot{X}_1 &= -X_2 + aX_1(X_1^2 + X_2^2) \\ \dot{X}_2 &= X_1 + aX_2(X_1^2 + X_2^2) \end{cases}$$

The only fixed point of the system is $\begin{pmatrix} 0 \\ 0 \end{pmatrix}$. The jacobian matrix in this point takes the value:

$$\mathcal{L}|_{(0,0)} = \begin{pmatrix} 0 & -1 \\ 1 & 0 \end{pmatrix}$$

$T = 0$ and $\Delta = 1$. Consequently the fixed point is a center.

In this example we can determine the stability of the fixed point by considering the whole system. Let's use the following change of variable $Z = X_1 + iX_2$. The system of equation can be reformulate in the following way:

$$\dot{Z} = iZ + aZ|Z|^2$$

Consider now the module and the phase of that complex number: $Z = Re^{i\Theta}$

$$\begin{cases} \dot{R} &= aR^3 \\ \dot{\Theta} &= 1 \end{cases}$$

We find that:

- if $a = 0$, R is constant, the system is in fact a consevative system and the trajectories are circles of radius fixed by the initial condition.
- if $a < 0$, $\dot{R} < 0$ and the radius of the trajectory decreases with time. The fixed point $\begin{pmatrix} 0 \\ 0 \end{pmatrix}$ is stable.
- if $a > 0$, $\dot{R} > 0$, the radius of the trajectory increases with time. The fixed point is unstable.

1.3 Limit cycles

1.3.1 Definition and existence

1.3.1.a Definition

A limit cycle is a **closed isolated trajectory** in the phase space. In the vicinity of a limit cycle, the trajectories spiral towards or away of the cycle depending of its stability (respectively stable and unstable). There is no other closed trajectory in the immediate vicinity of a limit cycle.

Such cycles can only exist for nonlinear dissipative systems. For a conservative system, closed orbits correspond to center and there are an infinity of them nested into each other. We saw an example of such a system in the case of the simple pendulum (Subsection 1.1.3.a). The amplitude of the closed orbits are fixed by the initial condition. On the contrary, in the case of a limit cycle, the frequency, the form and the amplitude of the oscillations do not depend on the initial conditions.

1.3.1.b Existence: Poincaré-Bendixson theorem

This mathematical theorem is only valid for $n = 2$. Given $\frac{d\mathbf{x}}{dt} = \vec{F}(\mathbf{x})$ with $\mathbf{x} \in \mathbb{R}^2$ an autonomous flow with $\vec{F}$ continuously differentiable. Given a sub-set $\mathcal{R}$ closed and bounded of $\mathbb{R}^2$ which **does not contain any fixed point**. If there exists a trajectory confined in $\mathcal{R}$, then $\mathcal{R}$ contains a limit cycle.

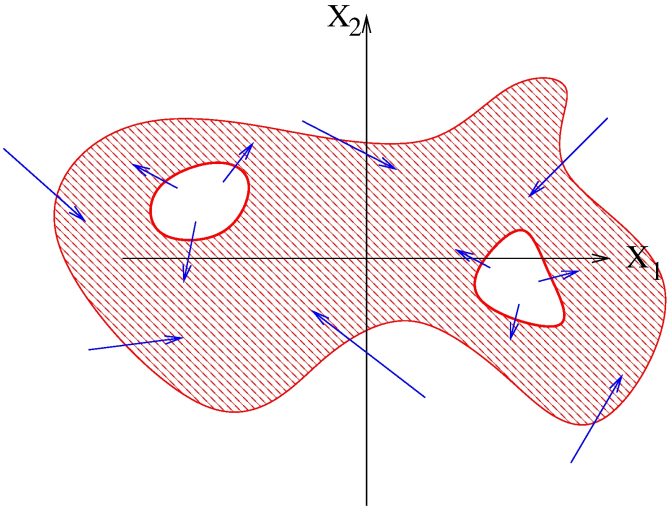

Figure 1.15: Illustration of how the Poincaré-Bendixson theorem works. If we can draw a set as the hatched one containing no fixed points and so that on all the frontiers of that set the flow (represented by the blue arrows) is going *inside* the set, then the trajectories are trapped in this set and there is a cycle limit in the hatched area.

A consequence of that theorem is that in two dimensions the only possible asymptotic

behaviors for a dissipative system are stationary solutions (fixed points) and periodic solutions (limit cycles).

1.3.1.c Example

Read the example 7.3.2 about the glycolysis cycle in the book of S. Strogatz.

1.3.2 Van der Pol oscillator

A very famous model giving rise to periodic oscillations is the Van der Pol oscillator.

We start with the linearized version of the damped pendulum:

$$\ddot{\theta} + \gamma\dot{\theta} + \omega^2\theta = 0,$$

but we suppose that the damping is not anymore a constant but depends on θ and can change of sign. This last point means that when $\gamma < 0$, it is not anymore a damping term but an amplification term (consequently some energy is injected in the system during the process).

A simple possible function $\gamma(\theta)$, which depends only on the amplitude of the oscillations, is quadratic:

$$\gamma(\theta) = \gamma_0 \left(\left(\frac{\theta}{\theta_0} \right)^2 - 1 \right)$$

with $\gamma_0 > 0$. Then, we have:

- when $|\theta| > |\theta_0|$, i.e. for large amplitude oscillations, $\gamma > 0$, so that those oscillations are damped and their amplitude decreases,
- when $|\theta| < |\theta_0|$, i.e. for small amplitude oscillations, $\gamma < 0$, and gives rise to an amplification of the oscillation, pushing the system away from the origin in the phase plane.

The nondimensionalisation of the equations: $t' = \omega t$, $x = \frac{\theta}{\theta_0}$, $\mu = \frac{\gamma_0}{\omega} > 0$ leads to the following equation:

$$\ddot{x} + \mu(x^2 - 1)\dot{x} + x = 0,$$

where the derivatives are now relative to t'.

Let's proceed to the usual reformulation $X_1 = x$ and $X_2 = \dot{x}$,

$$\left\{ \begin{array}{rcl} \dot{X}_1 & = & X_2 \\ \dot{X}_2 & = & -X_1 - \mu(X_1^2 - 1)X_2 \end{array} \right.$$

The only possible fixed point is $\begin{pmatrix} 0 \\ 0 \end{pmatrix}$. The jacobian matrix at this point is:

$$\mathcal{L}|_{(0,0)} = \begin{pmatrix} 0 & -1 \\ 1 & \mu \end{pmatrix}$$

$T = \mu > 0$ and $\Delta = 1 > 0$, the fixed point is always unstable (either a node or a spiral depending of the value of the non-dimensionalised damping parameter μ. Consequently, trajectories goes away from the origin. But they are not going to infinity as the damping increases with the amplitude of the oscillation.

The application of the Poincaré-Bendixson theorem in this case is tricky. First we trace the curves corresponding to $f_1(X_1, X_2) = 0$ on one hand and $f_2(X_1, X_2) = 0$ on the other hand. Those particular curves are called **nullclines**. They delimit the part of the phase plane where the general direction of the vector field changes because of the change of sign of one of its composant. Here the nullclines are

$$X_2 = 0, \text{ and } X_2 = -\frac{1}{\mu}\frac{X_1}{X_1^2 - 1}$$

and are represented thereafter.

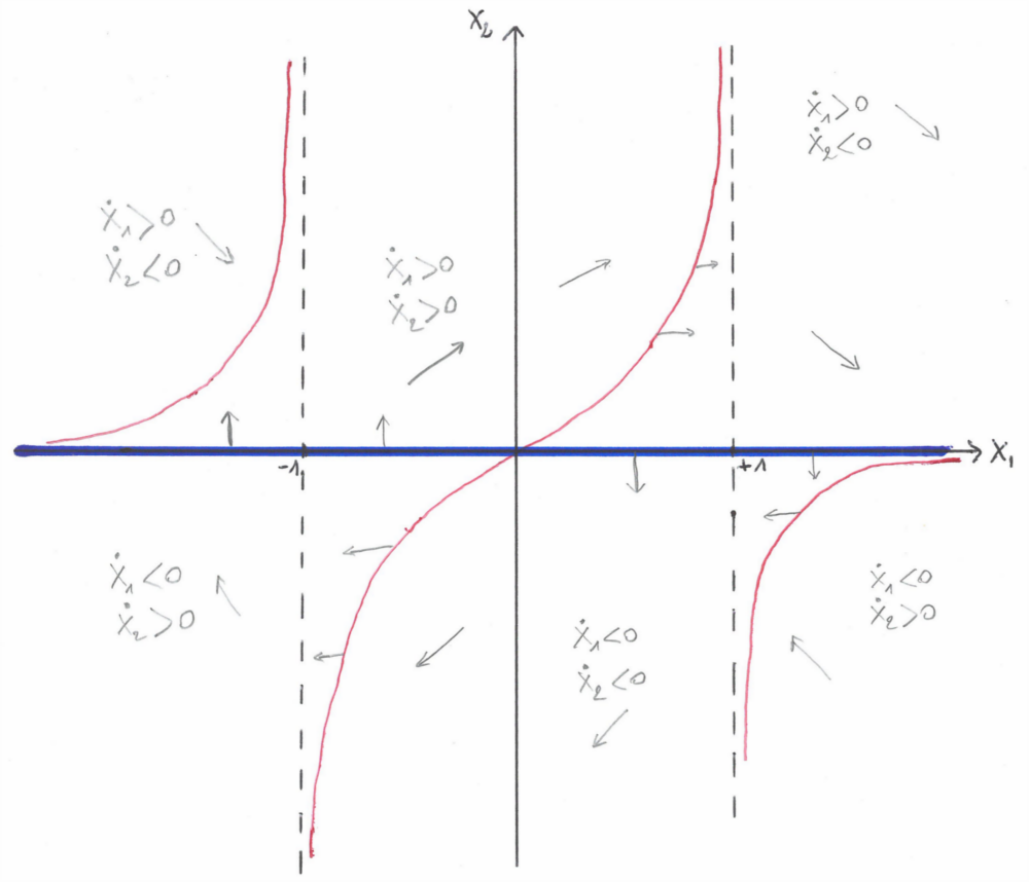

Figure 1.16: Nullclines of the Van der Pol oscillator: in blue $f_1(X_1, X_2) = 0$, in red $f_2(X_1, X_2) = 0$. In light grey, general trends of the vector field in the part of the phase space delimited by the nullclines.

Note that the intersections of the nullclines correspond to the fixed points as those points verify simultaneously $f_1(X_1, X_2) = 0$ and $f_2(X_1, X_2) = 0$. In the example the only

intersection is at the origin.

The orientation of the flow when $X_1 \in [-1, +1]$ in figure 1.16 is at the origin of the difficulty for a direct application of the Poincaré-Bendixson theorem. Nevertheless, it is possible to draw a curve fitting the theorem criteria, the appearance of which is shown in the following figure.

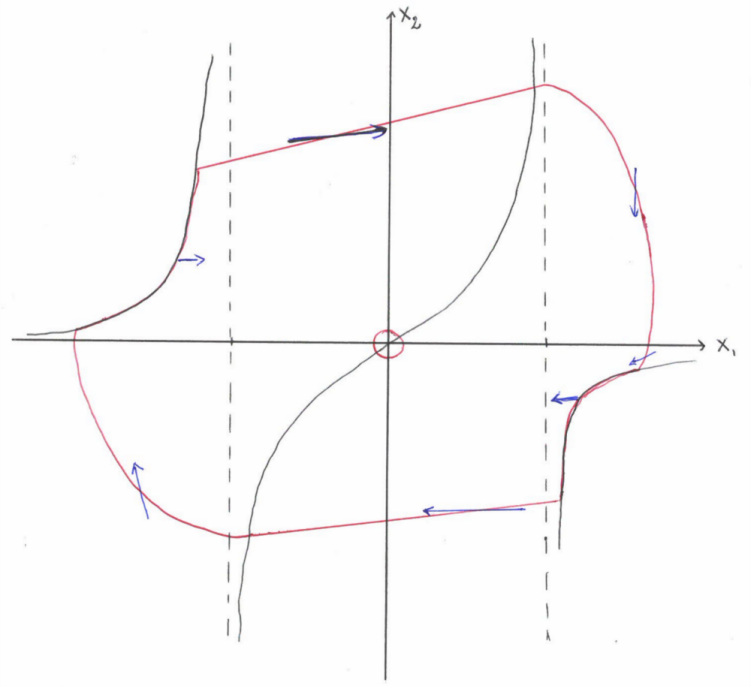

1.3.3 Poincaré map

The stability analysis of a limit cycle is much more complicated than for a fixed point. We are going to use a tool which is in fact very general to study the dynamics of a system of dimension larger than 2.

To reduce the dimension of the dynamics of the system we will not study the whole trajectory but only **the intersection points of this trajectory with a surface** (generally a plane) and only the points corresponding to a crossing of the surface **in a given orientation**.

Those intersection points form a pattern in the plane called a **Poincaré section**. The transformation T linking a point to the next one is a continuous map of the cutting plane in itself and is called **Poincaré map** or **first return map**.

$$P_{k+1} = T(P_k) = T(T(P_{k-1})) = T^2(P_{k-1}) = T^{k+1}(P_0)$$

We have consequently transformed a continuous flow in a discrete map. Notice that the time that elapsed between successive points is not constant in general. Nevertheless, in the case of driven systems at a fixed frequency ω_0, a Poincaré section can be obtained by

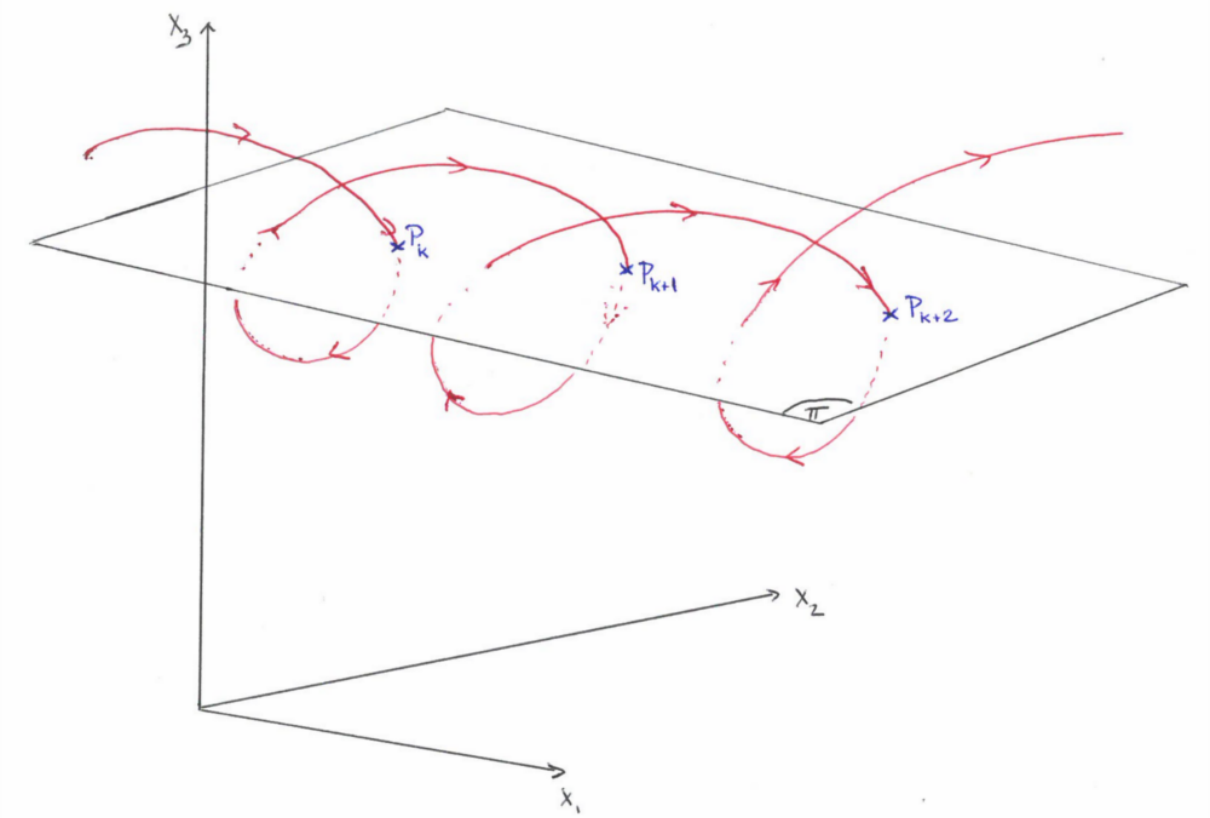

Figure 1.17: Principle of a Poincaré section. In red: trajectory of the system in the phase space. This trajectory intersect the plane (Π). We select the intersection points for a given orientation of the crossing of the plane (here when the trajectory cut the plane from top to bottom). The serie of points $\{P_0, P_1, \dots, P_k, \dots\}$ is called the Poincaré section.

taking points at each period $T_0 = \frac{2\pi}{\omega_0}$, as for a stroboscopy.

The Poincaré section has the same topological properties as the flow from which it has been obtained, in particular it also presents area contraction.

Case of a limit cycle

When studying a limit cycle for the flow, a wise choice of the surface Π will lead to a Poincaré section displaying a unique point P^*[10]. P^* is then a fixed point of the first return map:

$$P^* = T(P^*).$$

Consequently, the study of the stability of a limit cycle can be reduced to the problem of the stability of a fixed point but of a discrete map and not a continuous flow. The underlying principle of the analysis of the stability is exactly the same as the one we

[10] And in all cases a finite number of points.

studied in the previous section but the implementation is slightly different because of the discrete nature of the dynamics, as we will see in the next section.

1.3.4 Floquet multipliers

Using a Poincaré section, the study of the stability of a limit cycle is thus replaced by the study of the stability of the point P^*. To obtain the stability of this point we procced to a linear stability analysis taking into account of the fact that we deal with a discrete dynamics.

Considering the map: $T : \Pi \to \Pi$, the fixed point $P^* \in \Pi$, $T(P^*) = P^*$, and the matrix $\mathcal{L}|_{P^*}$ obtained by the linearization of T around P^*. As Π is an hyperplane of dimension $n-1$ in the phase space of dimension n, $\mathcal{L}|_{P^*}$ is a $(n-1) \times (n-1)$ matrix.

If $P_0 = P^* + \delta P_0$ is a point near P^* and calling $P_{i+1} = T(P_i) = P^* + \delta P_{i+1}$ the successive iterates:

$$\begin{aligned}
T(P^* + \delta P_0) &\simeq T(P^*) + \mathcal{L}|_{P^*}.\delta P_0 \\
P_1 &\simeq P^* + \mathcal{L}|_{P^*}.\delta P_0 \\
\delta P_1 &\simeq \mathcal{L}|_{P^*}.\delta P_0 \\
\\
T^2(P^* + \delta P_0) &= T(P^* + \delta P_1) \\
P_2 &\simeq T(P^*) + \mathcal{L}|_{P^*}.\delta P_1 \\
\delta P_2 &\simeq \left(\mathcal{L}|_{P^*}\right)^2.\delta P_0 \\
&\vdots \\
T^k(P^* + \delta P_0) &= P^* + (\mathcal{L}|_{P^*})^k.\delta P_0 \\
\delta P_k &\simeq \left(\mathcal{L}|_{P^*}\right)^k.\delta P_0
\end{aligned}$$

The stability of P^* is given by the evolution of the sequence of distances δP_k between the k^{th} iterate P_k and the fixed point P^*. If the sequence diverges, P^* is unstable: a small perturbation is amplified and the successive points are going away from P^*. If the sequence of δP_k converge to 0, P^* is stable. The behavior of the sequence is governed by the incremental powers of $\mathcal{L}|_{P^*}$.

We can again study the diagonal case to understand how $(\mathcal{L}|_{P^*})^k$ behave. If

$$\mathcal{L}|_{P^*} = \begin{pmatrix} \lambda_1 & & 0 \\ & \ddots & \\ 0 & & \lambda_n \end{pmatrix} \text{ then } (\mathcal{L}|_{P^*})^k = \begin{pmatrix} \lambda_1^k & & 0 \\ & \ddots & \\ 0 & & \lambda_n^k \end{pmatrix}$$

Consequently, what is now important is the values of the module of the λ_i compared to 1. We have the following rules:

- if **all the eigenvalues of $\mathcal{L}|_{P^*}$ have their module strictly less than 1**, then for all the λ_i, $\lambda_i^k \to 0$ when $k \to \infty$ and the fixed point (and consequently the limit cycle) is **stable**.
- if **at least one of the eigenvalues of $\mathcal{L}|_{P^*}$ has its module strictly greater than 1**, then for this eignevalue λ_i, λ_i^k diverges when $k \to \infty$ and the fixed point (and consequently the limit cycle) is **unstable**.
- if **all the eigenvalues of $\mathcal{L}|_{P^*}$ have their module ≤ 1, and at least one eigenvalue is of module strictly equal to 1**, then the linear stability analysis does not give the stability of the fixed point.

$\mathcal{L}|_{P^*}$ is called the **Floquet matrix** and its eignevalues $\{\lambda_i\}_{i=1\ldots n-1}$ are called the **Floquet multipliers**. People also use the **Floquet exponents**: $\left\{\mu_i = \frac{1}{\tau}\ln|\lambda_i|\right\}_{i=1\ldots n-1}$, where τ is the period of the limit cycle. The previous rules, when applied to the Floquet exponents are then similar to the ones we gave for the stability of the fixed points of continuous flows: the rules are then on the sign of the μ_i.

Conclusion

In this first chapter, we have learned different tools allowing the visualization of the dynamics of a system.

We have seen that for dissipative systems all the trajectories converge towards attractors which organize the phase space. We have studied in details two types of attractors, the fixed points, which live in a space of dimension ≥ 1 and the limit cycles which live in a space of dimension ≥ 2.

In the next chapter we will study the modification of the nature or number of attractors when the values of the parameters are modified.

Bibliography

- In English:
  - **Nonlinear dynamics and chaos**, S. Strogatz
- In French:
  - **L'ordre dans le chaos**, P. Bergé, Y. Pomeau, C. Vidal
  - **Cours DEA** de V. Croquette, `http://www.phys.ens.fr/cours/notes-de-cours/croquette/index.html`
  - **Les maths en physique**, J.P Provost, G. Vallée *(Pour une révision d'algèbre linéaire: ch. 4, sur les systèmes dynamiques: ch. 6)*

Chapter 2

Bifurcations

In the previous chapter we discuss the fact that disspatives systems possess attractors. Generally, in a model, the vector field $\vec{F}$ depends on parameters and the behavior of the system may depend on the values of those parameters. It means that the the number and/or nature of attractors may change when parameters are tuned. Such a change is called a **bifurcation**. The value of the parameter for which such qualitative change of the structure of the phase space happens is called the **critical value of the parameter**.

The *bifurcation theory* studies this problem for any numbers of parameters. Here we will study only the simple case of a vector field $\vec{F}$ depending only on **one** parameter. Moreover, we will only study the cases where a limited part of the phase space is involved in the change. Those particular kind of bifurcations are **local and of codimension 1**.

Near a bifurcation, the dynamical system can be reduced to a generic mathematical form by a change of variables and a reduction of its dimension to keep only the directions implied in the bifurcation. Those reduced mathematical expressions are called **normal forms** and each form is associated to a type of bifurcation.

2.1 Saddle-node bifurcation

This bifurcation corresponds to the apparition or anihilation of a pair of fixed points. Its normal form is:

$$\boxed{\dot{x} = \mu - x^2}$$

where $x \in \mathbb{R}$.

The study of the stability of the normal form gives two fixed points $\pm\sqrt{\mu}$ which can exist only when $\mu \geq 0$. As $\frac{\partial F}{\partial x} = -2x$, we obtain $\frac{\partial F}{\partial x}|_{+\sqrt{\mu}} = -2\sqrt{\mu} < 0$ and $\frac{\partial F}{\partial x}|_{-\sqrt{\mu}} = 2\sqrt{\mu} > 0$ so that the fixed point $+\sqrt{\mu}$ is stable and the other one $-\sqrt{\mu}$ is unstable.

Those fixed points are then plotted in a graph as a function of the value of the parameter. We call such graph **bifurcation diagram**. The set of stable fixed points is drawn with a solid line, the set of unstable fixed points is drawn with a dashed line.

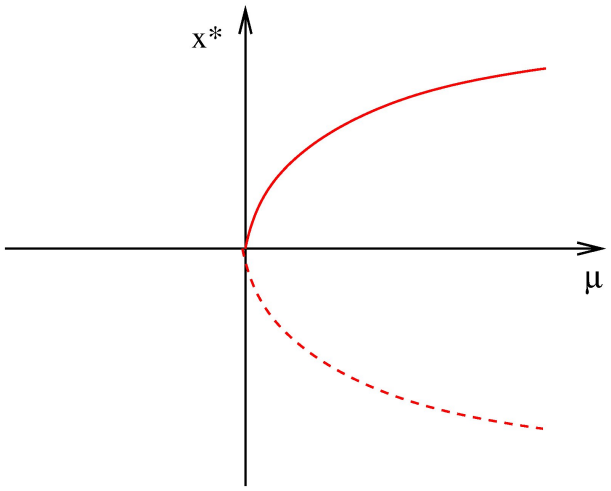

Figure 2.1: Saddle-node bifurcation. The solid red line is the function $x^* = +\sqrt{\mu}$ corresponding to the set of stable stationary solutions, the dashed one $x^* = -\sqrt{\mu}$ giving the set of unstable stationary solutions.

We obtain **branches of solutions**. A point of the bifurcation diagram from which several branches emerge is a bifurcation point. In the case of Figure 2.1, the bifurcation point is 0 and the critical value of the parameter μ is also 0.

For each normal form, an inverse bifurcation is obtained by changing the sign of the nonlinearity. Here the inverse bifurcation is:

$$\dot{x} = \mu + x^2$$

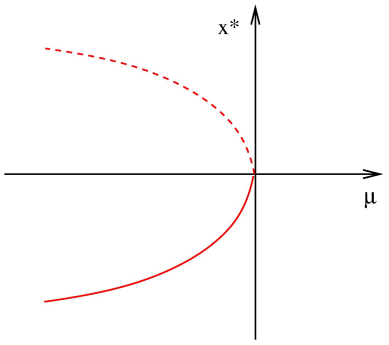

Figure 2.2: Inverse saddle-node bifurcation.

2.2 Transcritical bifurcation

This bifurcation corresponds to an exchange of stability between two fixed points. Its normal form is:

$$\boxed{\dot{x} = \mu x - x^2}$$

The fixed points are $x^* = 0$ and $x^* = \mu$. $\frac{dF}{dx} = \mu - 2x$, which gives:

- $\frac{dF}{dx}\big|_0 = \mu$, thus the fixed point 0 is stable when $\mu < 0$ and unstable when $\mu > 0$,
- $\frac{dF}{dx}\big|_\mu = -\mu$, the fixed point μ is unstable when $\mu < 0$ and stable when $\mu > 0$.

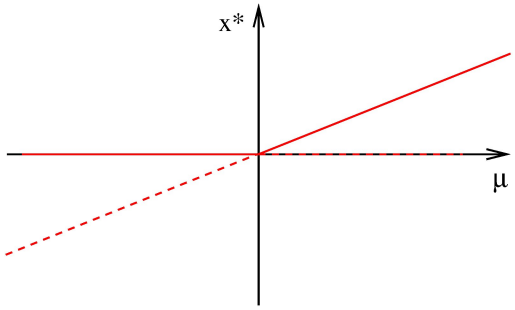

Figure 2.3: Transcritical bifurcation.

2.3 Pitchfork bifurcation

2.3.1 Supercritical bifurcation

The normal form of the bifurcation has the symetry $x \to -x$:

$$\boxed{\dot{x} = \mu x - x^3.}$$

We can find 1 or 3 fixed points depending on the sign of μ: the fixed point $x^* = 0$ exists for all values of μ, while the two symetric fixed points $\pm\sqrt{\mu}$ exist only for $\mu > 0$.

The stability analysis gives:

- $\frac{dF}{dx}\big|_0 = \mu$, the fixed point 0 is stable when $\mu < 0$ and unstable when $\mu > 0$,
- $\frac{dF}{dx}\big|_{\pm\sqrt{\mu}} = -2\mu < 0$, the two symetric fixed point $\pm\sqrt{\mu}$ are stable when they exist.

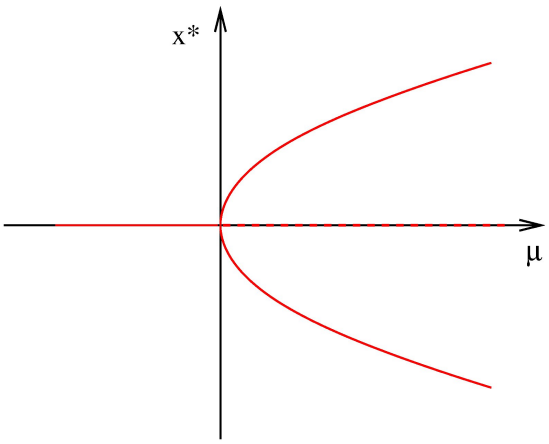

Figure 2.4: Supercritical pitchfork bifurcation.

When the system crosses the bifurcation coming from $\mu < 0$, it has to choose one of the two stable branches of the pitchfork. This choice is called a **symetry breaking**: the chosen solution has lost the symetry $x \to -x$.

2.3.2 Subcritical bifurcation

In the supercritical case, the nonlinear term $-x^3$ saturates the linear divergence for $\mu > 0$, leading to two new stable solutions when $x^* = 0$ becomes unstable. In the subcritical (inverse) case, the nonlinear term is $+x^3$ is destabilizing:

$$\dot{x} = \mu x + x^3$$

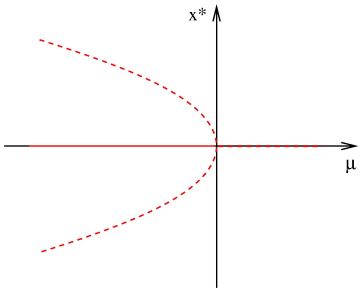

Consequently, to obtain stable solutions for $\mu > 0$, one has to take into account higher order terms in the normal form. Keeping the symetry $x \to -x$ of the system, we get:

$$\boxed{\dot{x} = \mu x + x^3 - x^5} \tag{2.1}$$

To obtain this bifurcation diagram, one has to study the fixed points of eq (2.1) and their stability.

The solutions of $\mu x + x^3 - x^5 = 0$ are either $x^* = 0$ or the solutions of the polynomial $\mu + x^2 - x^4 = 0$. Let $y = x^2$, we search the solutions of $y^2 - y - \mu = 0$ which are $y_\pm = \frac{1 \pm \sqrt{1+4\mu}}{2}$ for $\mu \geq -1/4$. As $y = x^2$, we can use the $y_\pm$ only when they are positive.

- $y_+ = \frac{1+\sqrt{1+4\mu}}{2}$ is always positive in its existence domain $\mu \geq -1/4$
- $y_- = \frac{1-\sqrt{1+4\mu}}{2}$ is positive only when $1 \geq \sqrt{1+4\mu}$, i.e. when $-1/4 \leq \mu \leq 0$.

To summarize:

- when $\mu < -1/4$ there is only one stationary solution, $x^* = 0$, and as $\frac{dF}{dx}|_0 = \mu < 0$, it is stable.
- when $-1/4 \leq \mu \leq 0$, there are five fixed points. $x^* = 0$ still exists and is still stable. The four other fixed points are given by $\pm\sqrt{y_+}$ and $\pm\sqrt{y_-}$. We will not detail the linear stability analysis but you can make the calculation and show that the two solutions $\pm\sqrt{\frac{1-\sqrt{1+4\mu}}{2}}$ are unstable while $\pm\sqrt{\frac{1+\sqrt{1+4\mu}}{2}}$ are stable.

- when $\mu \geq 0$, only 3 fixed points remain because the solutions $\pm\sqrt{y_-}$ do not exist anymore. The fixed point $x^* = 0$ is now unstable as $\mu > 0$, while the solutions $\pm\sqrt{\frac{1+\sqrt{1+4\mu}}{2}}$ are still stable.

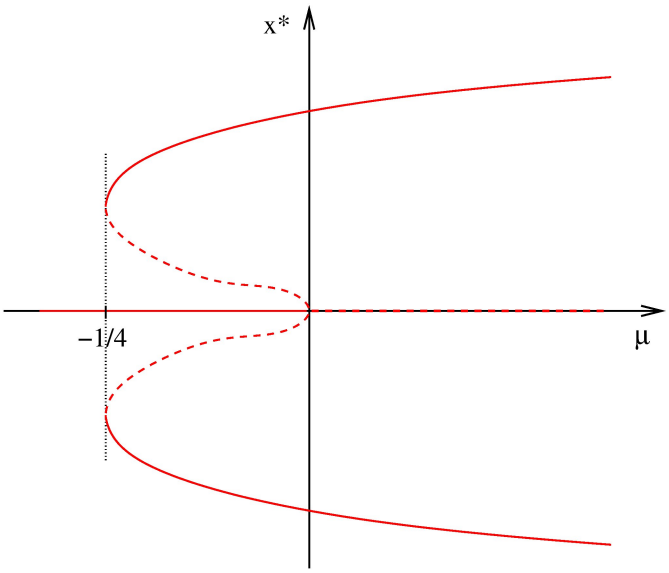

Figure 2.5: Subcritical pitchfork bifurcation.

In the interval $[-1/4; 0]$, several stable solutions coexist: there is **bistability** between the solutions. The choice between the 0 solution and one or the other of the symetric stable branches depends on the history of the system. An **hysteresis cycle** will be observed when the parameter μ is tuned one way and the other around the values $-1/4$ and 0.

2.4 Hopf bifurcation

This bifurcation corresponds to the emergence of a periodic solution from a stationary solution.

For all the previous bifurcations between different fixed points, a one-dimensional normal form was sufficient to describe each bifurcation. But now, as a limit cycle is a bidimensional object, one needs a bidimensional normal form to describe the bifurcation. This is taken into account by writting an equation on a complex:

$$\boxed{\dot{z} = (\mu + i\gamma)z - z|z|^2} \tag{2.2}$$

with $z \in \mathbb{C}$, μ and γ in $\mathbb{R}$ and $\gamma \neq 0$.

Fixed points are given by: $(\mu + i\gamma)z = |z|^2 z$, and if $\gamma \neq 0$, the only solution is $z = 0$ (because $|z|^2 \in \mathbb{R}$).

To do the linear stability analysis, we want more conventional writting of the equations with two equations on variables in $\mathbb{R}$. Writing $z = x + iy$, we have:

$$\left\{ \begin{array}{rcl} \dot{x} & = & \mu x - \gamma y - x(x^2 + y^2) \\ \dot{y} & = & \mu y + \gamma x - y(x^2 + y^2) \end{array} \right.$$

The linearization in $(0, 0)$ gives

$$\mathcal{L}|_{(0,0)} = \left[\begin{array}{cc} \mu & -\gamma \\ \gamma & \mu \end{array} \right],$$

from which we deduce $\Delta = \mu^2 + \gamma^2 > 0$ and $T = 2\mu$. Consequently, the fixed point $(0, 0)$ is stable for $\mu < 0$ and unstable for $\mu > 0$. At the bifurcation, the behavior around the fixed point changes from a convergent spiral to a divergent spiral. To understand what happens to the trajectories when $\mu > 0$, we use the other decomposition of a complex number with modulus and phase: $z = re^{i\theta}$ which gives:

$$\left\{ \begin{array}{rcl} \dot{r} & = & \mu r - r^3 \\ \dot{\theta} & = & \gamma \end{array} \right.$$

We recognize for the evolution of the modulus the normal form of a supercritical pitchfork bifurcation, while the phase has a linear dependence in time. We deduce from this system that the stable solution for $\mu > 0$ is a solution of fixed modulus but linearly increasing phase with time. It is a periodic solution which verifies $r = \sqrt{\mu}$ and $\theta = \gamma t + \theta_0$. The bifurcation diagram of a Hopf bifurcation is given in Figure 2.6.

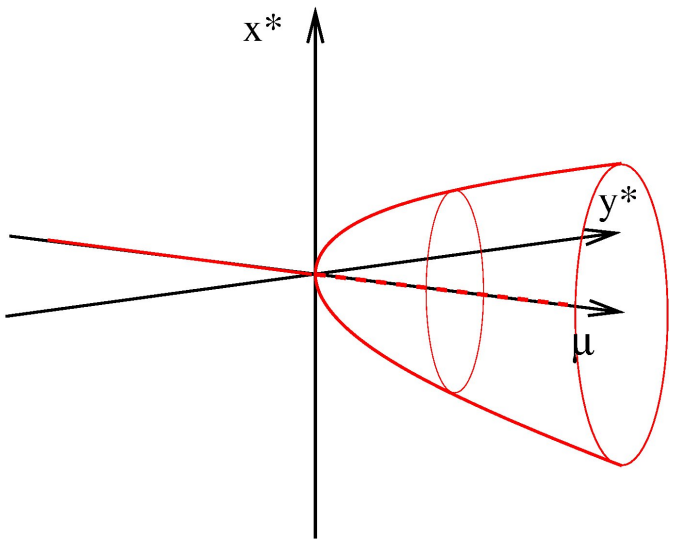

Figure 2.6: Hopf bifurcation.

The subcritical case exists: $\dot{z} = (\mu + i\gamma)z + z|z|^2$. The study is exactly the same as the supercritical case, leading to unstable limit cycles solution for $\mu < 0$.

2.5 Imperfect bifurcation. Introduction to catastrophe theory

Bibliography:

- *Nonlinear dynamics and chaos, S. Strogatz,*
- *Dynamiques complexes et morphogénèse, C. Misbah.*

Coming back to the pitchfork bifurcation, you can have the intuition that the bifurcation diagram we draw was idealized and that in fact, in a real system a branch will be always chosen preferentially because of some imperfection of the system.

This problematic deals with the question of the *robustness* of the model to a perturbation (note that we speak of the perturbation of the *model* and not of a given solution of the equations).

In this part, we want to know how the pitchfork bifurcation will be modified if a new parameter h is added to its normal form:

$$\dot{x} = \mu x - x^3 + h$$

Do we observe the same qualitative bifurcation or not ? Does it keep its general properties ?

Let's find the fixed points of this new equation. They are given by the intersection of the curve $y = g(x)$ with $g(x) = x^3 - \mu x$ with the line $y = h$.

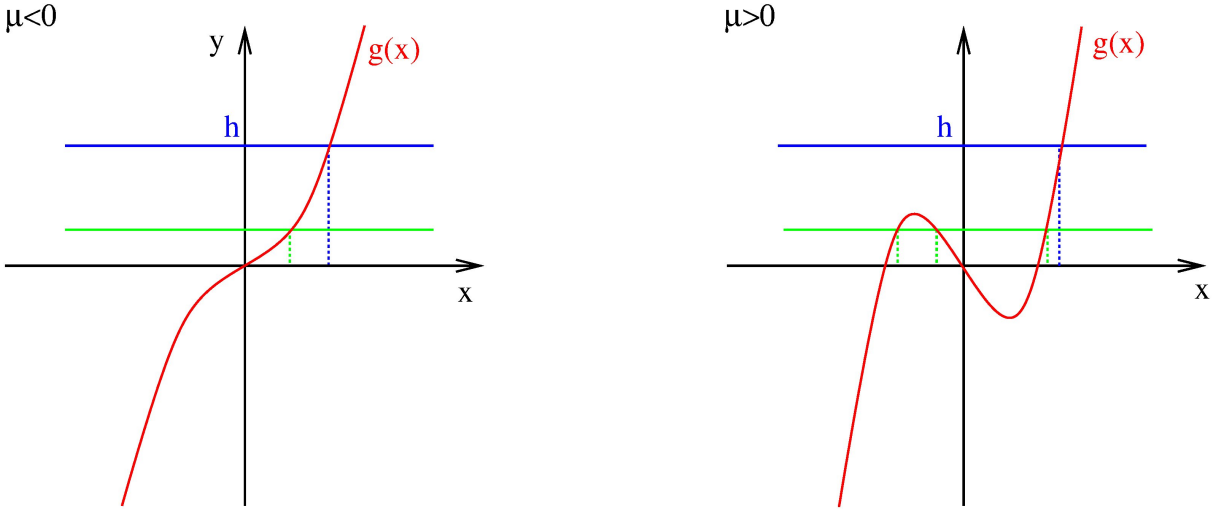

Figure 2.7: Finding the fixed points of $\dot{x} = \mu x - x^3 + h$: intersection of the curve $y = g(x)$ and of $y = h$.

By studying the function $g(x)$, we obtain that $g(x)$ is strictly growing when $\mu < 0$, so that there is a unique fixed point x^* for given values of the parameters μ and h. For

$\mu > 0$, the derivative of $g(x)$ is negative in the interval $[-\sqrt{\frac{\mu}{3}}, +\sqrt{\frac{\mu}{3}}]$, so that depending on the value of h, we can find either 1 or 3 fixed points (respectively blue and green cases on the right part of Figure 2.7). A straightforward calculation gives that we find 3 fixed points when $h \in [-\frac{2\mu}{3}\sqrt{\frac{\mu}{3}}, +\frac{2\mu}{3}\sqrt{\frac{\mu}{3}}]$, while for values of h outside this interval there is only one fixed point.

In the space of the parameters (μ, h), we can then draw a **stability diagram** as shown in Figure 2.8 The hatched area is delimited by the curves $h = \frac{2\mu}{3}\sqrt{\frac{\mu}{3}}$ and $h = -\frac{2\mu}{3}\sqrt{\frac{\mu}{3}}$.

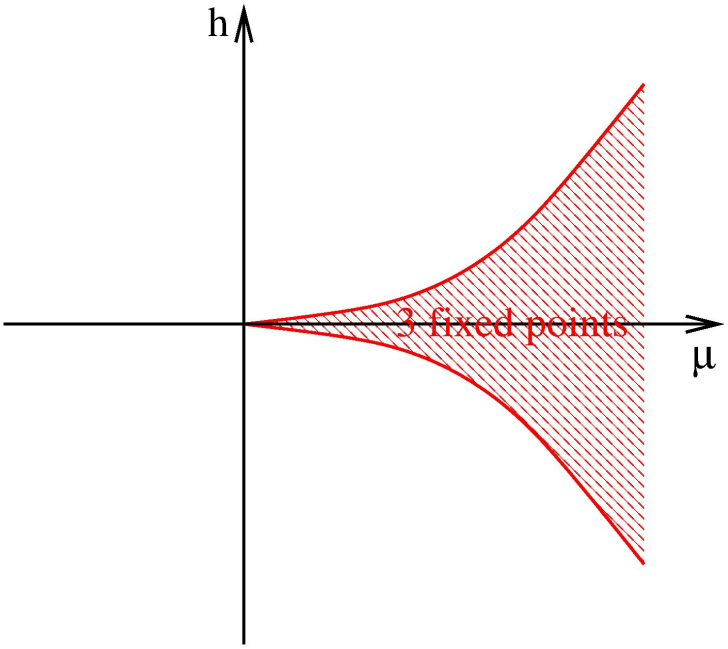

Figure 2.8: Stability diagram of the imperfect pitchfork bifurcation.

Their junction point in $(0, 0)$ is a singular point called a **cusp**.

To find the stability of the fixed points, we can use the fact that if $F(x) = \mu x - x^3 + h$, $dF/dx = -g'(x)$, so that we can deduce the stability of a fixed point from the sign of the derivative of g. We see that in the case $\mu < 0$, the only existing fixed point is stable. When $\mu > 0$, the fixed points obtained in the increasing part of g (the rightmost and leftmost ones) are stable, while the one obtained in the decreasing part (middle fixed point) is unstable.

We can now draw different types of bifurcation diagrams: bifurcation diagrams at fixed μ and varying h and the ones at fixed h and varying μ.

The bifurcation diagram for a fixed value of μ and considering as a varying parameter h depends on the sign of μ (see figure 2.9).

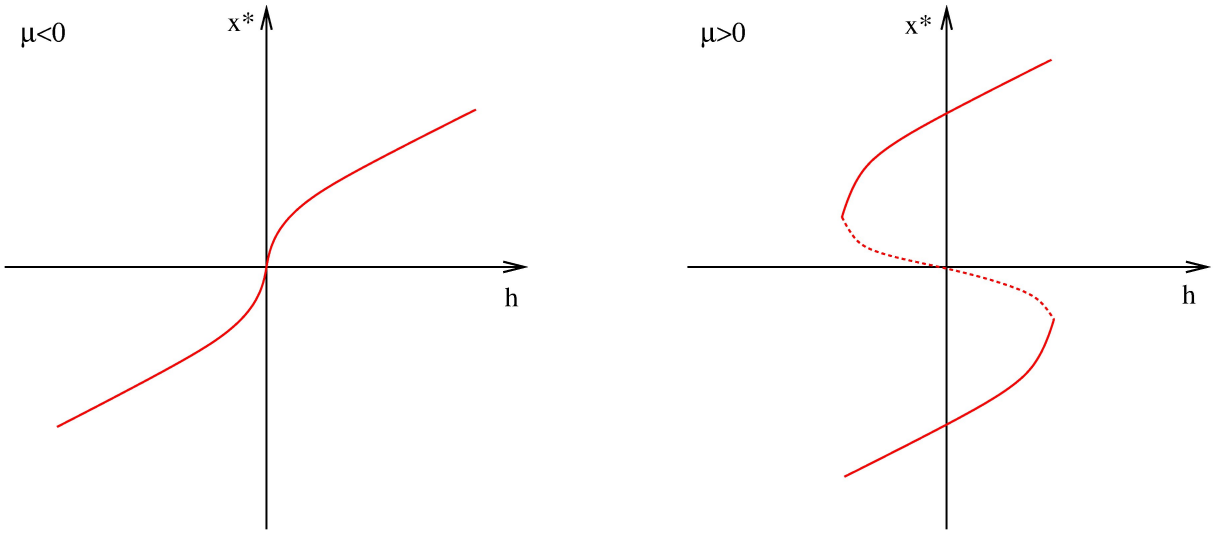

Figure 2.9: Bifurcation diagrams in function of the parameter h.

We see in figure 2.9 that a bifurcation occurs only in the case $\mu > 0$, more precisely the bifurcation diagram displays two saddle-node bifurcations which corresponds in figure 2.7 right to the tangency of the line $y = h$ with the curve $y = g(x)$.

We can also deduce the bifurcation diagram at fixed $h > 0$ and for varying μ (you can draw the case $h < 0$ by yourself as an exercise):

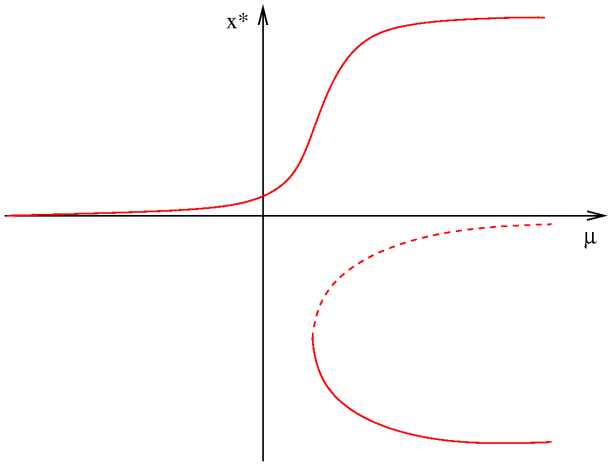

Figure 2.10: Bifurcation diagram of the imperfect pitchfork bifurcation when $h > 0$.

This bifurcation is called the **imperfect pitchfork bifurcation**.

Finally the full representation of the stationary solutions in function of the 2 parameters h and μ is the following one:

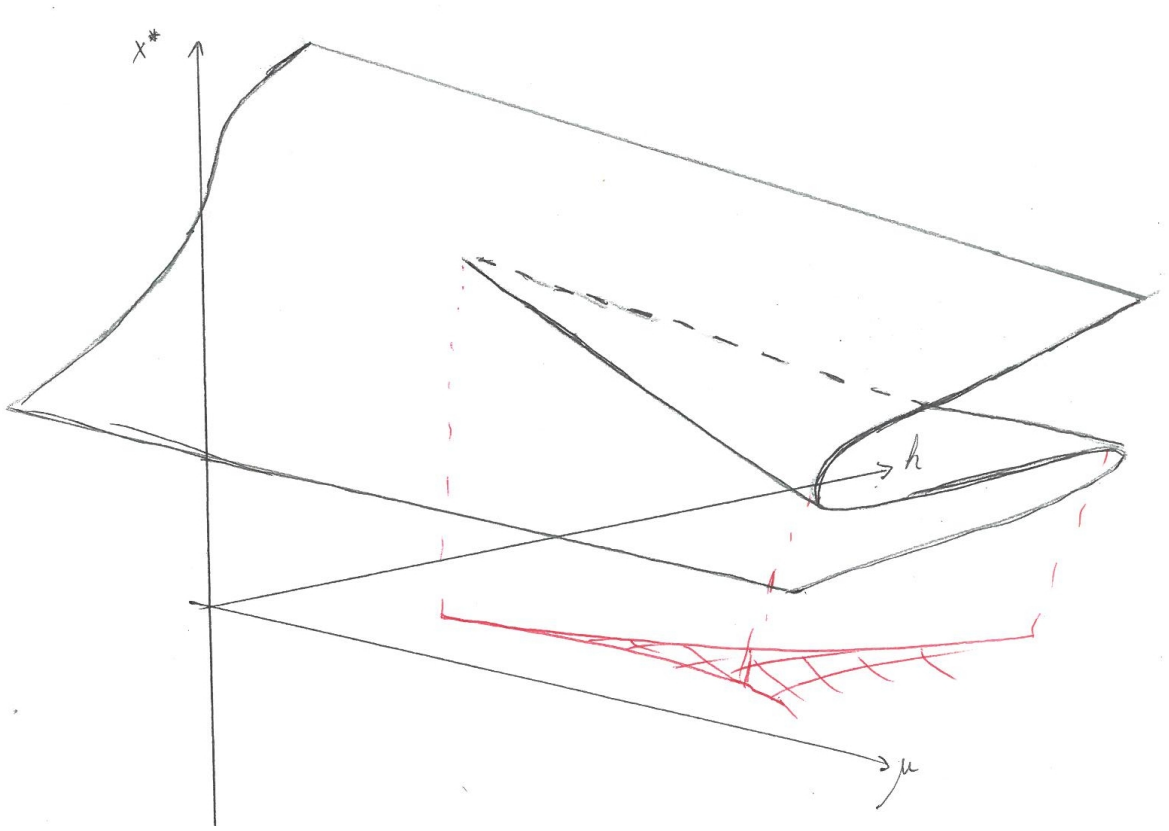

Figure 2.11: Cusp catastrophe.

This is an example of what is called a **catastrophe**. In this precise case it is called *cusp catastrophe*.

2.6 Examples

2.6.1 Start of a laser

Bibliography: Les lasers, D. Dangoisse, D. Hennequin, V. Zehnlé

2.6.1.a Model

A laser is a device emitting coherent light. It consists of a gain medium enclosed in a resonant cavity formed by mirrors. At least one of those mirrors is partially transparent, ensuring the output emission.

We will study one of the simpliest model for the gain medium: only two states for the atoms constituting this medium will be considered. The states will be called 1 and 2 and the associated energy will be called E_1 and $E_2 > E_1$. The lowest level E_1 is not the fundamental state. The relationship between the frequency ν of the light emitted by the

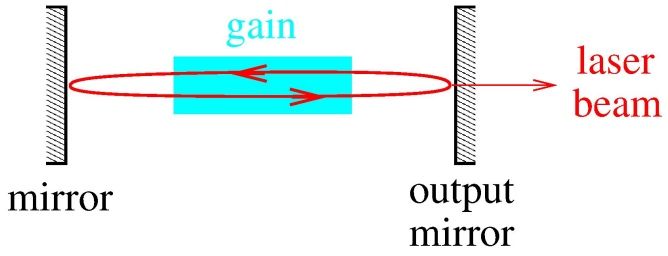

laser and the energy gap $E_2 - E_1$ is :

$$E_2 - E_1 = \hbar\omega = h\nu.$$

Let's defined the following variables :

- $N_1(t)$ is the number of atoms in the state 1 per unit volum at time t,
- $N_2(t)$ is the number of atoms in the state 2 per unit volum at time t,
- $\mathcal{I}(t)$ is the photons flux in the gain medium, i.e. the number of photons crossing a unit surface by unit time.

The mechanisms governing the light emission and absorption have been described by A. Einstein in 1916 :

- **absorption** :

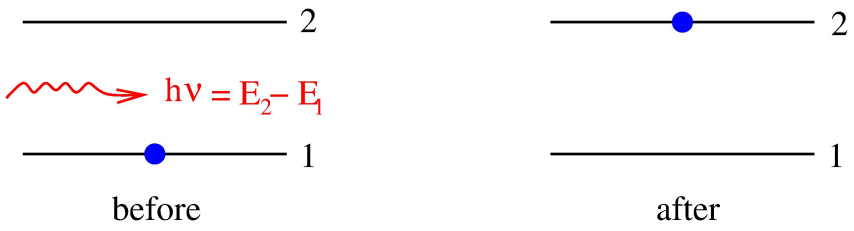

During this process, a photon of energy $h\nu$ is absorbed and an atom switches from state 1 to state 2. The number of atoms shifting from state 1 to state 2 is thus proportional to N_1 and $\mathcal{I}$. The proportionality coefficient has the dimension of a surface, it is called the *absorption cross section* and will be noted σ_a. Consequently, we have for the variation of the population of atoms in each states between times t and $t + \Delta t$:

$$\begin{aligned} (\Delta N_2)_{abs} &= \sigma_a \mathcal{I} N_1 \Delta t \\ (\Delta N_1)_{abs} &= -\sigma_a \mathcal{I} N_1 \Delta t \end{aligned}$$

To calculate the variation of the photons flux, we consider a cylinder in the gain medium along the direction propagation of the photons :

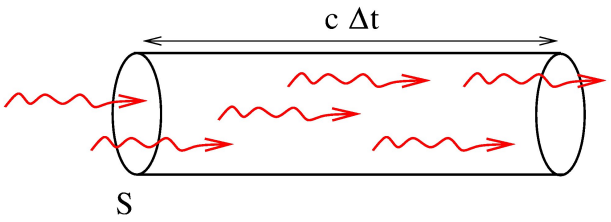

Per unit time, $\mathcal{I}(t)S$ photons enter in the volume $Sc\Delta t$ and $\mathcal{I}(t+\Delta t)S$ photons exit. Besides, $\sigma_a \mathcal{I} N_1$ photons are absorbed per unit time and unit volume, so:

$$\begin{aligned} \mathcal{I}(t+\Delta t)S - \mathcal{I}(t)S &= -(\sigma_a \mathcal{I} N_1)(c\Delta t S) \\ (\Delta \mathcal{I})_{abs} &= -\sigma_a \mathcal{I} N_1 c \Delta t \end{aligned}$$

- **Stimulated emission**: symetrically to the process of absorption, there is emission of photons stimulated by photons already present in the cavity:

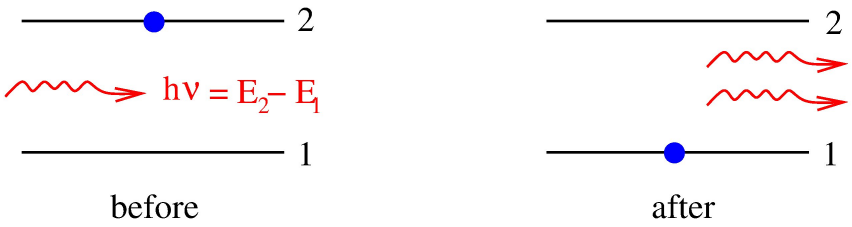

It is very important to note that this emission is not spontaneous : the photons that are generated when the atoms decay from state 2 to state 1 are clones of the photons already present in the gain medium. They share all the properties of the photon that have stimulated the emission, in particular its wave vector. We have for the variations of the quantities that describe our system:

$$\begin{aligned} (\Delta N_2)_{sti} &= -\sigma_{sti} \mathcal{I} N_2 \Delta t \\ (\Delta N_1)_{sti} &= \sigma_{sti} \mathcal{I} N_2 \Delta t \\ (\Delta \mathcal{I})_{sti} &= \sigma_{sti} \mathcal{I} N_2 c \Delta t \end{aligned}$$

In the case considered here, we have $\sigma_{sti} = \sigma_a = \sigma$.

- **Losses and decay**: Independantly of the presence of photons already in the cavity, atoms which are not in the fundamental state tend to decay spontaneously towards lower states by emitting photons which are not coherent with the ones constituting the photons flux and consequently do not contribute to $\mathcal{I}$. Atoms may also decay by other modes than the emission of photons: collisions, vibrations... For the sake

of simplicity, we will consider that the decay rate of the atom population does not depend of the state level:

$$\begin{aligned}(\Delta N_2)_d &= -\gamma N_2 \Delta t \\ (\Delta N_1)_d &= -\gamma N_1 \Delta t\end{aligned}$$

Two other effects have to be taken into account. First because of the partially transparent output mirror, a term of loss for the flux has to be included for the evolution of $\mathcal{I}$:

$$(\Delta \mathcal{I})_{loss} = -\kappa \mathcal{I} \Delta t.$$

Finally, a laser is an out-of-equilibrium system but we have until now not discussed the energy input in the system. Indeed, with only the terms described right now, the levels would decay until they are empty and the photons flux would decrease until the extinction of the light flux. In a laser, the energy injection consists in a feeding of the higher level, i.e. state 2, enforcing what is called a *population inversion*. The process is called the "pumping" of the laser and the pumping rate will be denoted λ.

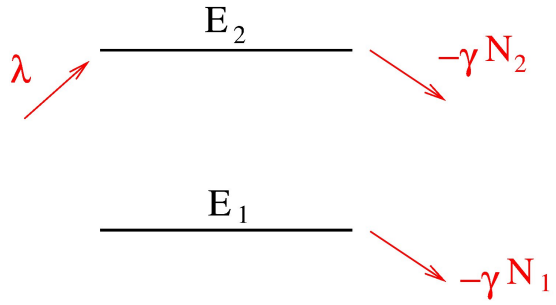

Putting everything together, we obtain a model describing the evolution of a laser:

$$\begin{aligned}\frac{dN_2}{dt} &= \sigma \mathcal{I} N_1 - \sigma \mathcal{I} N_2 - \gamma N_2 + \lambda \\ \frac{dN_1}{dt} &= -\sigma \mathcal{I} N_1 + \sigma \mathcal{I} N_2 - \gamma N_1 \\ \frac{d\mathcal{I}}{dt} &= -c\sigma \mathcal{I} N_1 + c\sigma \mathcal{I} N_2 - \kappa \mathcal{I}\end{aligned}$$

We can notice that the relevant variables for the description of the medium are not the individual values of the population of atoms but only the difference $\mathcal{D} = N_2 - N_1$ which is called the *population inversion*, and the system can be rewritten with only two variables :

$$\left\{\begin{array}{rcl}\dot{\mathcal{D}} &=& -2\sigma \mathcal{I} \mathcal{D} - \gamma \mathcal{D} + \lambda \\ \dot{\mathcal{I}} &=& c\sigma \mathcal{I} \mathcal{D} - \kappa \mathcal{I}\end{array}\right.$$

We can non-dimensionnalize the system using the following change of variables : $D = \frac{\sigma c}{\kappa}\mathcal{D}$, $I = \frac{2\sigma}{\gamma}\mathcal{I}$, $\tau = \gamma t$, and $A = \frac{\sigma c}{\kappa\gamma}\lambda$ and we obtain :

$$\begin{cases} \dot{D} &= -D(I+1)+A \\ \dot{I} &= kI(D-1) \end{cases}$$

where the time variable governing the derivatives is now τ and the control parameter is A, the pumping parameter. Indeed it corresponds to the parameter that can generally easily be tuned experimentally, for example by the variation of an electrical current which is used to excite the atoms to a higher state, or any other mean of pumping. The parameter k depends of the loss of the mirrors through κ and of the gain medium through γ, so that this parameter is constant for a given laser.

2.6.1.b Study of the dynamical system

We thus have to study the dynamical system of dimension 2:

$$\begin{cases} \dot{D} &= -D(I+1)+A \\ \dot{I} &= kI(D-1) \end{cases}$$

Fixed points

$$\begin{cases} A &= D(I+1) \\ 0 &= I(D-1) \end{cases}$$

There are two fixed points:

- $I = 0$ and $D = A$, the laser is not emitting any light.
- $D = 1$ and $I = A - 1$, the light flux increases with the pumping while the population inversion is saturated to a constant value.

Jacobian matrix

$$\mathcal{L} = \begin{pmatrix} -(I+1) & -D \\ kI & k(D-1) \end{pmatrix}$$

Stability of $(D = A, I = 0)$

$$\mathcal{L}|_{(A,0)} = \begin{pmatrix} -1 & -A \\ 0 & k(A-1) \end{pmatrix}$$

The trace is $T = k(A-1) - 1$ and the determinant $\Delta = -k(A-1)$.

- when $A < 1$, $\Delta > 0$ and $T < 0$, the fixed point is stable.
- when $A > 1$, $\Delta < 0$, the fixed point is a saddle point and is unstable.

Stability of $(D = 1, I = A - 1)$

$$\mathcal{L}|_{(1,A-1)} = \begin{pmatrix} -A & -1 \\ k(A-1) & 0 \end{pmatrix}$$

The trace $T = -A$ is always negative and the determinant is $\Delta = k(A-1)$.

- when $A < 1$, $\Delta < 0$ the fixed point is a saddle point and is unstable.
- when $A > 1$, $\Delta > 0$, the fixed point is stable.

Bifurcation From the study of the stability of the fixed points, we deduce that a bifurcation occurs for the value of the control parameter $A = 1$. There is an exchange of stability between two different fixed points so that it is a *transcritical bifurcation.*

Taking into account the fact that I and A are both positive, we can draw the bifurcation diagrams :

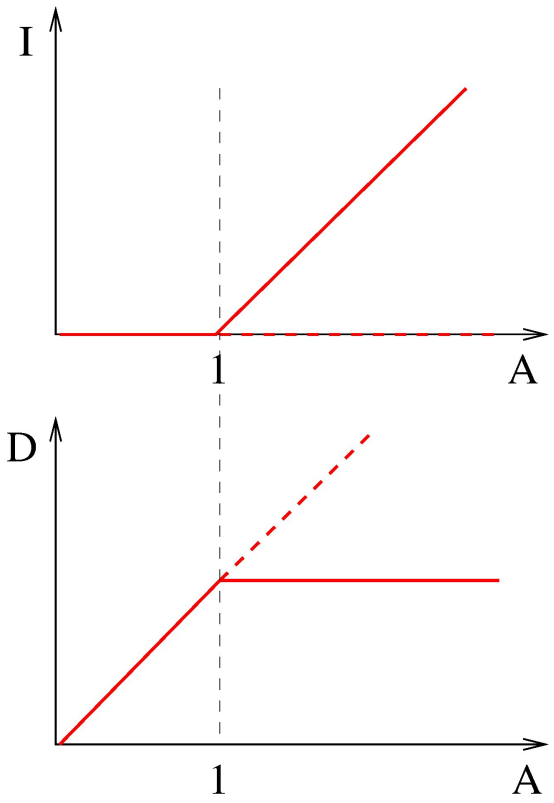

The diagrams show that there is a threshold for the start of a laser. The existence of such threshold is typical of a nonlinear system. When the laser is emitting, the population inversion saturates.

2.6.2 Oscillating chemical reactions

2.6.2.a Chemical kinetics

Bibliography: Instabilités, Chaos et Turbulence, P. Manneville.

Let's consider the elementary step of a chemical reaction :

$$\sum_{i=1}^{N} n_i A_i \rightarrow \sum_{i=1}^{N} n'_i A_i$$

where the A_i are the N chemical species implied in the reaction (either reactants or products), of concentration $[A_i]$, n_i (resp. n'_i) is the number of mole of A_i before (resp. after) the reaction and can be 0.

The reaction rate is proportional to the number of reactional collisions per unit of time. A reactional collision implies all the reactants at a same location. The probability to have one species A_i at a given location is proportional to its concentration. Consequently, the reaction rate is of the form $k \prod_{i=1}^{n} [A_i]^{n_i}$ with k the reaction rate constant (which depends on the temperature). When a collision happen, n'_i moles of A_i are producted and n_i moles consumed, leading to a variation $n'_i - n_i$ of the number of mole of the species A_i. Consequently, the dynamics of the reaction is given by the N equations :

$$\frac{d[A_i]}{dt} = (n'_i - n_i) k \prod_{i=1}^{n} [A_i]^{n_i}$$

If there are several steps to the reaction, the total variation of $[A_i]$ is given by the sum of the variations corresponding to each individual reaction step.

2.6.2.b Belousov-Zhabotinsky oscillating reaction

Bibliography: L'ordre dans le chaos, P. Bergé, Y. Pomeau, C. Vidal.

B. Belousov was a Russian chemist who discovered the existence of oscillating chemical reactions. Such reactions have been studied more deeply afterwards by A. Zhabotinsky in the 60s.

Reactants are[1] : sulfuric acid H_2SO_4, malonic acid $CH_2(COOH)_2$, sodium bromate $NaBrO_3$ and cerium sulfate $Ce_2(SO_4)_3$. Those reactants, in aqueous solution with certain concentrations, can lead to oscillations in the concentrations of some ions implied in the reaction. Those oscillations can be visualized using a colored redox indicator (e.g. ferroin).

If the reaction is done by simply mixing a given quantity of reactants in a closed container, the oscillations are transitory. To maintain the reaction, you have to supply continuously some reactants, to stir continuously the solution and to have an outlet for

[1] There are several variants of the reaction.

the overflow.

The dynamical variables of the system are the instantaneous values of the concentration of all the species in the reactor. But in that kind of experiment only a few variables are practically measurable. It can be (see *L'ordre dans le chaos*) :

- the electrical potential difference between two electrodes immersed in the solution. The relationship between the measured voltage and the concentration in Br^- (in the case of the reaction described previously) is given by the Nernst equation.

- the transmission of light through the tank at a given wavelength. The Beer-Lambert law is then used to describe the absorption of the light. For example, for $\lambda = 340$ nm, the absorption is mainly due to the Ce^{4+} ions.

Another concern is the parameters which can be tuned in such a system. It can be the temperature, which will change the constants of the reactions k_j, or the concentration of the species in input, or the flux rates of the pumps that provide the reactants which changes the time spent by the reactants in the tank.

Concerning the modeling of the experiment, the problem is that such reactions are very complicated and can imply a lot of elementary steps which are not known. In fact the complete reaction schematics of some of those reactions is still debated. Among the tips that help for the modeling of such complicated systems is the fact that the characteristic times of the steps of the reaction can be very different so that for example the faster ones can be considered to be instantaneous. Using that kind of approximation it is possible to consider simplier models with a reduce number of differential equations containing only the dynamics of interest for the phenomenon studied.

2.6.2.c The Bruxellator

Bibliography:

- *Nonlinear dynamics and chaos, S. Strogatz,*

- *Instabilités, Chaos et Turbulence, P. Manneville*

From a theoretical point of view, because of the complexity of real chemical reactions, an approach consists in the search of minimal models which will lead to an oscillating dynamics. The *"Bruxellator"* is such a kinetical model proposed by I. Prigogine and R. Lefever in 1968. They considered the global reaction

$$A + B \rightarrow C + D$$

constituted of four steps of elementary reactions and implying two free intermediates species X and Y. The sequence of elementary reactions considered is:

$$\begin{aligned} A &\rightarrow X \\ B+X &\rightarrow Y+C \\ 2X+Y &\rightarrow 3X \\ X &\rightarrow D \end{aligned}$$

The control parameters of the system are the concentration of species A and B and we suppose that those concentrations can be maintained at constant values by a continuous supply. All the reaction constant rates are supposed equal to 1. We note $[A] = A$.

The kinetics laws give us the following system of differential equations :

$$\begin{aligned} \frac{dX}{dt} &= (1-0)A + (0-1)BX + (3-2)X^2Y + (0-1)X \\ \frac{dY}{dt} &= (1-0)BX + (0-1)X^2Y \\ \frac{dC}{dt} &= (1-0)BX \\ \frac{dD}{dt} &= (1-0)X \end{aligned}$$

Note that C and D are directly given by X so that there are finally only two pertinent variables for the understanding of the dynamics of the system: X and Y. Consequently, we want to study the dynamical system:

$$\begin{aligned} \frac{dX}{dt} &= A - (B+1)X + X^2Y \\ \frac{dY}{dt} &= BX - X^2Y \end{aligned}$$

Fixed points. They are given by :

$$\begin{aligned} A &= [(B+1) - XY]\, X \\ BX &= X^2Y \end{aligned}$$

For $A > 0$, we have necessarily $X \neq 0$. We deduce that the only fixed point has for coordinates in the phase space :

$$X = A \text{ and } Y = \frac{B}{A}.$$

Jacobian matrix.

$$\mathcal{L} = \begin{pmatrix} -(B+1)+2XY & X^2 \\ B-2XY & -X^2 \end{pmatrix}$$

Stability of the fixed point.

$$\mathcal{L}|_{(A,\frac{B}{A})} = \begin{pmatrix} B-1 & A^2 \\ -B & -A^2 \end{pmatrix}$$

The determinant of the jacobian matrix is $\Delta = A^2 > 0$, and the trace is $T = B - 1 - A^2$. When $B < 1 + A^2$, the fixed point is stable, when $B > 1 + A^2$, it is unstable. At the bifurcation, the fixed point shifts from a stable spiral point to an unstable spiral point.

Consequently, if the concentration A is constant, for low concentration of B, the reaction will reach a stationary state: the concentration of C and D are constant after a transient. When increasing B, there is a destabilisation of this state through a Hopf bifurcation leading to a limit cycle. The concentrations in C and D then display oscillations.

Poincaré-Bendixson. We want to apply the Poincaré-Bendixson theorem for given values of A and B with $B > 1 + A^2$.

We search the nullclines, i.e. the two curves along which the vector field is parallel to one of the axis of the phase plane.

- The first curve is given by $A - (B+1)X + X^2Y = 0$, which leads to:

$$Y = f(X) = \frac{(B+1)X - A}{X^2}.$$

To study this function, we compute its derivative: $f'(x) = \frac{-(B+1)X^2+2A}{X^3}$, which changes of sign when $X = \frac{2A}{B+1}$:

X	0	$\frac{2A}{B+1}$	$+\infty$
f'	$+$	0	-
f	$\nearrow$		$\searrow$

- The second function is given by $BX - X^2Y = 0$, leading to:

$$Y = g(X) = \frac{B}{X}.$$

To draw the curves, we need to know the position of the fixed point (which is the intersection of the two nullclines) compared to the maximum of $f(X)$. When the fixed point is unstable:

$$\begin{aligned} B &> A^2+1 \\ B+1 &> 2 \\ 1 &> \frac{2}{B+1} \\ A &> \frac{2A}{B+1} \end{aligned}$$

The two curves can then be drawn:

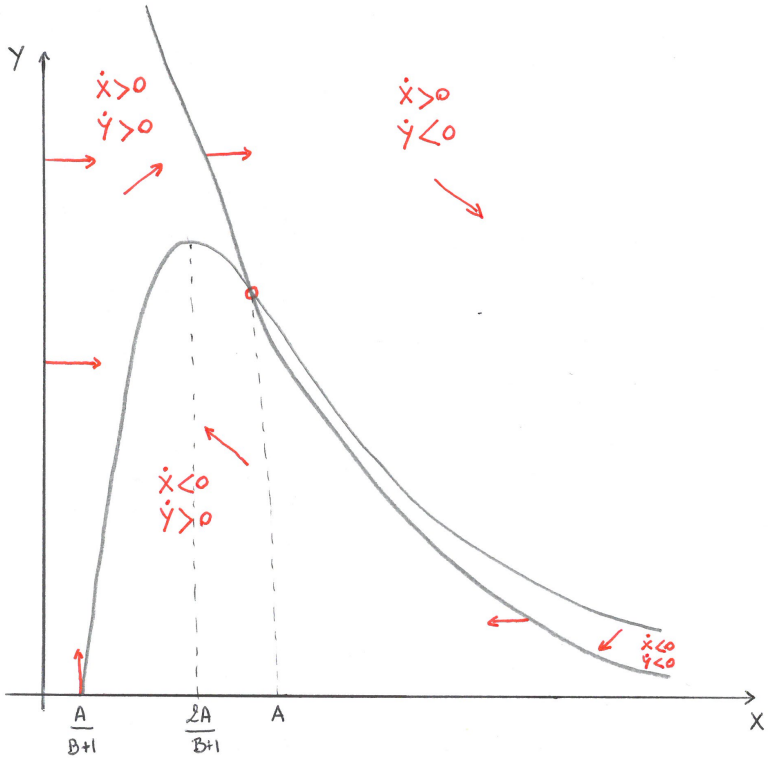

To find a domain on the frontier of which the vector field always points inside the domain, we need to find a line of negative slope smaller than the one of the vector field in the case $\dot{Y}<0$ and $\dot{X}>0$.

$$\begin{aligned} \frac{dY}{dX} &= \frac{BX-X^2Y}{A-(B+1)X+X^2Y} \\ &= -1+\frac{A-X}{A-(B+1)X+X^2Y} \end{aligned}$$

when $X>A$, we thus have $\frac{dY}{dX}<-1$ so that any line of negative slope strictly larger than -1 will do, here we used a $-1/2$ slope:

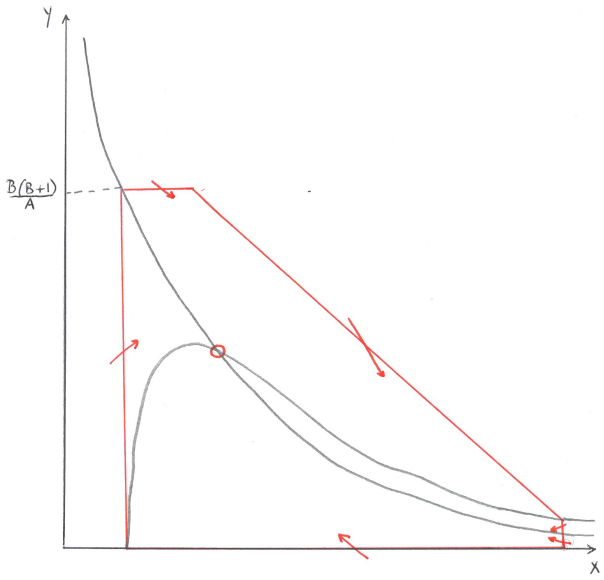

Integration with Matlab We can also for given values of the parameter draw the nullclines (f in cyan and g in green), the vetor field (in blue, rescaled) and an example of trajectory (in red, after a transient the trajectory settle on the limit cycle):

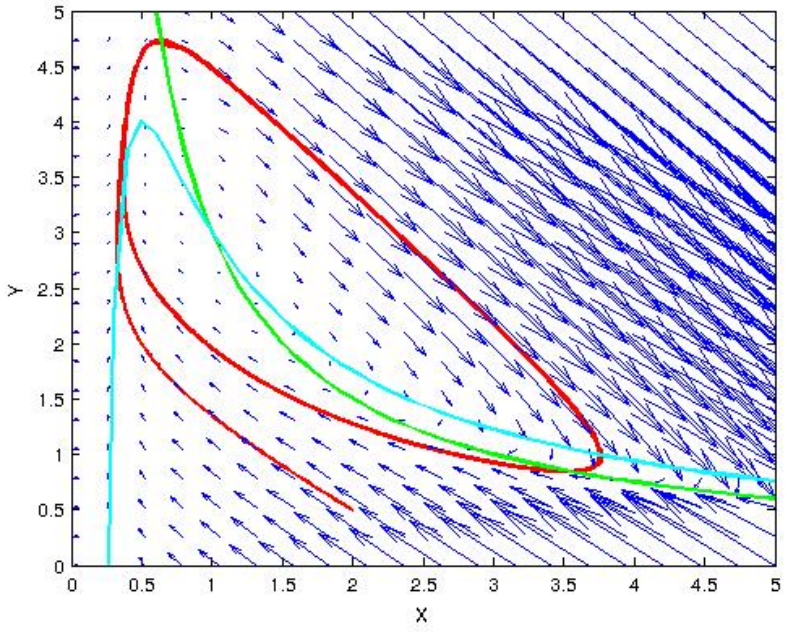

Figure 2.12: Integration of the system for $A = 1$ and $B = 3$ superimposed with the nullclines and the general directions of the vector field (the size of the vectors have been rescaled).

Conclusion

We have presented in this chapter several *bifurcations*, which correspond to the modification of the number and/or the nature of the attractors of a dynamical system.

We have illustrated some of those bifurcation by few examples coming from different field (start of a laser, chemical reactions).

Bibliography

- In English:
  - **Nonlinear dynamics and chaos**, S. Strogatz
- In French:
  - **L'ordre dans le chaos**, P. Bergé, Y. Pomeau, C. Vidal
  - **Cours DEA** de V. Croquette, `http://www.phys.ens.fr/cours/notes-de-cours/croquette/index.html`
  - **Dynamiques complexes et morphogénèse**, C. Misbah
  - **Les lasers**, D. Dangoisse, D. Hennequin, V. Zehnlé
  - **Instabilités, Chaos et Turbulence**, P. Manneville

Chapter 3

Strange attractors

We want now to study new kind of attractors that can only exist for dimension of the phase space at least of three. We will study two kind of attractors, first the torus and the associated quasi-periodic regime, and then strange attractors which are the attractors associated to chaotic signals.

The central subject of this chapter is the study and understanding of irregular (or aperiodic) temporal dynamics sustained on a long-term basis. From an experimental point of view, when we measure an irregular signal at the output of a system, it can have several origins. It can be a very noisy signal, so that the deterministic behavior we want to study is blurred by a stochastic signal. But we can also have signals for which noise is negligible but the dynamics itself lead to the observation of an irregular behavior, which is exactly the case of interest for us. We will discuss in this chapter how to distinguish those two kinds of aperiodic behaviors.

In the following we will first study the dynamics on a torus, which will lead us to the description of complicated behaviors coming from a dynamics on a high-dimensional torus in the phase space and to the Landau's theory of transition to the turbulence. In opposition to this vision of complexity coming from high dimensional dynamics, we will study in the second part of this chapter strange attractors, which can exhibit an irregular dynamics even with a small number of degrees of freedom (at least 3). In the last part we will study tools to characterize those attractors.

Most of this chapter is based on the book *L'ordre dans le chaos* of P. Bergé, Y. Pomeau and C. Vidal.

3.1 Beyond periodicity

3.1.1 Dynamics on a torus

If a system has a two-dimensional torus as an attractor in the phase space, its dynamics is characterized by two frequencies f_1 and f_2 which are linked to the typical rotation rates around the two axes of the torus.

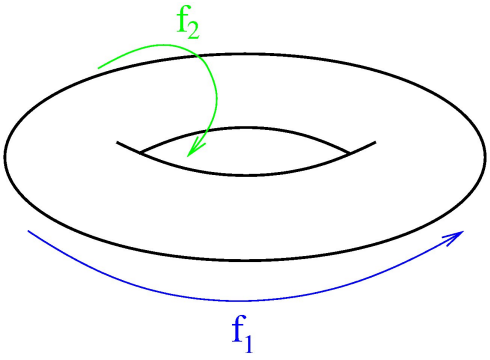

To visualize the trajectories, it is much easier to cut the torus in order to obtain a plane (the variables $\omega_i t = 2\pi f_i t$ have been chosen for the axes):

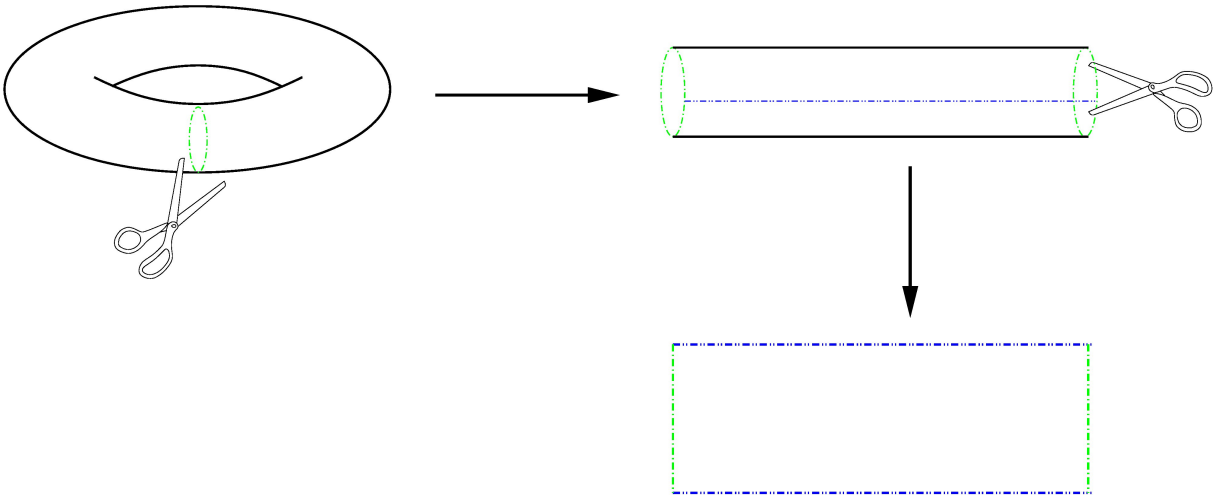

Then the trajectories have to be represented by taking into account periodic boundary conditions:

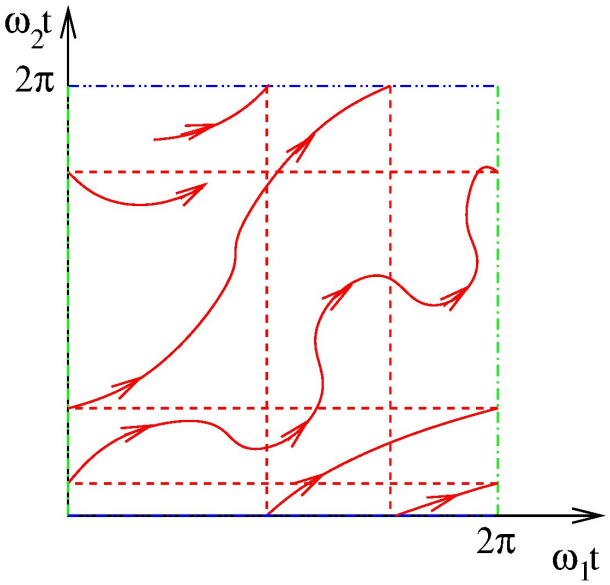

As the trajectories can not cross themselves and as they are confined on the surface of the torus, we see that the general direction of the trajectories is bounded. There are in fact two possibilities: either the trajectory closes on itself and it is in fact a periodic orbit, or it is not closed but in this last case it needs to have enough space to go round and round again without crossing itself. Consequently, the trajectory must have the same general form over and over again, so that we can put an inifnite number of them ones beside the others. In fact, from a topogical point of view, we see then that we can work with lines of constant slope to think about those trajectories, the slope being necessarily constant to avoid any crossing.

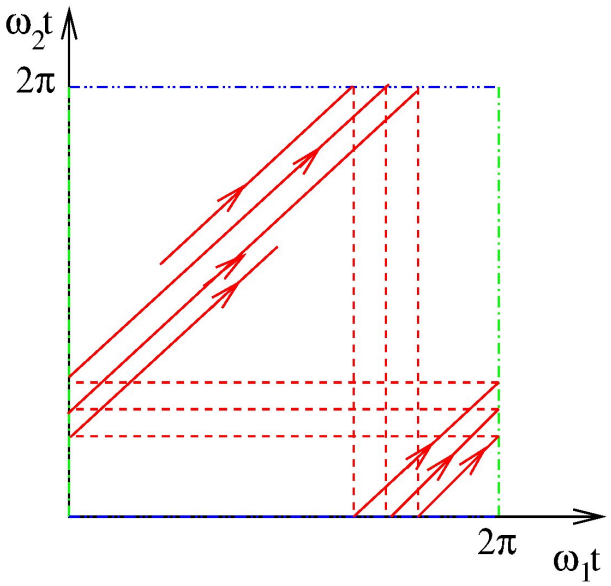

The slope of the lines is given by the ratio f_2/f_1. When this ratio is a rationnal p/q ($p, q \in \mathbb{N}$), the trajectory will necessarily close on itself after q revolutions along f_1 (and p along f_2). When the ratio f_2/f_1 is irrational (we say then that f_1 and f_2 are *incommensurable*), i.e. when it is not possible at all to write it as a ratio of two integers, then the trajectory will never close on itself and it will have enough space to go round and round all over the torus. We then say that the trajectory will cover the torus in a *dense* manner.

When the ratio f_2/f_1 is a **rational**, the period of the temporal signal is then $pT_1 = qT_2$. A Poincaré section of the trajectory will give a finite number of points.

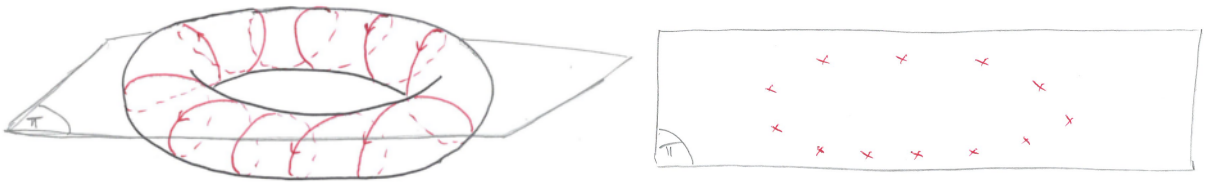

The number of points obtained depend on the orientation of the Poincaré plane Π compared to the torus. For example, if the plane is orthogonal to the f_1 axis of rotation

as on the figure above, we will obtain p points, while if Π is orthogonal to the f_2 plane of rotation, we will obtain q points. If we note r the finite number of points of intersection $P_1, P_2, \ldots, P_r$, the first return map T gives:

$$T(P_i) = P_{i+1} \text{ and } T^r(P_i) = P_i.$$

Figure 3.1 and 3.2 are examples of such behavior. They correspond to the following parametric equations:

$$\begin{aligned} X_1(t) &= 3\cos(\omega_1 t) + \cos(\omega_2 t)\cos(\omega_1 t) \\ X_2(t) &= 3\sin(\omega_1 t) + \cos(\omega_2 t)\sin(\omega_1 t) \\ X_3(t) &= \sin(\omega_2 t) \end{aligned} \tag{3.1}$$

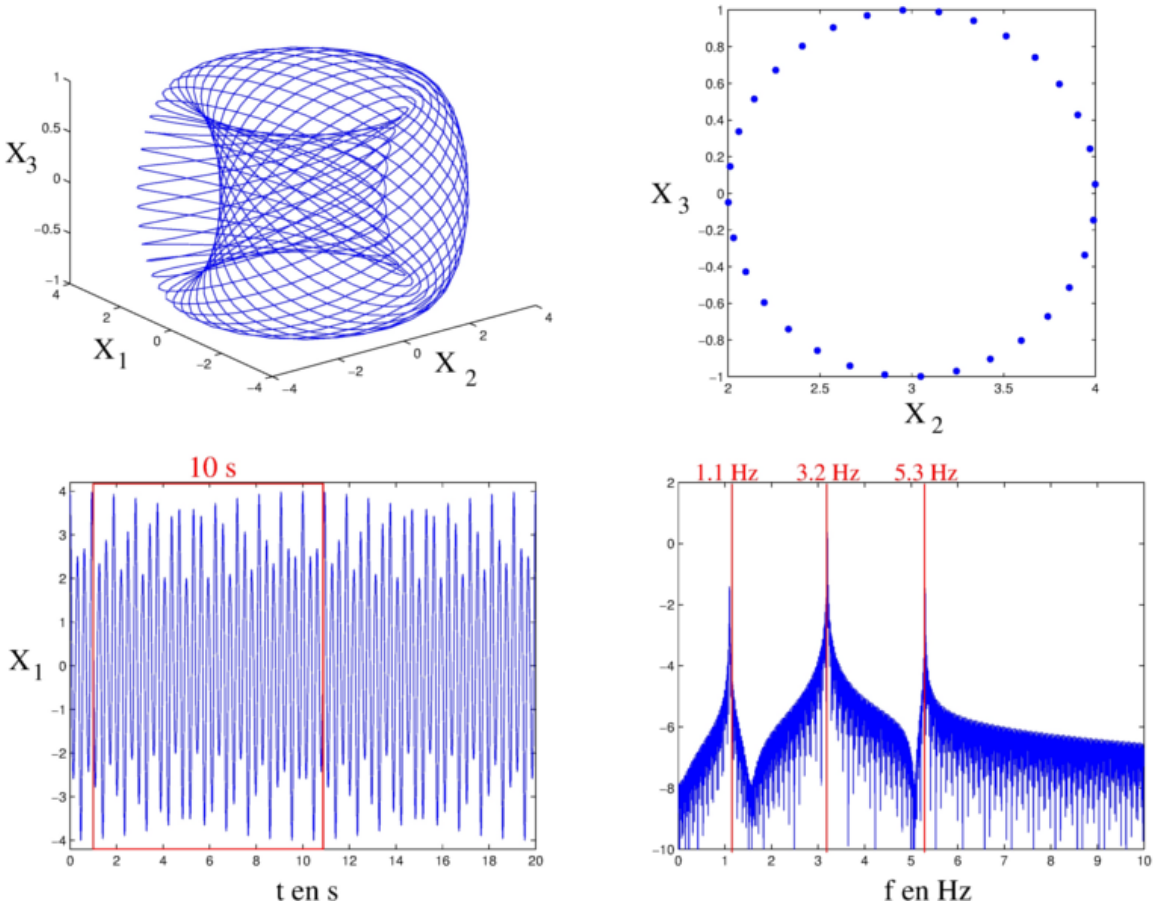

Figure 3.1: System (3.1) for $\omega_1 = 2\pi \times 3.2$ and $\omega_2 = 2\pi \times 2.1$. (a) Representation of the periodic orbit in the phase space. (b) Poincaré section using the plane $X_1 = 0$, consisting in 32 points. (c) Temporal dynamics of X_1. (d) FFT of the temporal signal $X_1(t)$ in a logarithmic scale.

On the other hand, when the ratio f_2/f_1 is **irrational**, the Poincaré section will give an infinite number of points which will form a closed curve.

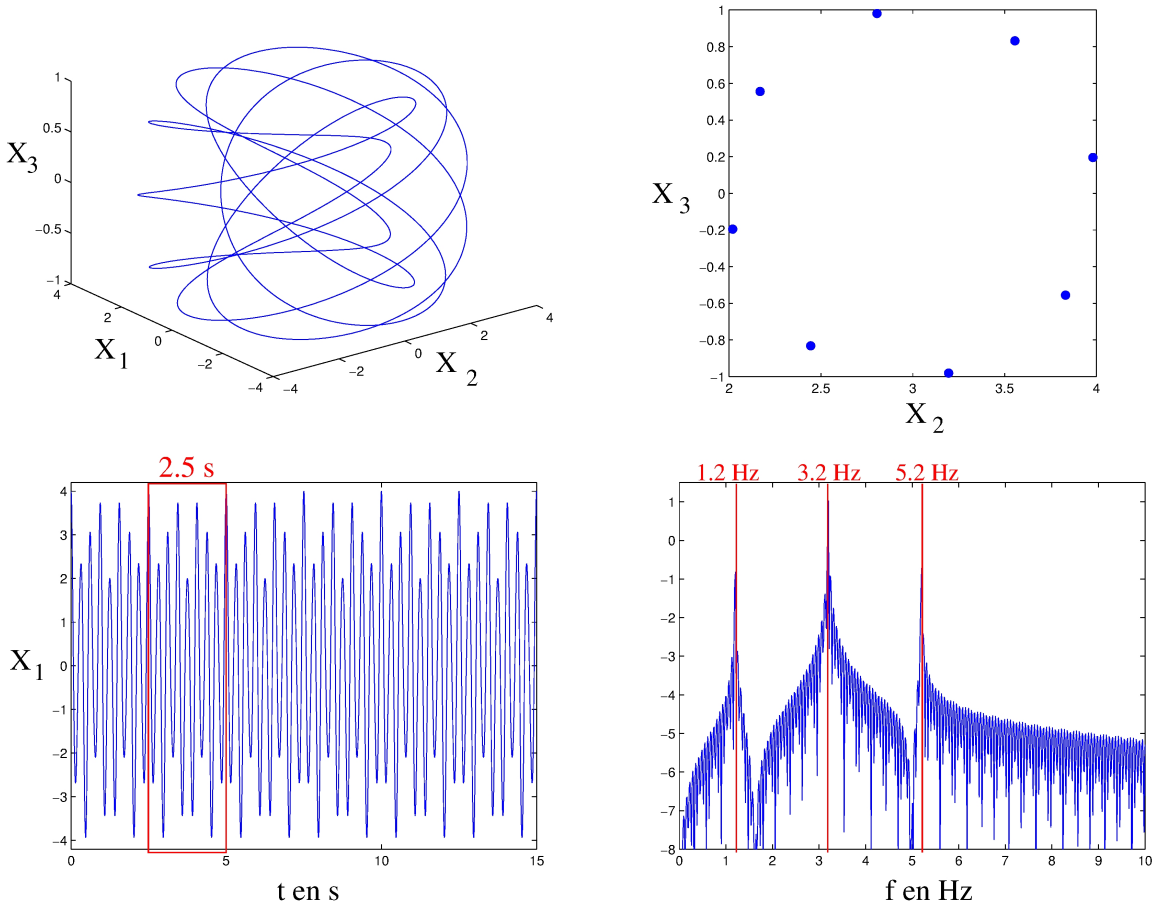

Figure 3.2: System (3.1) for $\omega_1 = 2\pi \times 3.2$ and $\omega_2 = 2\pi \times 2$. (a) Representation of the periodic orbit in the phase space. (b) Poincaré section using the plane $X_1 = 0$, forming a continuous curve. (c) Temporal dynamics of X_1. (d) FFT of the temporal signal $X_1(t)$ in a logarithmic scale.

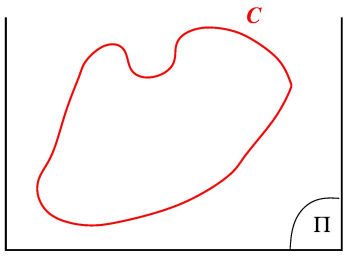

The first return map T verifies in this case $T(\mathcal{C}) = \mathcal{C}$, i.e. the curve $\mathcal{C}$ is invariant under the action of T.

The kind of temporal behavior observed in the case f_1 and f_2 incommensurable and corresponds to what is called **quasi-periodicity**.

Figure 3.3 shows such kind of response. The dynamics is not periodic, as can be seen by the infinite number of points in the Poincaré section, nevertheless the temporal signal is not chaotic either. Indeed, the spectral analysis of the temporal signal displays only three peaks, showing that the underlying dynamics is in fact quasi-periodic.

More generally, the spectrum of a quasi-periodic signal can be more complicated with harmonics corresponding to combinations $|a_1 f_1 + a_2 f_2|$ with $a_1, a_2 \in \mathbb{Z}$. Nevertheless the dynamics is "simple" because it is composed only of a countable number of peaks in the Fourier space.

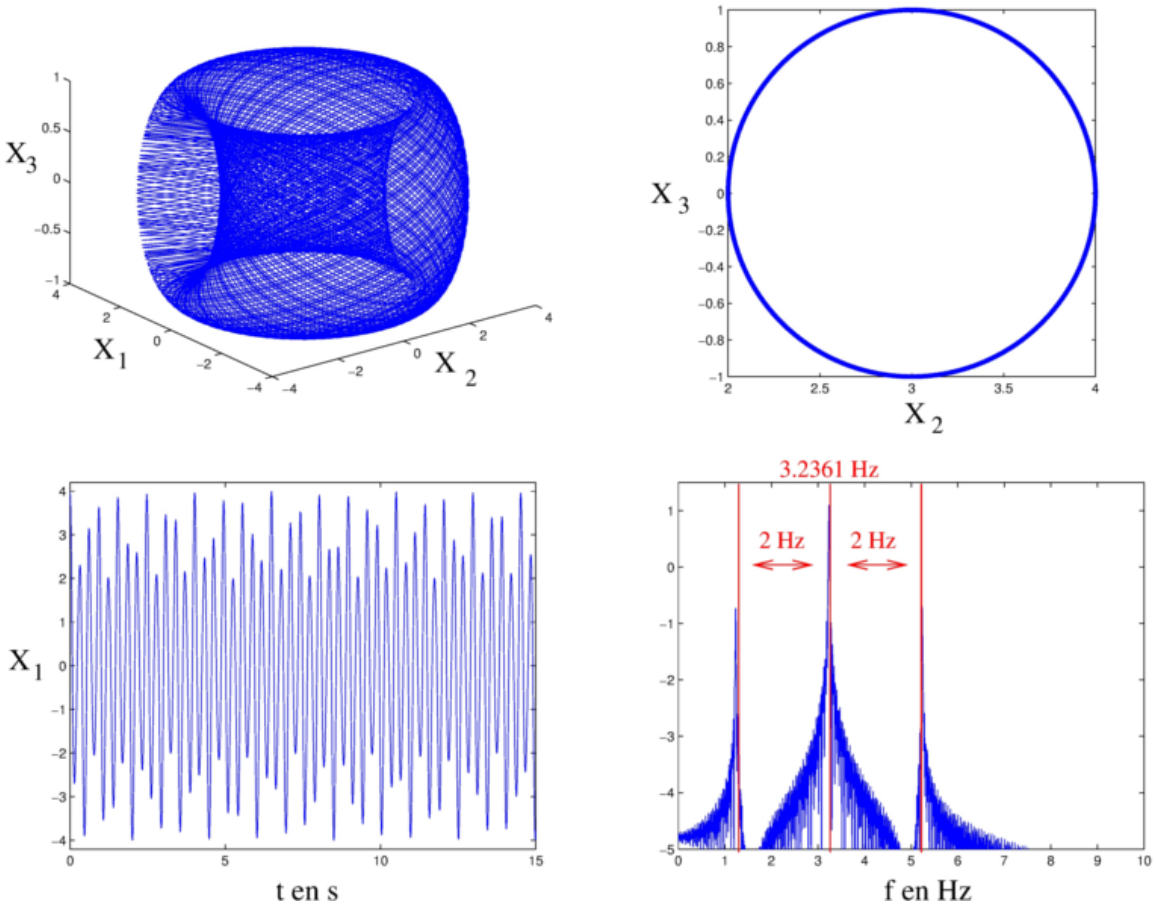

Figure 3.3: System (3.1) for $\omega_1 = 2\pi \times (1+\sqrt{5})$ and $\omega_2 = 2\pi \times 2$. (a) Representation of the periodic orbit in the phase space. (b) Poincaré section using the plane $X_1 = 0$, consisting in 8 points. (c) Temporal dynamics of X_1. (d) FFT of the temporal signal $X_1(t)$ in a logarithmic scale.

We have considered here only the biperiodic case, and a T^2 torus which exists in a phase space of dimension at least 3. Higher dimensional T^n tori exist implying n frequencies and living in spaces of dimension at least $n+1$. As each frequency is indepedent of all the others, dynamics on a very high dimensional torus implying a lot of harmonics will have a spectrum with so much peaks that it can be considered almost as continuous. The signal is then very close to a white noise.

3.1.2 First characterization of an aperiodic behavior

The previous discussion about quasi-periodicity shows the importance of the study of the spectrum of a signal for the identification of its dynamics.

An important feature of aperiodic signals is that we cannot deduce the future behavior of the system using the signal we have already recorded, however long that recording may

be. This loss of memory can be evidenced using the auto-correlation function:

$$C(\tau) = \langle X(t)X(t+\tau)\rangle_t = \frac{1}{t_2 - t_1}\int_{t_1}^{t_2} X(t)X(t+\tau)dt$$

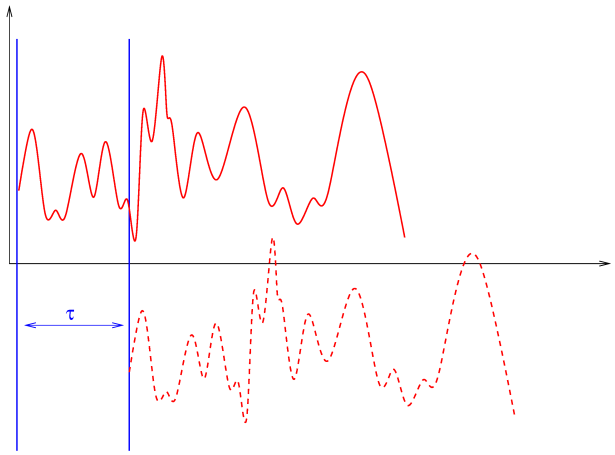

The function $C(\tau)$ gives an indication of the similarity of the signal at time t with the signal at time $t+\tau$. If $X(t)$ and $X(t+\tau)$ are totally decorrelated, $\langle X(t)X(t+\tau)\rangle_t = \langle X(t)\rangle_t\langle X(t+\tau)\rangle_t = \langle X\rangle_t^2$. If $X(t)$ and $X(t+\tau)$ are identical, $\langle X(t)X(t+\tau)\rangle_t = \langle X^2\rangle_t$. Consequently, the function $C(\tau)$ is bounded by those values.

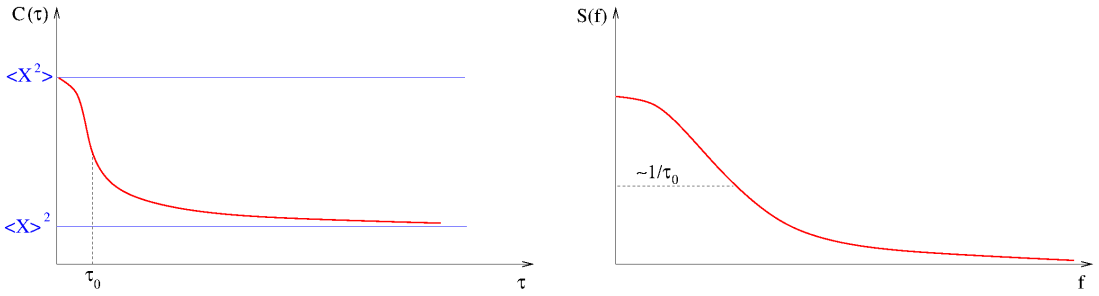

For a periodic signal, $C(\tau)$ periodically takes its maximal value. Conversely, for an aperiodic signal, the temporal autocorrelation function goes to a minimal value[1] for a large enough delay τ. Its shape is thus roughly the one shown on the left in the above figure. The Fourier transform of such a curve is shown on the right. The width of the continuous band in the Fourier space increases when the typical time of decay of the auto-correlation function $C(\tau)$ decreases. The Fourier transform of the function $C(\tau)$ is the power spectral density of X (Wiener-Khintchine theorem). Consequently, **an aperiodic signal displays a continuous part in its spectrum**.

A first characterization of an irregular signal is thus always the study of its power spectral density. When a continuous band exists in the spectrum, possibly superimposed

[1] 0 for a signal verifying $\langle X\rangle = 0$ or after normalization of the function C.

to several lines of definite frequency, it is a first indication that the signal may be chaotic. However, such a characterization is not enough to evidence chaos, as a large continuous band in the spectrum can be linked to the measurement of a very noisy signal or of a quasi-periodic signal containing a lot of harmonics of several incommensurable frequencies measured with a spectrum analyzer of limited resolution.

3.1.3 Landau's theory of turbulence

Between the 40's and the 70's, the accepted theory for the description of how chaos appears in a system was in fact a vision based on quasi-periodicity and was developed by L. Landau and E. Hopf. They proposed an interpretation of the transition from a laminar regime in a fluid to a turbulent one when the Reynolds number increases, as a succession of Hopf bifurcations.

If the dynamical variable we consider is the velocity of the fluid in a point (typically where a captor is placed), a laminar regime is a stationnary state. When the Reynolds number (Re) increases, the stationnary state becomes unstable and a first Hopf bifurcation takes place. Increasing further the Reynolds number, the observed regime becomes more and more complicated. In the Landau theory, this phenomenon is due to a succession of Hopf bifurcations which take place successively when the Reynolds number is increased giving rise to new frequencies. Each of those successive bifurcations leads to an enrichment of the spectral density of the signal by the emergence of the new frequencies, of their harmonics and of the numerous combination of all those frequencies. After several successive Hopf bifurcations, with a spectrum analyzer of finite resolution, the spectrum observed in such a scenario is a continuous one.

The trajectory of such a system lives on a high-dimensional torus in a higher-dimensional phase space. Such a theory is thus based on the idea that for a signal to be chaotic, it needs to have a very large number of degrees of freedom and that the observed complexity reflects this high dimensionality. The change of point of view that occured at the end of the 70's with the chaos theory is that you do not need a high dimensional phase space to have complexity: chaos may arise in a three-dimensional space, and a nonlinear deterministic system with only three degrees of liberty can give birth to aperiodic signals.

Nevertheless, the breakthrough of the chaos theory does not give an understanding of the turbulence transition. And while in the beginning of this paragraph I left some confusion between what is called "chaos" and what is called "turbulence", I want now to distinguish what is generally designated by those two words. In most of the works concerning dynamical systems, *chaos* designates aperdiodic deterministic behavior of *finite-number* of degrees of freedom systems, while *turbulence* implies spatially-extended systems, i.e. systems possessing an infinite numbers of dimensions and which need partial differential equations for the description of dynamics. As you will see in the following, most of the tools presented in this chapter for the study of chaos and strange attractors can only be used for systems of low dimensions. Dynamics in phase space of high dimension is more accuratly studied using tools coming from statistics.

3.2 Strange attractors

3.2.1 General properties

In 1971, D. Ruelle and F. Takens published an article called *"On the Nature of Turbulence"* and introduced a new kind of attractors of topological nature different from a torus: the *strange attractors*. The essential characteristics of those attractors is the sensitivity to initial conditions: two trajectories, however close to each other initially, will diverge one from the other after some time, the distance between the trajectories growing exponentially with time.

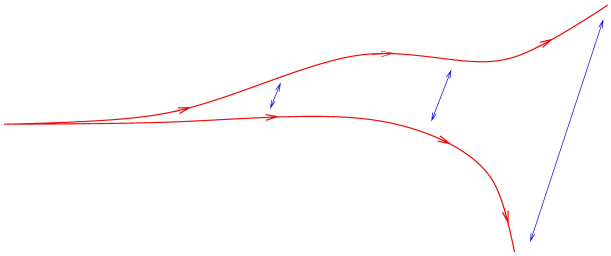

Such a behavior is not possible on a torus: we saw in the first section of this chapter that the topology of the torus combined with the impossibility for the different trajectories to cross each others leads either to closed orbits or to trajectories parallel one to the others.

Consequently, *strange attractors* need to possess something in their topology that allow divergence of the trajectories, a feature which is called *"stretching"*. But as they are *attractors*, their topology also need to ensure that all the trajectories stay in a bounded part of the phase space, and thus have to be re-injected back in the same sub-space. Some *"folding"* is thus also needed in the structure of the attractor.

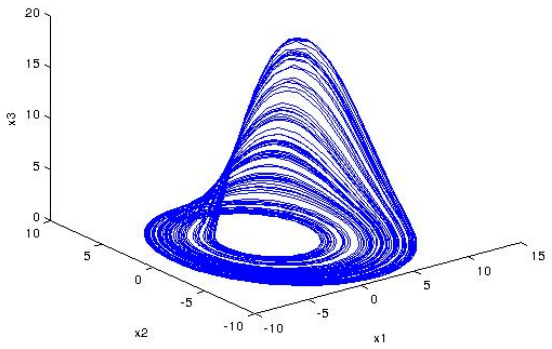

Figure 3.4: Rössler attractor (cf. Matlab session).

What is called *"stretching"* and *"folding"* can be observed on the Rössler attractor shown in Figure 3.4. It is a three-dimensional system we will study during the practicals

in the computer lab. We observe that a part of the trajectory is in the (X_1, X_2) plane but it needs to go out of the plane for some divergence between the trajectories to take place. The trajectory is then re-injected on the plane to stay on the attractor.

Because of the successive stretching and folding underlying its structure and as a trajectory on the attractor never intersect itself, a strange attractor has a foliated structure. The dimension of such a structure cannot be an integer. We say that the attractor is a *fractal* object. Such feature ensures that objects of dimension larger than 2 have a null volume in the phase space.

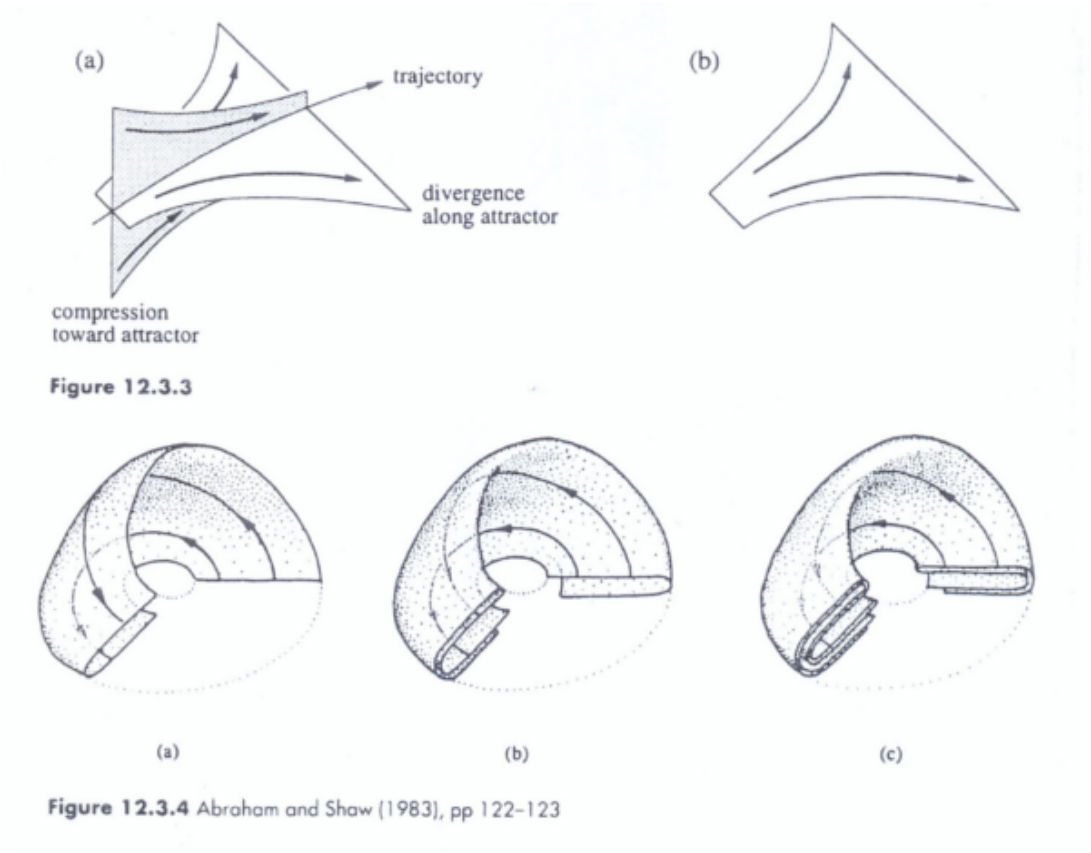

Figure 3.5: From *L'ordre dans le chaos*. Principle of the successive stretching and folding underlying the structure of the Rössler attractor.

3.2.2 A theoretical illustrative example: the Smale attractor

To understand practically the mechanisms of stretching and folding, we will study in this part a model illustrative of those mechanisms. The Smale attractor is a theoretical model of a discrete chaotic dynamics. It consists of the iteration of a map on the plane. The attractor is obtained through the iteration of a procedure described hereafter.

Stretching. A rectangle is stretched of a factor 2 along one axis and compressed of a

factor $1/(2\eta)$ in the other direction. For $\eta > 1$, the area of the rectangle decreases, which introduces some dissipation in the model (area contraction).

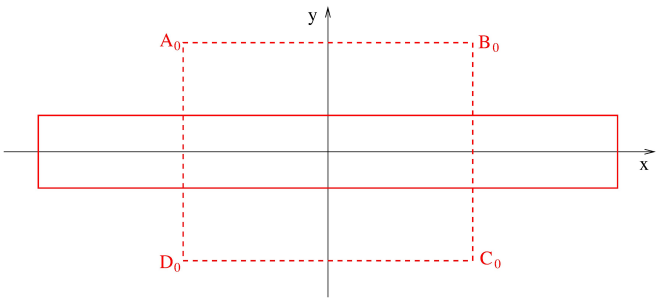

Folding. If we keep only the stretching transformation: $\begin{pmatrix} x \\ y \end{pmatrix} \to \begin{pmatrix} 2 & 0 \\ 0 & 1/2\eta \end{pmatrix} \begin{pmatrix} x \\ y \end{pmatrix}$, the size of the rectangle along the x direction will grow indefinitely. A folding of the rectangle ensures that the new set of points remains in the initial domain:

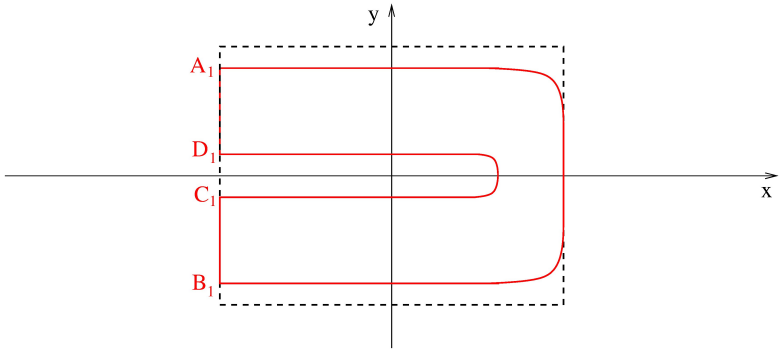

Iteration. The whole process is then iterated.

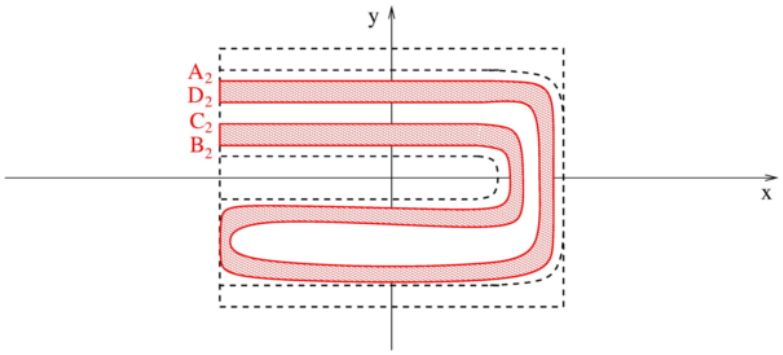

Finally, the attractor is the set obtained in the limit of an infinite number of iteration of the process. The set obtained in this limit has a complex foliated structure: a *fractal* structure. Its dimension is smaller than 2 but still larger than 1. This limit set is an attractor and exhibits sensitivity to initial conditions. Indeed if we consider two adjacents

points in the initial rectangle $A_0B_0C_0D_0$, because of the infinite number of successive stretching, their distance will increase exponentially along the x direction.

Note that we said that strange attractors only exists in phase space of dimension larger or equal to three and we have just presented an example in dimension 2, which seems to be contradictory. But the affirmation that chaos arises only from dimension 3 concerns only continuous time dynamical systems. For iterative maps, we will see that chaos may arise even for one-dimensional map.

3.2.3 Experimental point of view: the delay embedding method

Experimentally, one has access only to a very limited number of measurable variables. Typically, only one variable $X(t)$ is recorded during time.

Consequently, the usual situation is to have a long aperiodic serie of data $X(t)$ and a problem is to deduce a prospective strange attractor from those data. In certain conditions, which correspond to dynamics with a low number of degrees of freedom, each variable entails the main characteristics of the dynamics. It is then possible to reconstruct an attractor of the same topology of the underlying one governing the dynamics using a representation in a space of arbitrary dimension n using the following coordinates:

$$\{X(t), X(t+\tau), X(t+2\tau), \ldots, X\left(t+(n-1)\tau\right)\},$$

where τ is a chosen delay. This method corresponds more or less to a numerical calculation of the successive derivatives of the time series $X(t)$.

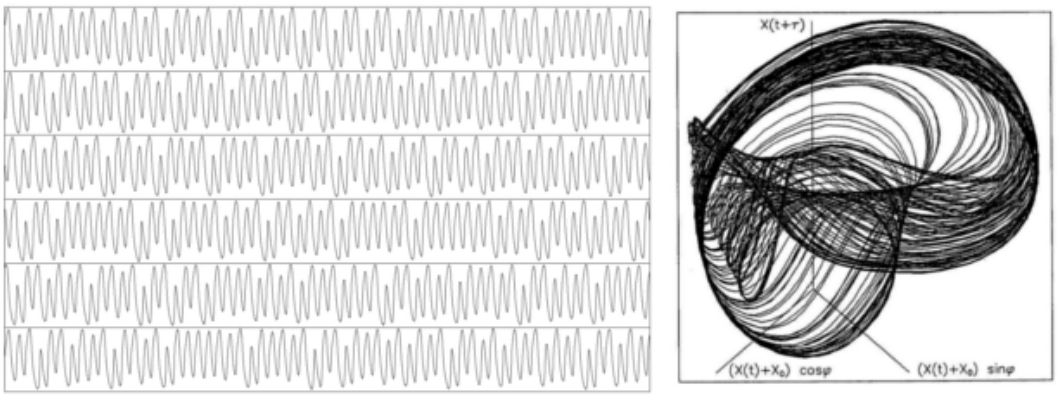

Left: Chaotic time series $X(t)$ delivered by a CO_2 laser with modulated losses ; Right: reconstruction of the underlying strange attractor in a phase space with cylindrical coordinates $\{X(t), X(t+\tau), \phi\}$ where τ is a suitably chosen time delay and ϕ is the modulation phase.

Figure 3.6: Example of the application of the delay embedding method on an experimental signal from *Topological analysis of chaotic signals from a CO2 laser with modulated losses*, M. Lefranc and P. Glorieux, Int. J. Bifurcation Chaos Appl. Sci. Eng. **3** 643-649 (1993).

The *embedding dimension* n is chosen as the smallest dimension for which there are no crossing of the trajectories in the phase space, i.e. the smallest dimension for which

the attractor is unfolded. The choice of τ has to be done mainly by trials. It has to be of the order of a fraction of the typical time the trajectory spent to go around the attractor. The attractors obtained for different values of τ are different but have the same topology.

3.3 Strange attractors characterization

In this last part we will present some tools that can be used to characterize the structure of strange attractors.

3.3.1 First return map

To visualize the structure of an attractor, Poincaré sections can be done. In the example shown in Figure 3.7 the successive sections evidenced the stretching and folding process that takes place along the attractor. As you can easily imagine those kind of representations are only useful when the embedding dimension of the attractor is of dimension 3 and the Poincaré section of dimension 2.

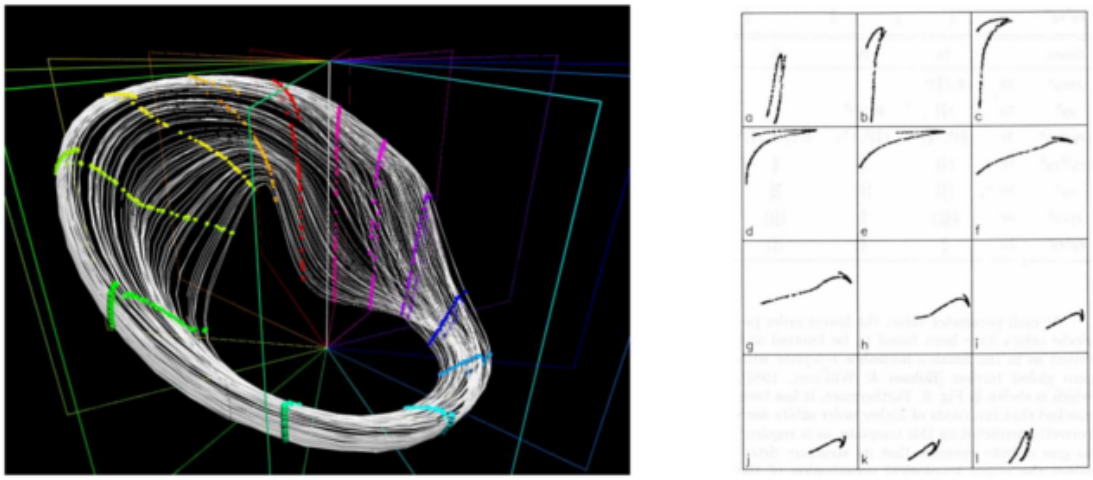

Left: Intersections of a chaotic attractor with a series of section planes are computed. Right: Their evolution from plane to plane shows the interplay of the stretching and squeezing mechanisms.

Figure 3.7: Example of successive Poincaré section of an attractor obtained from experimental time series of the intensity of a CO2 laser with modulated losses (from M. Lefranc, *The topology of deterministic chaos: Stretching, squeezing and linking*, NATO Security Through Science Series D – Information and Communication Security, **7**, 71 (2007)).

When the system is dissipative enough and the section is made in a region of the phase space where the contraction is high, a part of the attractor is approximatively a surface and the section obtained in this region is almost unidimensional. The Poincaré map is then an unidimensional map. The study of this map can give information on the dynamics of the system.

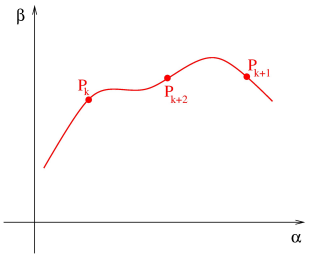

The first return map, which links P_{k+1} to P_k, has in general $(n-1)$ dimensions and in the case considered in this part only 2 dimensions:

$$\begin{pmatrix} \alpha_{k+1} \\ \beta_{k+1} \end{pmatrix} = T \begin{pmatrix} \alpha_k \\ \beta_k \end{pmatrix}$$

But as the curve is unidimensional, a single coordinate (α or β or a curvilign coordinate) is suficient to describe the one-dimensional map dynamics. This means that generally we will keep only the α or the β coordinate or a combination of the two and we will finally end up with a one-dimensional map.

A very common experimental method to obtain a one-dimensional first return map is in fact to collect the successive values of the local maxima and to plot each value as a function of the previous one.

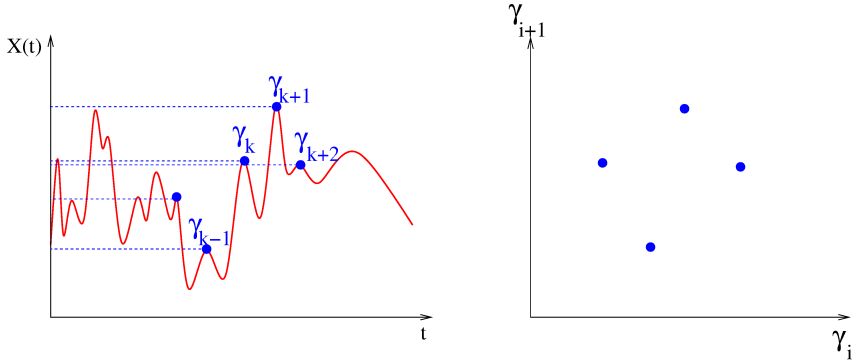

Using this method we can for example obtain the first-return map corresponding to the Lorenz attractor (see Matlab session):

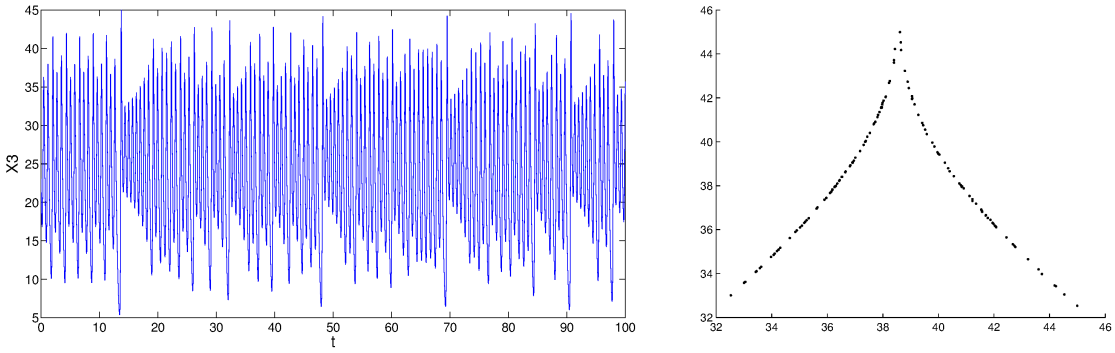

Figure 3.8: Left: temporal trace of one of the coordinates of the Lorenz model. Right: first-return map obtained from the temporal trace by plotting each local maxima as a function of the previous one.

When such an unidimensional map can be obtained, a lot of information qualitative or even quantitative can be deduced from it. The first thing being that the obtention of a well defined curve for the first return map allows to assert that the dynamics is indeed

deterministic. As a matter of fact, the knowledge of a point in the section allows to deduce the whole sequence of its iteratives and thus the future of the system.

Practically, this method is limited to low dimensional dynamics with a high level of contraction. Surprisingly, a wealth of experimental systems can be analyzed using this tool. This is linked to the fact that several well-known "roads" towards chaos can be described using one-dimensional maps. We will come back on the subject in the next chapter.

3.3.2 Lyapounov exponents

3.3.2.a Introduction

As the main characteristic of a strange attractor is its sensitivity to initial conditions, a quantification of this feature is essential. This divergence between trajectories is quantified using the *Lyapounov exponents*.

Consider $\vec{X}(t)$, a trajectory on the attractor. Practically to obtain such a trajectory numerically, we integrate during a time long enough the system with an arbitrary initial condition until we can consider the transients have vanished. Then we use the end point of this integration as an initial condition $\vec{X}(0)$ for a new trajectory $\vec{X}(t)$ (see practicals in computer lab). Consider $\vec{X}'(t)$ a trajectory stemming from a point $\vec{X}'(0)$ very close to $\vec{X}(0)$. We note $\delta(t) = \|\vec{X}'(t) - \vec{X}(t)\|$ the distance between the two trajectories at time t. We study the evolution of this difference with time.

When there is sensitivity to initial conditions, there is an exponential divergence between the two trajectories. This means that the plot of $\ln \delta(t)$ as a function of time presents a linear part with a positive slope.

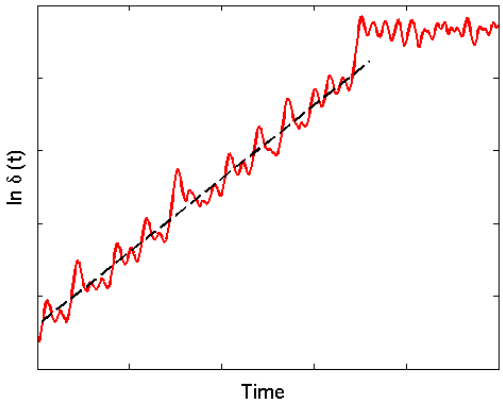

The slope of that line, λ, is what is usually called the Lyapounov exponent. It characterizes the divergence of the trajectories as it means that $\delta(t) \sim \delta_0 e^{\lambda t}$. The saturation of the curve at long time is due to the fact that δ has reached the size of the attractor and cannot become larger. The exponent has the dimension of the inverse of a time: it is a growing rate.

A positive Lyapounov exponent is the unambiguous signature of a chaotic regime.

To be rigorous, the rough point of view presented here has to be refined: there are in fact several Lapounov exponents: the same number as the dimension of the phase space. But at long time, the behavior of $\delta(t)$ will be dominated by the largest exponent, which is usually called "the" Lyapounov exponent. Another approximation in the previous rough representation is that the value of λ depends on the trajectory considered and of the position along the attractor. Consequently, a good estimation of the Lyapounov

exponent requires to repeat the previous procedure on several trajectories and to perform an average of the slopes obtained.

3.3.2.b Mathematical point of view

The mathematical formulation of the calculation of all the Lyapounov exponents is the following. Consider the following dynamical system: $\frac{d\vec{X}}{dt} = \vec{F}(\vec{X})$.

We will consider a linearization of the equations **all along a trajectory**: $\vec{X}(t)$ is a trajectory on the attractor and $\vec{X}'(t) = \vec{X}(t) + \delta\vec{X}(t)$

$$\begin{aligned} \frac{d\vec{X}'}{dt} &= \vec{F}(\vec{X} + \delta\vec{X}) \\ \frac{d\vec{X}}{dt} + \frac{d\delta\vec{X}}{dt} &\simeq F(\vec{X}) + \mathcal{L}|_{\vec{X}(t)} .\delta\vec{X}(t) \end{aligned}$$

Consequently,

$$\frac{d\delta\vec{X}}{dt} \simeq \mathcal{L}|_{\vec{X}(t)} .\delta\vec{X}(t),$$

where you have to note that the coefficients of $\mathcal{L}|_{\vec{X}(t)}$ depend on time. This study differs consequently from the one we did for the fixed points. In spite of this dependence of the jacobian matrix on time, an integration is still possible, at least numerically, leading to the obtention of a matrix $\mathfrak{L}(t)$ such as $\delta\vec{X}(t) = \mathfrak{L}(t)\delta\vec{X}(0)$. The eigenvalues of $\mathfrak{L}(t)$ give the evolution with time of the difference between the trajectories.

Let's reasoning in the case when the jacobian matrix $\mathcal{L}|_{\vec{X}(t)}$ is independent of time[2] and of eigenvalues $\lambda_1, \lambda_2, \ldots, \lambda_n$ constants. Then $\mathfrak{L}(t)$ has for eignevalues $e^{\lambda_1 t}, e^{\lambda_2 t}, \ldots, e^{\lambda_n t}$. Then:

$$Tr\left(\mathfrak{L}^+(t)\mathfrak{L}(t)\right) = e^{(\lambda_1+\lambda_1^*)t} + e^{(\lambda_2+\lambda_2^*)t} + \cdots + e^{(\lambda_n+\lambda_n^*)t}$$

For time t large enough, the exponential with the largest real value dominates over all the other exponentials, so that:

$$\lambda_{\vec{X}} = \lim_{t\to\infty}\left[\frac{1}{2t}\ln\left(Tr\left(\mathfrak{L}^+(t)\mathfrak{L}(t)\right)\right)\right] \tag{3.2}$$

This formula is valid even when the coefficients of $\mathcal{L}|_{\vec{X}(t)}$ depend on time, and it gives the (largest) Lyapounov exponent linked to the trajectory $\vec{X}(t)$. You still need to average over several trajectories to have a good estimate of the Lyapounov exponent.

3.3.2.c Experimental point of view

An experimental estimation of the Lyapounov exponent is not easy to obtain. A possible method is based on the first return map: In the case when you are able to reduce the

[2]It is a massive simplification but it allows to obtain a mathematical expression which is in fact valid in the general case.

dynamics to a first return map (not necessarily an unidimensional one) T, an analytical fit of this application can be obtained numerically.

Taking a point Y_1 in the Poincaré section, the orbit of the point can be calculated using the map: $Y_2 = T(Y_1), \ldots, Y_p = T(Y_{p-1})$. If now we consider another point of the section very close to Y_1: $Y_1' = Y_1 + \delta Y_1$, we have:

$$\begin{aligned} \delta Y_2 &= L_{Y_1} \delta Y_1 \\ \delta Y_3 &= L_{Y_2} \delta Y_2 = L_{Y_2} L_{Y_1} \delta Y_1 \\ &\vdots \quad\quad \vdots \\ \delta Y_p &= L_{Y_p} \ldots L_{Y_2} L_{Y_1} \delta Y_1 \end{aligned}$$

In the previous expressions, the matrices L_{Y_i} are directly obtained by the linearization of the analytical expression of the fit of the first return map around Y_i.

If we note the matrix $J_p = L_{Y_p} \ldots L_{Y_2} L_{Y_1}$, we have:

$$\tilde{\lambda} = \frac{1}{2p} \ln \left[Tr \left(J_p^+ J_p \right) \right]$$

Contrary to the case of the calculation in the full phase space where the exponent has the dimension of the inverse of time (see equation (3.2)), the exponent obtained by the study of the first return map has no dimension. $\tilde{\lambda}$ gives the rate of divergence of the trajectories per average period of time between two intersections of the section plane.

In the particular case of an unidimensional dynamics described by the function $f(x)$, we have:

$$J_p = \prod_{i=1}^{p} f'(x_i) \text{ and } \tilde{\lambda} = \frac{1}{p} \sum_{1}^{p} \ln |f'(x_i)|.$$

Example: Chaos in the Belousov-Zhabotinskii reaction, J. L. Hudson and J. C. Mankin, J. Chem. Phys. **74**, 6171 (1981)

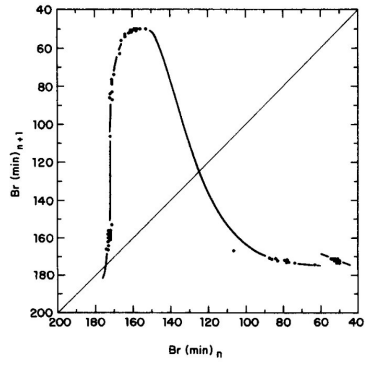

Figure 3.9: Dots: first return map obtained experimentally. Lines: fit by intervals, see expressions on the right.

$$\begin{aligned} x \geq 172 \quad & y = 175 - 4.62(1.44 - (x - 172))^{1/3} \exp(0.0126x) \\ 172 > x \geq 150 \quad & y = 175 - 4.42(1.44 + (172 - x))^{1/3} \exp(0.0126x) \\ 150 > x \geq 60 \quad & y = 175 - 182(175 - x)^{2.04} \exp(0.0918x) \\ x < 60 \quad & y = 191 - 0.375x \end{aligned}$$

Average value obtained for the Lyapounov exponent:

$$\bar{\lambda} \simeq 0.62$$

But this value is very sensible to the parameters used in the fit: see the discussion in the original article.

3.3.3 Fractal dimension

We mention previously that another characteristic of a strange attractor is that the dimension of this attractor is *fractal*. We now give a more precise definition of this word and examples of calculation of this quantity in model or practical cases.

3.3.3.a Box counting dimension

There exists different manner to give a measurement of the dimension of an object. All those methods give exactly the same values for lines, surfaces and other common objects, but their implementation differ slightly practically. We will present here the box counting method to understand how such methods work.

Consider a set of points in a n-dimensional space. To cover all the points of the set using cubes of side size ϵ, we need a minimal number of cubes which is $\mathcal{N}(\epsilon)$. The dimension of the set is then:

$$\boxed{d = \lim_{\epsilon \to 0} \frac{\ln\left(\mathcal{N}(\epsilon)\right)}{\ln\left(1/\epsilon\right)}}$$

This expression means that for ϵ small enough, we have $\mathcal{N}(\epsilon) \sim \epsilon^{-d}$.

We can apply this definition on sets of known dimension:

An isolated point. Then, whatever the value of ϵ, $\mathcal{N}(\epsilon) = 1$, and consequently $d = 0$.

A line. You need L/ϵ to cover a line of size L with boxes of size ϵ. consequently:

$$\begin{aligned} d &= \lim_{\epsilon \to 0} \frac{\ln\left(L/\epsilon\right)}{\ln\left(1/\epsilon\right)} \\ d &= \lim_{\epsilon \to 0} \frac{\ln L - \ln \epsilon}{-\ln \epsilon} \xrightarrow[\epsilon \to 0]{} 1 \end{aligned}$$

A surface. You need S/ϵ^2 to cover a surface of area S with boxes of side size ϵ. consequently:

$$\begin{aligned} d &= \lim_{\epsilon \to 0} \frac{\ln\left(S/\epsilon^2\right)}{\ln\left(1/\epsilon\right)} \\ d &= \lim_{\epsilon \to 0} \frac{\ln S - 2\ln \epsilon}{-\ln \epsilon} \xrightarrow[\epsilon \to 0]{} 2 \end{aligned}$$

3.3.3.b Examples of fractal sets

We will now apply this method to fractals obtained by iteration of a procedure.

Cantor ternary set

This mathematical object is obtained by the iteration of the process of removing the middle third of segments:

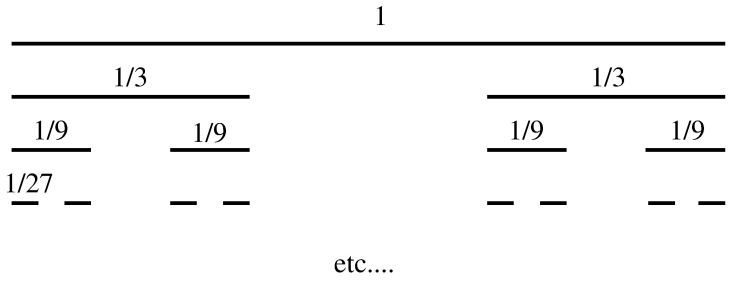

The set obtained when the process is iterated an infinite number of time is called the *Cantor ternary set*. It consists in an infinite number of points, so that it is not of zero dimension, but it is much "smaller" than a line. We can calculate its dimension by using the box counting method. We will take a particular sequence of ϵ: $\epsilon_p = (1/3)^p$. We have indeed $\epsilon_p \xrightarrow[p\to\infty]{} 0$ and using the method of construction of the set, we can deduce: $\mathcal{N}(\epsilon_p) = 2^p$. Consequently:

$$d = \lim_{p\to\infty} \frac{\ln\left(\mathcal{N}(\epsilon_p)\right)}{\ln\left(1/\epsilon_p\right)} = \lim_{p\to\infty} \frac{\ln(2^p)}{\ln(3^p)} = \lim_{p\to\infty} \frac{p\ln 2}{p\ln 3}$$

$$\boxed{d = \frac{\ln 2}{\ln 3} \simeq 0.63}$$

Koch curve

Another construction of a fractal structure is based on the adding of equilateral triangles in the middle third of each segments instead of removing it:

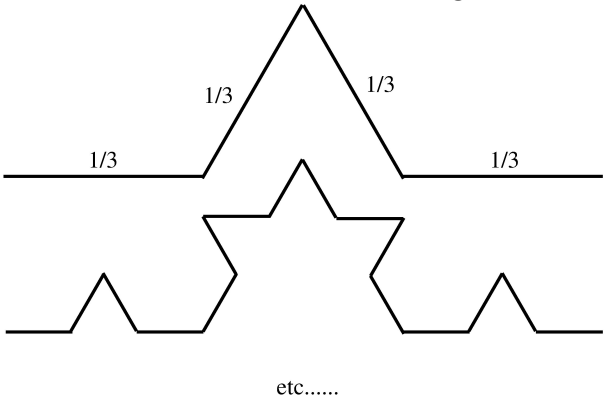

As in the previous example, using $\epsilon_p = (1/3)^p$, we find $\mathcal{N}(\epsilon_p) = 4^p$, so that:

$$\boxed{d = \frac{\ln 4}{\ln 3} \simeq 1.26}$$

3.3.3.c Application to strange attractors

If we want to calculate the fractal dimension of an attractor obtained either by an embedding of experimental data or numerical integration, we have to analyze a set of discrete points in a n-dimensional phase space. It is a finite sequence of points: $X_1, X_2, \ldots, X_N$.

We will not use the box counting method but a variant[3]: we count the average number of points $\mathcal{C}(\epsilon)$ of the attractor in spheres of given size ϵ:

[3]See Matlab session and *L'ordre dans le chaos*.

$$\mathcal{C}(\epsilon) = \frac{1}{N^2} \sum_{i,j=1}^{N} H\left(\epsilon - \|X_i - X_j\|\right),$$

where H is the Heaviside function: if $x < 0$, $H(x) = 0$ and if $x \geq 0$, $H(x) = 1$.

An average along the attractor is necessary as the density of points along the attractor varies a lot depending on the amount of stretching or folding in the area considered.

The relationship between the density $\mathcal{C}(\epsilon)$ computed here and the number of boxes considered in the previous part is the following: if we use spheres instead of cubes in the box counting method, $\mathcal{N}(\epsilon)\mathcal{C}(\epsilon)$ is a constant: it is the total number of points of the recording. If d is the dimension of the attractor, we await that the number of spheres necessary to cover the set is of the form $\mathcal{N}(\epsilon) \sim \epsilon^{-d}$. The average number of points by sphere is thus awaited to be of the form: $\mathcal{C}(\epsilon) \sim \epsilon^{d}$.

We will see during the Matlab session that the typical observed behavior for $\mathcal{C}(\epsilon)$ in function of ϵ is the following one:

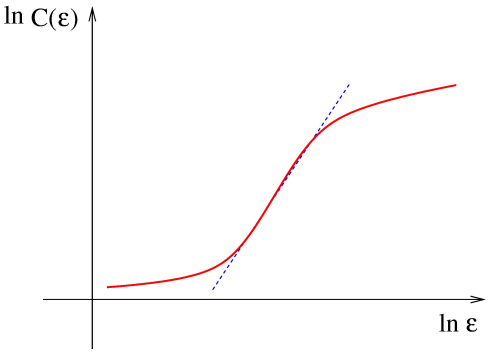

The saturation at large values of ϵ is linked to the finite size of the attractor. The plateau at small values of ϵ is linked to the sampling rate and the fact that we have a discrete sequence of points. The slope of the linear part between the two plateaus gives the dimension of the attractor.

Conclusion

For a phase space of dimension 3 or higher, a nonlinear dynamical system may present a peculiar aperiodic dynamics called chaos. The main property of this dynamics is the sensitivity to initial conditions, which can be characterized by Lyapounov exponents. The attractors corresponding to this dynamics are called strange attractors, which are fractal structures. The topology of those attractors are governed by two processes: *stretching* and *folding*.

Bibliography

- **L'ordre dans le chaos**, P. Bergé, Y. Pomeau, C. Vidal

Chapter 4

Transition towards chaos

In this chapter we will study how successive bifurcations can lead to chaos when a parameter is tuned. It is not an extensive review : there exists a lot of different manners to transit to chaos, we will just spend some time on the transistions that are rather well known.

The understanding of the successive bifurcations leading to chaos is mostly based on the study of one-dimensional maps so that the first section of the chapter will be dedicated to some general useful tools for those kind of studies. The following parts are each dedicated to a transition towards chaos: the second part describes the subharmonic cascade, the third one the intermittency phenomenon, and the last part the transition towards chaos by quasi-periodicity. The description of each of those transitions will be done using a generic one-dimensional map typical of each road to chaos.

The one-dimensional maps that will be studied can have several meanings. They can correspond to a model of a discrete dynamics: for example, the logistic function is used to describe successive generations in population dynamics. But we have also seen that a high-dimensional dynamics can be reduced in some conditions to a first return map which can be unidimensional. Finally, from a pure mathematical point of view, the mere study of a one-dimensional map (as the study of the logistic map by M. J. Feigenbaum) can lead to a very good understanding of the mechanisms underlying chaos by itself.

4.1 One-dimensional maps

Let's consider a one-dimensional map $f : \mathbb{R} \to \mathbb{R}$. We study the discrete dynamics given by the successive iterates of the function from an initial point x_0, which is then the initial condition of the time serie defined by:

$$x_{n+1} = f(x_n).$$

4.1.1 Graphical construction

That kind of dynamics can be studied using a graphical construction. We draw the curve $y = f(x)$ and we obtain the successive points using the line $y = x$:

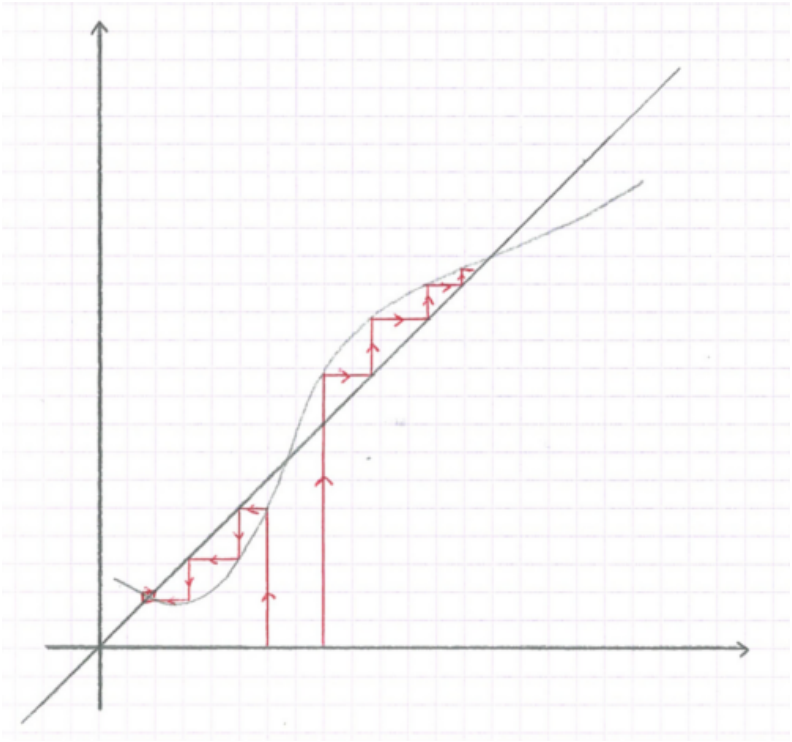

The intersection points of the curve $y = f(x)$ and of the line $y = x$ give the **fixed points** of the system as they obey to $x^* = f(x^*)$.

Those fixed points can be stable or unstable, depending on the behavior of the successive iterates from a point in the vicinity of x^*.

4.1.2 Stability of the fixed points

As in Chapter 1, to determine the stability of a fixed point x^* we study the iterates stemming from an initial condition x_0 very close to the fixed point x^*, i.e. $x_0 = x^* + \delta x_0$ with $\delta x_0 \ll x^*$. We can then compute the first approximation of the iterates:

$$x_1 = f(x_0) = f(x^* + \delta x_0) \simeq f(x^*) + f'(x^*)\delta x_0 = x^* + f'(x^*)\delta x_0$$

We deduce $\delta x_1 = x_1 - x^* = f'(x^*)\delta x_0$. By iteration, we obtain:

$$\delta x_n = [f'(x^*)]^n \, \delta x_0$$

Consequently, and as we have already seen in Chapter 1, if $|f'(x^*)| < 1$, the fixed point is stable and if $|f'(x^*)| > 1$ it is unstable. The stability of the fixed point can thus be deduced graphically by checking the slope of the tangent to the curve in x^*.

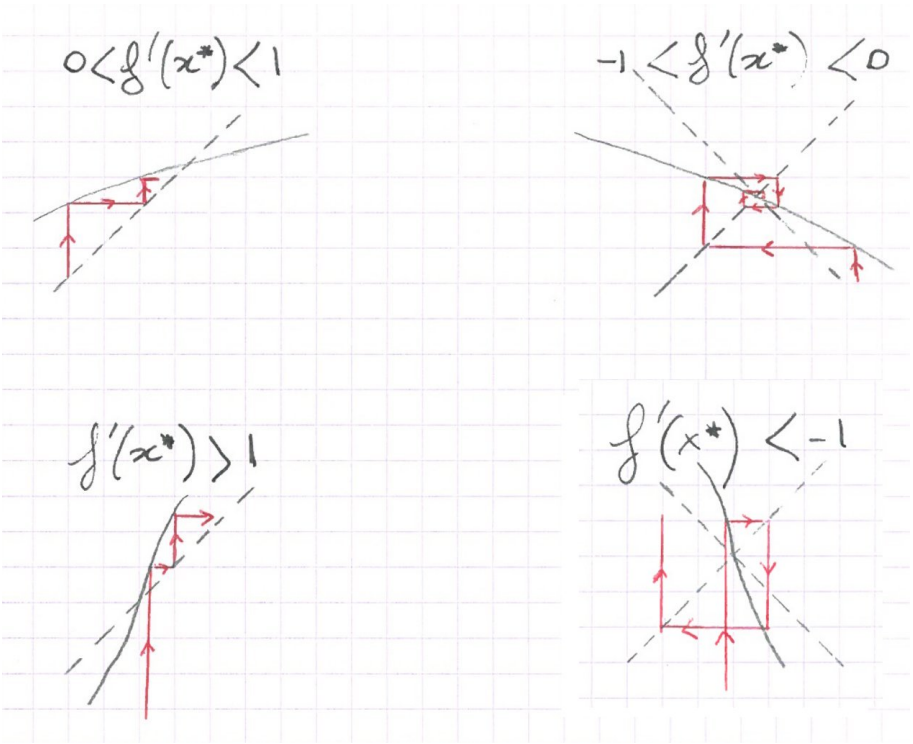

4.2 Subharmonic cascade

This transition is also named a "period-doubling" cascade: starting from a periodic behavior of period T, the increase of a parameter leads to a first bifurcation to a new periodic regime of period $2T$, then to another one of period $4T$, then $8T$ and so on. We thus observe successive $2^n T$ periodic regimes whith increasing n as the parameter is tuned until we reach a value of the parameter for which the system becomes chaotic.

This transition can be understood by studying the logistic map.

4.2.1 The logistic map

The logistic map is the function:

$$f(x) = rx(1-x),$$

where r is a parameter.

We will also study this discrete dynamics in the last computer session.

4.2.1.a Domain of study

First, we want the dynamics to be bounded, i.e. that no time series go to infinity. This condition reduces the set of values of x that can be taken as initial conditions. The curve $y = f(x)$ is a parabola whith a maximum for $x = 1/2$ and verifying $f(0) = 0$ and

$f(1) = 0$. As $f(1/2) = r/4$, if $0 \leq r \leq 4$, then for all $x \in [0, 1]$, $f(x) \in [0, 1]$. We will thus consider the dynamics only on the interval $[0, 1]$ and restrict the domain of variation of the parmaeter r to the interval $[0, 4]$.

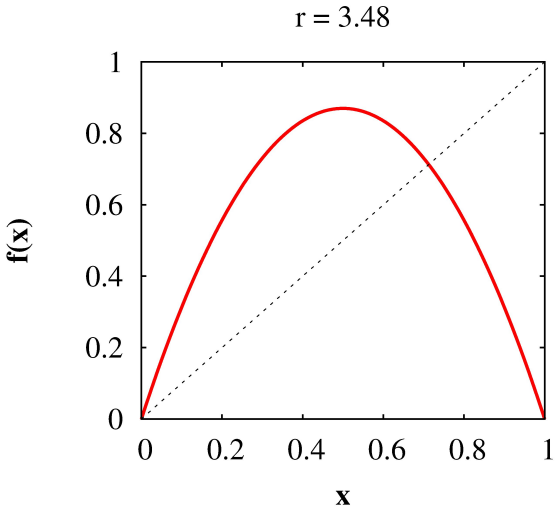

4.2.1.b Fixed points

The fixed points are given by : $x^* = rx^* - rx^{*2}$ from which we deduce 2 fixed points:

- $x^* = 0$ which is always a fixed point,
- $x^* = \frac{r-1}{r}$ which exists only when $0 < \frac{r-1}{r} < 1$, i.e. when $r > 1$.

We can see on the following graphs how this new fixed point appears when r increases:

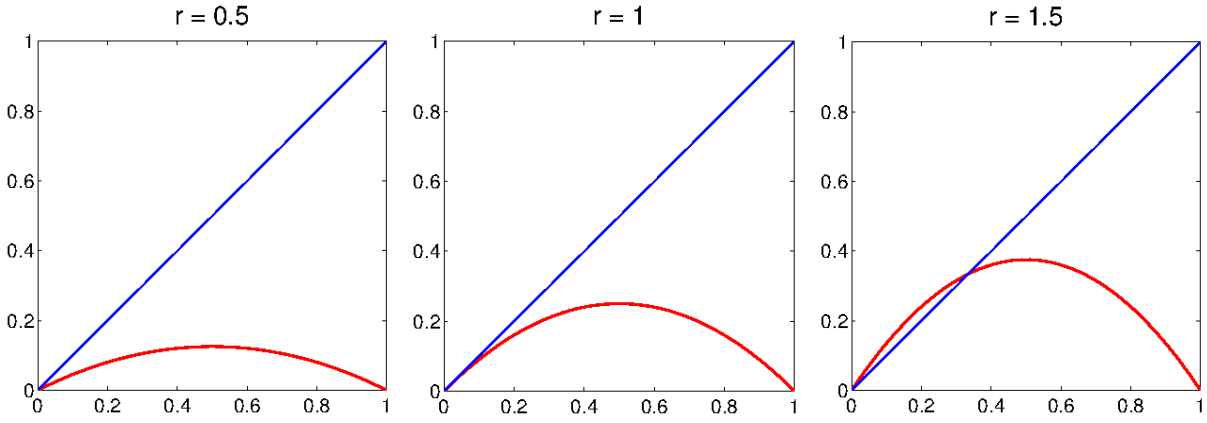

4.2.1.c Fixed points stabiity

- **For $0 < r < 1$** there is a unique fixed point $x^* = 0$. As $f'(0) = r$, $0 < f'(0) < 1$, the fixed point is stable (see also graphs above).

When r exceeds 1, the tangent in 0 becomes greater than 1 and the fixed point 0 becomes unstable. We can observe this change of slope of the curve at the origin on the previous figures. Simultaneously to that destabilization a new intersection of the curve with the line $y = x$ occurs.

- **For $1 < r < 3$**, the fixed point 0 is now unstable but there is a new fixed point : $x^* = \frac{r-1}{r}$.

$$f'\left(\frac{r-1}{r}\right) = 2 - r,$$

so that $-1 < f'(x^*) < 1$ for $1 < r < 3$ and the new fixed point is stable in this range.

When r increases above 3 the non-zero fixed point becomes unstable but no new fixed point appears. Consequently, for $r > 3$ there are two fixed points but the two of them are unstable.

4.2.1.d Periodic dynamics of the iterate map

For $3 < r < 3.569946$..., the response of the system is periodic[1]. Just after 3, in the permanent regime, the iterates oscillate between two values. This behavior can still be understood by a geometrical construction:

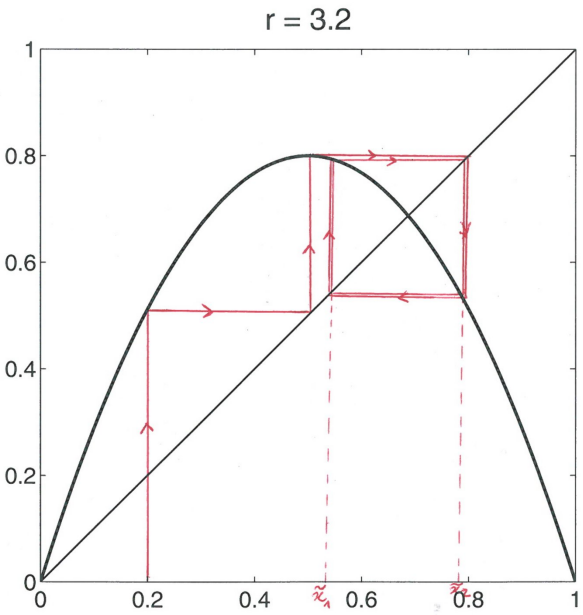

To understand this behavior, the function to study is $g = f \circ f$. Indeed, if we have an oscillation between $\tilde{x}_1$ and $\tilde{x}_2$, we have $\tilde{x}_2 = f(\tilde{x}_1)$ and $\tilde{x}_1 = f(\tilde{x}_2)$, so that $\tilde{x}_1 = f(f(\tilde{x}_1)) = g(\tilde{x}_1)$ and $\tilde{x}_2 = f(f(\tilde{x}_2)) = g(\tilde{x}_2)$, which means that $\tilde{x}_1$ and $\tilde{x}_2$ are fixed

[1] See Matlab session.

points of g. As a matter of fact, the drawing of the curves $y = g(x)$ before and after $r = 3$ shows that two new fixed points appear for the function g for $r > 3$ as shown in the Figures below:

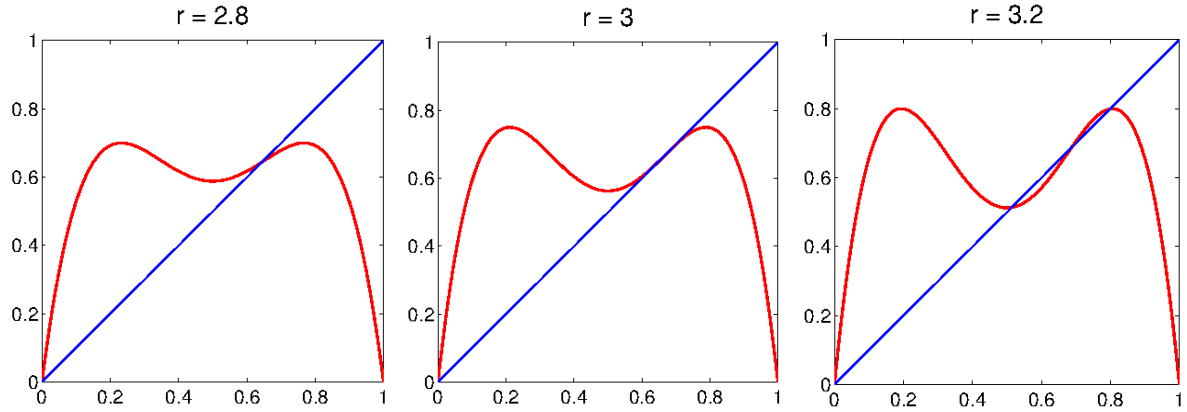

For $r \lesssim 3$ (left Figure), the curve $y = g(x)$ has two intersection points with the line $y = x$: 0 and $\frac{r-1}{r}$, i.e. the same fixed points as the function $f(x)$. Indeed, fixed points of f are perforce also fixed points of $f \circ f$.

When the parameter r crosses 3 (middle Figure), the slope of the tangent to the curve $y = g(x)$ in $x^* = \frac{r-1}{r}$ becomes greater than 1 and the fixed point x^* becomes unstable.

Two new fixed points then appear simultaneously on either side of x^* (right Figure). The fixed point $x^* = \frac{r-1}{r}$ is unstable and the two new fixed points are stable. The bifurcation that occurs is consequently a pitchfork bifurcation.

The mathematical study of g can be done. First, we compute the expression of g:

$$\begin{aligned} g(x) &= rf(x)\left(1 - f(x)\right) \\ &= r\left[rx(1-x)\right]\left[1 - rx(1-x)\right] \\ &= r^2x(1-x)\left[1 - rx(1-x)\right] \end{aligned}$$

To find the fixed points, we write

$$x = r^2x(1-x)\left[1 - rx(1-x)\right]$$

and then we factorize the polynom $r^2x(1-x)\left[1 - rx(1-x)\right] - x$ using the fact that $\frac{r-1}{r}$ is a known root. We can then demonstrate that :

$$\tilde{x}_1 = \frac{1 + r - \sqrt{(r-1)^2 - 4}}{2r} \text{ and } \tilde{x}_2 = \frac{1 + r + \sqrt{(r-1)^2 - 4}}{2r}$$

which only exist when $r \geq 3$.

To study the stability of those fixed points, we have to calculate $g'(\tilde{x})$. We have $g'(x) = f'(x)f'\left(f(x)\right)$ so that

$$g'(\tilde{x}_1) = f'(\tilde{x}_1)f'\left(f(\tilde{x}_1)\right) = f'(\tilde{x}_1)f'(\tilde{x}_2) = g'(\tilde{x}_2)$$

Consequently, the two points have necessarily the same stability. The computation gives:

$$g'(\tilde{x}_{1,2}) = -r^2 + 2r + 4.$$

The simultaneous destabilization of the two points happens when $g'(\tilde{x}) = -1$. The corresponding critical value of r can be computed: $r = 1 + \sqrt{6} = 3.449....$

This destabilization of g is totally similar to the one which has happened for the function f when $r = 3$ and is exactly of the same nature. The study of the new periodic regime that arise after the destabilization of $\tilde{x}_1$ and $\tilde{x}_2$ can thus be done by studying the iterates of the function g: $h = g \circ g$.

The drawing the curve of the function $h = g \circ g = f \circ f \circ f \circ f$ for $r = 3.56$ shows the four new fixed points of h after the destabilization of $\tilde{x}_1$ and $\tilde{x}_2$:

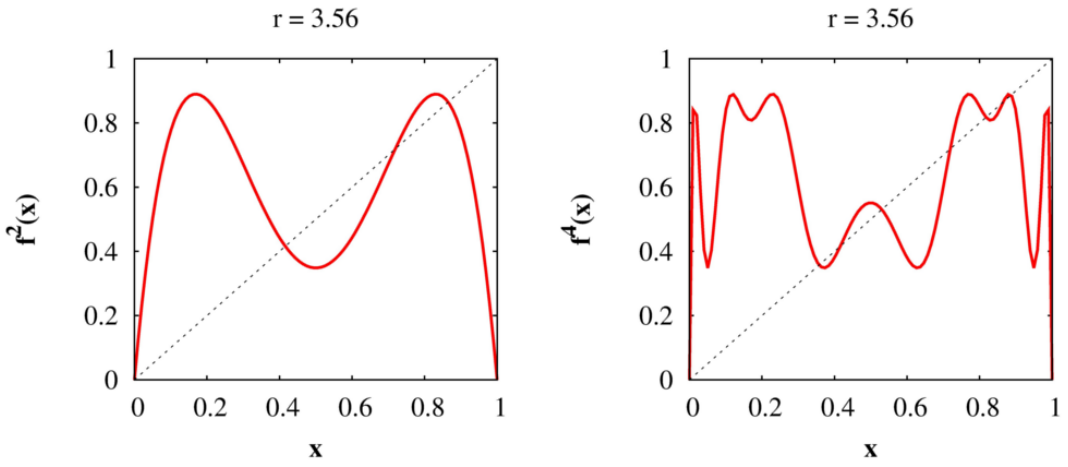

The scenario we have described for $r > 3$ is the following one: the fixed point $x^* = \frac{r-1}{r}$ of f becomes unstable at $r_1 = 3$ through a pitchfork bifurcation which gives rise to a periodic solution characterized by an oscillation between two points $\tilde{x}_1$ and $\tilde{x}_2$. This limit cycle becomes unstable when $r_2 \simeq 3.449$ leading to a new periodic behavior corresponding to an oscillation between four points. The bifurcation diagram is obtained by plotting the iterates of f in the permanent regime:

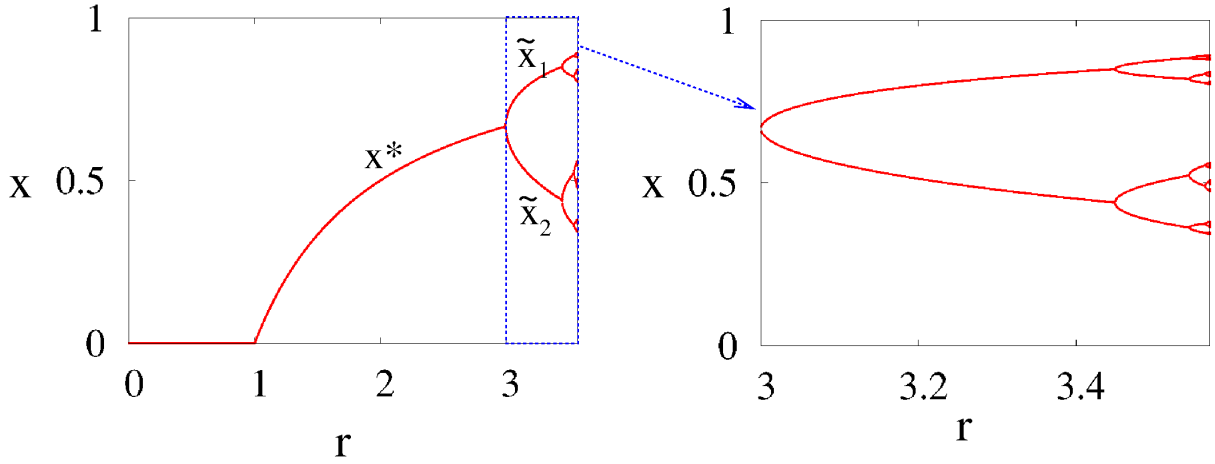

We could pursue the analysis of the iterates of f and observe successive pitchfork bifurcations giving each birth to a limit cycle of period twice the previous one. This process continues until a value of r called r_∞:

$$\begin{aligned} r_1 &= 3 \\ r_2 &= 3.449\ldots \\ r_3 &= 3.54409\ldots \\ r_4 &= 5.5644\ldots \\ r_5 &= 3.568759\ldots \\ &\vdots \quad \vdots \quad \vdots \\ r_\infty &= 3.569946\ldots \end{aligned}$$

If the logistic map is a unidimensional map that has been obtained from a dynamics of higher dimension, the fixed point x^* corresponds to a limit cycle which has a period T. Then, when this fixed point loses its stability at $r_1 = 3$ for a cycle between $\tilde{x}_1$ and $\tilde{x}_2$, it means when coming back to the full dynamics that the limit cycle has now two intersections in the Poincaré section and hence that the period of the new limit cycle is $2T$. Similarly, at the next bifurcation in r_2, the cycle complexifies again to reach a $4T$ period. At each following bifurcation the period is multiply by 2. This is the origin of the name "period-doubling" cascade.

4.2.2 Dynamics after r_∞

For r > 3.569946..., we can observe either chaotic or periodic dynamics depending on the value of r.
In the bifurcation diagram, by representing the iterates of f in the permanent regime, aperiodic responses correspond to vertical lines where the points almost cover segments.

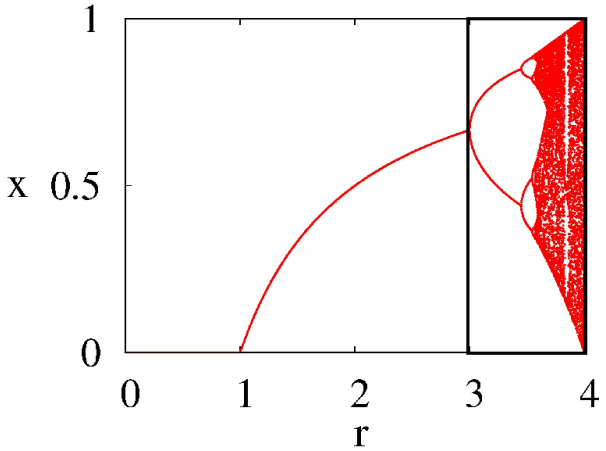

We observe in the following diagrams (which are enlargement of the above bifurcation diagram), that there are a lot of values of r for which the response is chaotic but there are also periodic windows, which correspond to values of r where periodicity is recovered. There are an infinity of such windows, we see only the larger ones on the following representations, the largest being the $3T$ window.

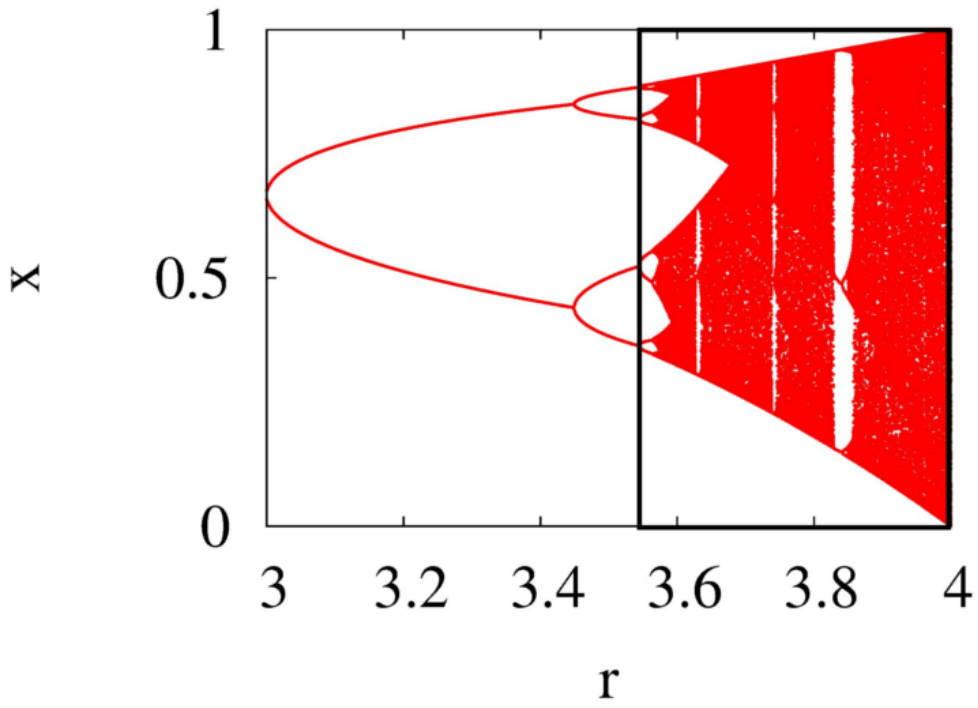
1
0.5
0
x
3
3.2
3.4
3.6
3.8
4
r

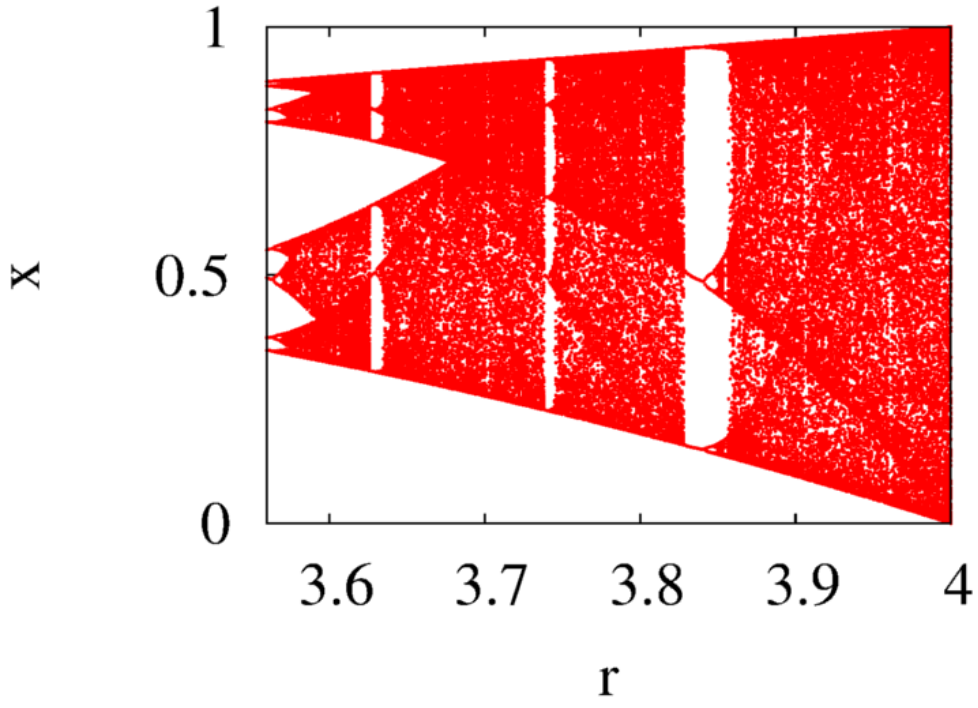
1
0.5
0
x
3.6
3.7
3.8
3.9
4
r

4.2.2.a Lyapounov exponent

The chaotic or periodic behaviors can be identified by computing the Lyapounov exponent for each values of r, following the method we saw in the previous chapter:

$$\tilde{\lambda} = \frac{1}{N}\sum_{i=1}^{N} \ln |f'(x_i)|.$$

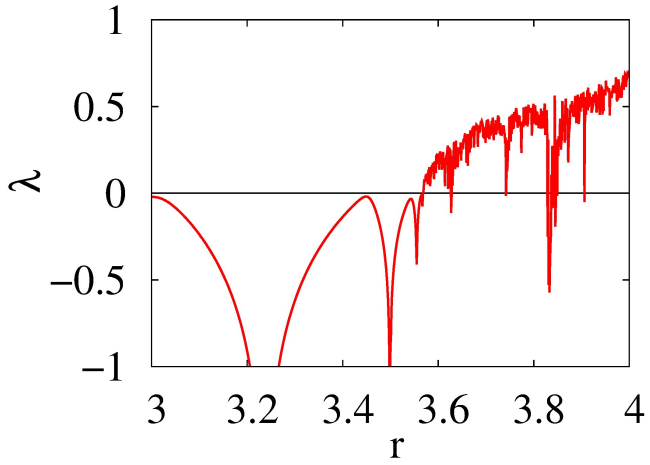

For $r < r_\infty$, the Lyapounov exponent is always negative. For $r > r_\infty$, for most of the values of r the Lyaponov exponent is positive, indicating a chaotic behavior.

In fact, chaotic and periodic domains are closely intertwined: between two values of r for which the behavior is chaotic you can always find a window of values of r for which the behavior is periodic. The Lyapounov exponent for the periodic windows is then negative. Most of the periodic windows are so small that we cannot see them on the figure above because of the lack of resolution of this graph. As for the bifurcation diagram representation, we only see the larger windows.

4.2.2.b $3T-$window

The study of the $3T-$window implies to study the function $f \circ f \circ f$ for values of r between 3.8 and 3.9. Representation of this function for two different values of r are shown below:

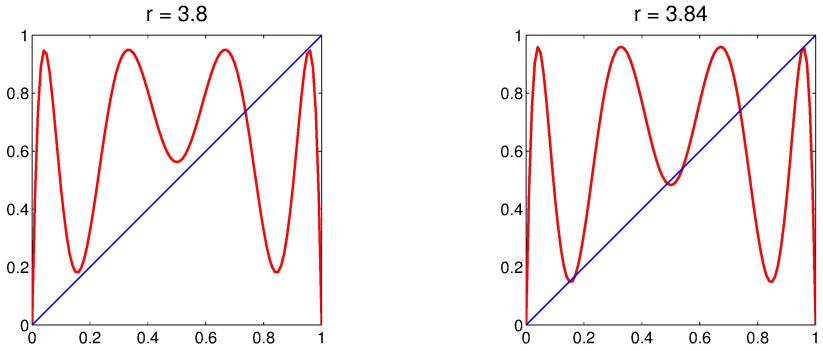

On the left side of the figure, $f \circ f \circ f$ intersects the $y = x$ line only in 0 and x^*: there is no $3T-$cycle. On the right side, we observe 6 new fixed points: 3 stable and 3 unstable. Those 6 fixed points appear by the crossing of the $y = x$ line by each local extrema of the curve as the parameter r increases. They thus all appear by pairs of a stable and an unstable point through saddle-node bifurcations.

The destabilization of the $3T$ window occurs through another cascade of period doubling leading to a succession of periodic behaviors: $6T$, $12T$, ..., $3 \times 2^n T$.

Other periodic windows ($5T$, $7T$, ...) can be found in the interval $r_\infty < r < 4$.

4.2.3 Universality

4.2.3.a Qualitative point of view

All the phenomenology that we have just studied using the logistic map is shared by a whole class of functions. All the functions that have the same general shape as the logistic function[2] present the same period-doubling cascade leading to a chaotic regime when the parameter is tuned. After r_∞, the order of apparition of the periodic windows is the same. This succession of periodic windows embedded in chaotic regimes is called the *universal sequence*.

For example, we show thereafter a study of the iterates of the function $f(x) = r \sin(\pi x)$, for $x \in [0, 1]$ and $r \in [0, 1]$ showing the similarity of the bifurcation diagrams between the logitic map and the sine one.

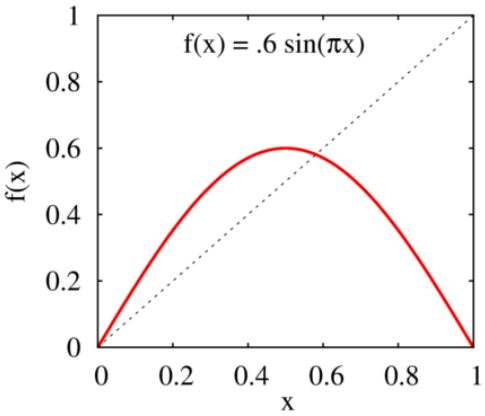

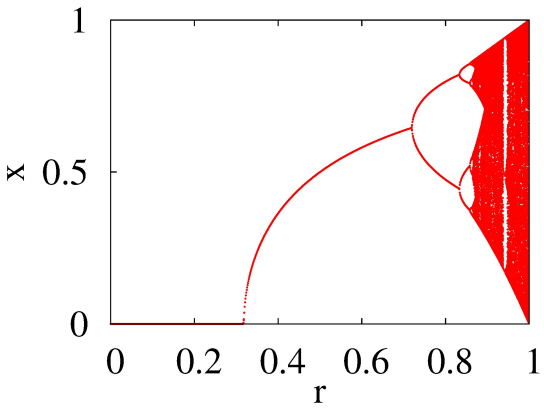

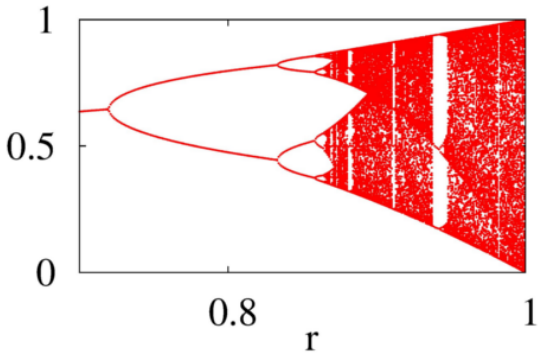

[2]The functions have to be *unimodal*, i.e., continuous, differentiable, concave and with a maximum. Consequently, all the curves that are bell-shaped.

4.2.4 Quantitative point of view

For all those functions, the cascade of period-doubling comes from the fact that the destabilization mechanism at each bifurcation is the same: only the scales on the axis change as well as the precise form of the function.

This similarity can be already seen in the iterates of the logistic function. The following curves show that the parts of the curve of the iterates we need to study to understand each bifurcation have the same shape as the one of the logistic curve but at a smaller scale.

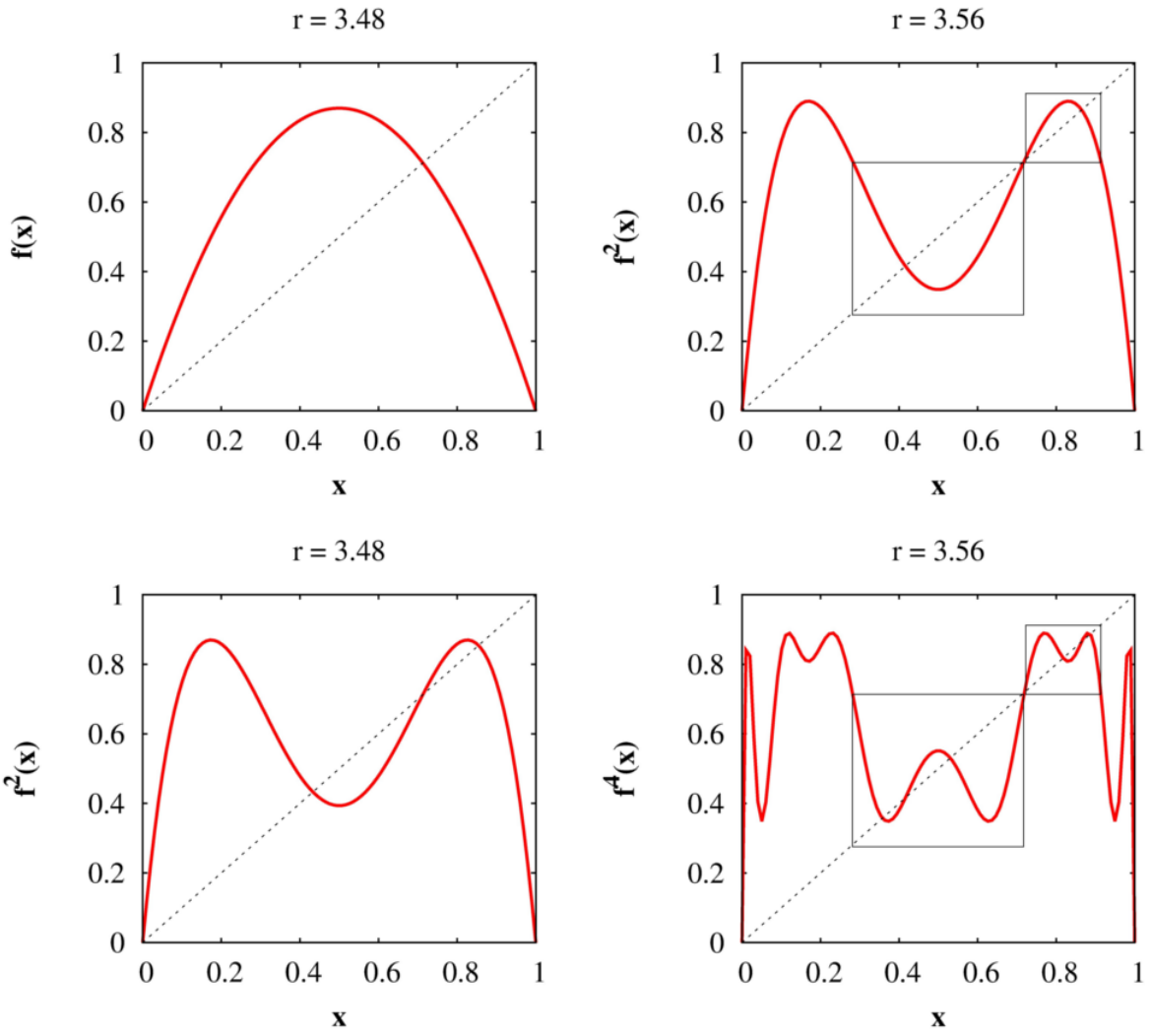

In fact, after a proper renormalisation (i.e. a change of the scales of the graphs to superimposed the curves), we obtain from any unimodal function a sequence of unidimensional functions using the iterates f^{2n} and those sequences all converge to the same universal function.

Because of this universal mechanism, the quantitative study of the values of the parameters for which the successive bifurcations occur: r_1, r_2, r_3, ..., r_n, ..., allows to define a universal constant δ:

$$\boxed{\frac{r_n - r_{n-1}}{r_{n+1} - r_n} \xrightarrow[n\to\infty]{} \delta}$$

δ is called the Feigenbaum constant and $\delta = 4.669....$

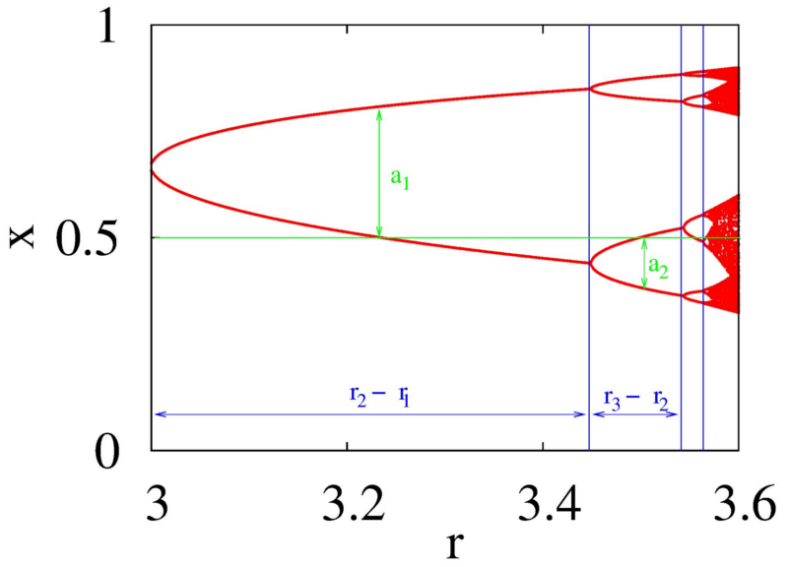

Another scaling law characterizes the change of the size of the successive pitchforks along the vertical axis in the bifurcation diagram.

This size corresponds to the distance between the location of the maximum of the initial function (1/2 in the case of the logistic map) and the closest fixed point:

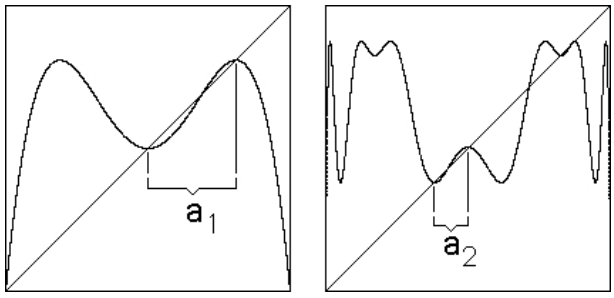

The ratio $\frac{a_n}{a_{n+1}}$ tends towards another universal constant:

$$\frac{a_n}{a_{n+1}} \xrightarrow[n\to\infty]{} \alpha,$$

with $\alpha = -2.5029....$ This constant is linked to the size factor necessary to rescale the successive curves at each iteration. The limit universal curve is then defined implicitely by:

$$f(x) = \alpha f^2\left(\frac{x}{\alpha}\right).$$

4.3 Intermittency

This kind of transition towards chaos is characterized by the apparition of bursts of irregular behaviors interrupting otherwise regular oscillations. When the parameter is tuned further towards chaos, those bursts are more and more prevalent until a fully chaotic regime is reached.

4.3.1 Type I intermittency

The dynamics is now described by the following one-dimensional map:

$$f(x) = x + \epsilon + x^2,$$

where ϵ is a small parameter ($|\epsilon| \ll 1$). We study orbits given by the iterates $x_{n+1} = f(x_n)$.

The fixed points are given by: $x^* = x^* + \epsilon + (x^*)^2$, so that:

- if $\epsilon < 0$, $x^* = \pm\sqrt{-\epsilon}$,
- if $\epsilon > 0$, there are no fixed point.

When $\epsilon < 0$, we can determine the stability of the fixed points:

- $f'(\sqrt{-\epsilon}) = 1 + 2\sqrt{-\epsilon} > 1$, so that the fixed point $+\sqrt{-\epsilon}$ is unstable
- $f'(-\sqrt{-\epsilon}) = 1 - 2\sqrt{-\epsilon} < 1$, the fixed point $-\sqrt{-\epsilon}$ is stable.

Consequently, when the parameter ϵ increases from a small negative value to a small positive one, a pair of fixed points, one stable, one unstable, disappears. This scenario corresponds to an inverse saddle-node bifurcation. You can understand from the figures below why a saddle-node bifurcation is also called a *tangent* bifurcation.

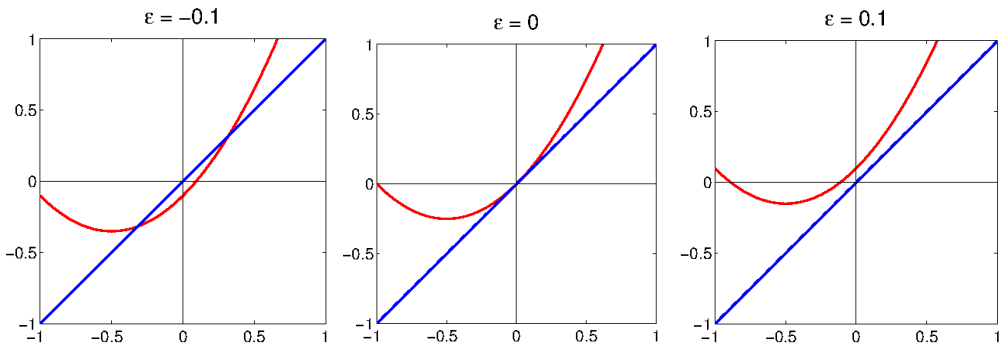

When $\epsilon \gtrsim 0$ there are no more fixed points but if ϵ is small enough, the system will spend a lot of time in the region where the function is very close to the line $y = x$, as can be obtained by a geometric construction.

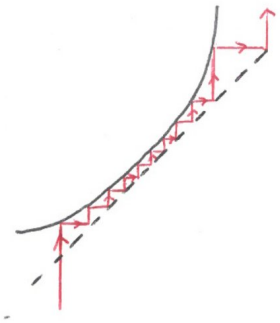

When the system is trapped in this region, the observed response is very close to the periodic response which was existing just before the bifurcation, and was corresponding to the stable fixed point $-\sqrt{-\epsilon}$. When the system exits the channel between the curve $y = f(x)$ and the line $y = x$, the next iterates can take very large values, which correspond to a burst in the temporal response. The system then explores the phase space before to be reinjected at the entrance of the channel where it will again be trapped. The closer to the bifurcation the system is, the longer the time spent in the channel will be. The observed behavior is then quasi-regular oscillations interrupted by irregular bursts. The duration of the sequences of quasi-regular oscillations between the bursts becomes shorter and shoter when moving away from the bifurcation.

4.3.2 Other intermittencies

There exists other types of intermittencies but the general behavior: regular oscillations interrupted by bursts of irregular behavior, are common to all those transitions[3].

For example, in the "type III" intermittency, the bursts display a subharmonic behavior and the one-dimensional map associated is:

$$f(x) = -(1 + \epsilon)x + ax^2 + bx^3.$$

4.4 Transition by quasi-periodicity

This transition has been proposed by D. Ruelle, F. Takens and S. Newhouse in 1978. The mathematical theorem underlying this transition is difficult. Roughly, it says that 3-frequencies quasi-periodicity is not robust, i.e. a T^3 torus does not withstand perturbations, however small. Consequently, if a system goes through three successive Hopf bifurcations, there is a very high probability that a strange attractor emerges after the third bifurcation.

[3]For more details read the corresponding chapter in *L'ordre dans le chaos*.

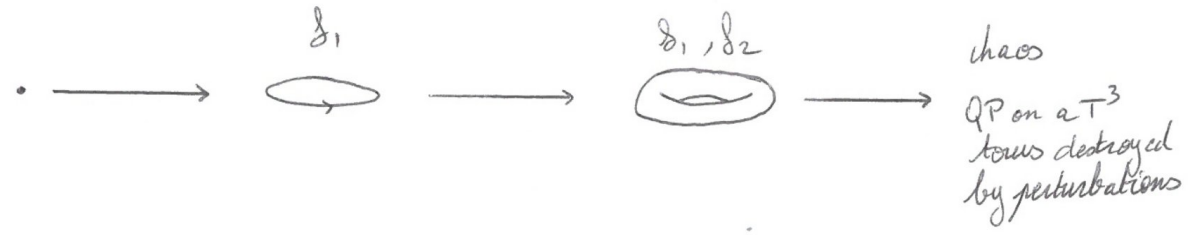

We will first study a model which gives rise to quasi-periodicity but also to frequency locking. Then we will describe how chaos can occur in this system.

4.4.1 First-return map

The one-dimensional map describing this transition is based on a Poincaré section of the torus supporting the 2-frequencies quasi-periodic regime just before the last bifurcation. This section is a closed curve when the regime is indeed quasi-periodic, i.e. when the two frequencies are incommensurable:

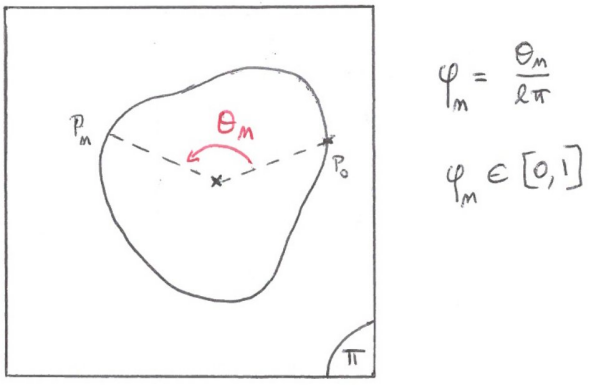

The one-dimensional variable used to described the system is the angle θ_n giving the position of the n^{th} point along the curve, using an arbitrary point as a reference (P_0 in the schematic example). For the sake of simplicity, a variable which takes its values in the interval $[0, 1]$ is preferred, so that finally the dynamical variable is: $\phi_n = \frac{\theta_n}{2\pi}$. The first return map is the function f such as $\phi_{n+1} = f(\phi_n)$.

We know that for this kind of dynamics we need to characterize the ratio of the two effective frequencies of the system around the torus. This quantity is given by the *winding number*:

$$\sigma = \lim_{n\to\infty} \frac{\phi_n - \phi_0}{n}.$$

When σ is irrational, the system is quasi-periodic.

When the system is locked in frequency, σ is a rational p/q, the system is periodic and the Poincaré section displays a finite number of points, q if the section is well chosen. We have then a q-cycle ϕ_1^*, ϕ_2^*, ..., ϕ_q^*, and

$$\underbrace{(f \circ f \circ \cdots \circ f)}_{q \text{ fois}}(\phi_i^*) = f^q(\phi_i^*) = \phi_i^* + p \pmod 1 = \phi_i^*.$$

The stability analysis is based on the calculation of:

$$\begin{aligned}
[f^q]'(\phi) &= \left[f^{q-1} \circ f\right]'(\phi) \\
&= f'(\phi) \cdot \left[f^{q-1}\right]'(f(\phi)) \\
&= f'(\phi) \cdot \left[f^{q-2} \circ f\right]'(f(\phi)) \\
&= f'(\phi) \cdot f'(f(\phi)) \cdot \left[f^{q-2}\right]'\left(f^2(\phi)\right) \\
&= f'(\phi) \cdot f'(f(\phi)) \cdot f'\left(f^2(\phi)\right) \cdots f'\left(f^{q-1}(\phi)\right)
\end{aligned}$$

If we apply this formula to any point of a $q-$cycle, we obtain:

$$[f^q(\phi_i^*)]' = f'(\phi_1^*) \cdot f'(\phi_2^*) \cdots f'(\phi_q^*),$$

and the $q-$cycle is stable when

$$\left| \prod_{i=1}^{q} f'(\phi_i^*) \right| < 1.$$

4.4.2 Arnold's model

The archetypal first-return function for the study of the transition to chaos by quasi-periodicity is the following one:

$$\phi_{n+1} = \phi_n + \alpha - \frac{\beta}{2\pi} \sin(2\pi\phi_n) \pmod 1,$$

the function is noted $f_{\alpha,\beta}$, so that $\phi_{n+1} = f_{\alpha,\beta}(\phi_n)$, and $f'_{\alpha,\beta}(\phi) = 1 - \beta\cos(2\pi\phi)$.

When $\beta = 0$, the dynamics obtained is simply given by $\phi_{n+1} = \phi_n + \alpha$ and corresponds exactly to the example of trajectories we studied at the beginning of chapter 3 of straight lines of constant slope on the unfold torus. Here the slope of the lines is α and corresponds to the ratio of the two frequencies. The behavior is then periodic or quasi-periodic depending on the value of α. In such a model, no locking of the frequencies coming from dynamical reasons is possible as there is no nonlinear term allowing the characteristic frequencies of the system to adjust spontaneously.

The coupling stems from the term $-\beta\sin(2\pi\phi_n)/2$. When $\beta > 0$ we will be able to obtain locking or unlocking of the oscillations depending on the value of β for a given value of α.

4.4.2.a Frequency locking: Arnold's tongues

Case $\sigma = 1$: a winding number $\sigma = 1$ corresponds to a a frequency locking $1:1$ and to a unique point on the Poincaré map. Consequently, it is a fixed point of the map:

$$\phi^* = \phi^* + \alpha - \frac{\beta}{2\pi}\sin(2\pi\phi^*)$$

which leads to the relation

$$\frac{2\pi\alpha}{\beta} = \sin(2\pi\phi^*).$$

A solution, and thus a limit cycle, thus exists only for $-1 < \frac{2\pi\alpha}{\beta} < 1$. This region of $1:1$ locking can be represented on a (α, β) diagram as a hatched area. Stable cycles verify $|1 - \beta\cos(2\pi\phi^*)| < 1$, so that for $0 < \beta < 1$ the obtained limit cycle is always stable.
If α and β are given, the stable fixed point can also be find using a graphical methods on the one-dimensional map:

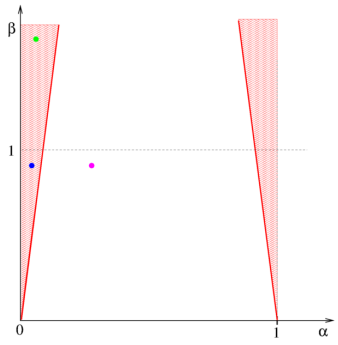

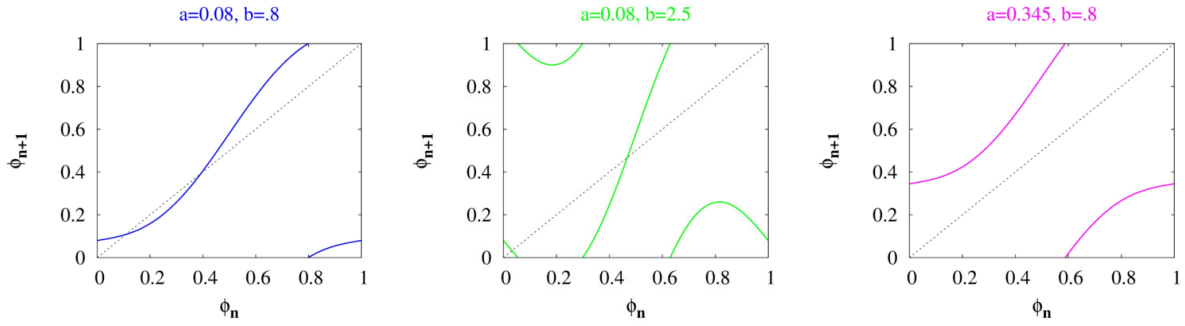

Each of those one-dimensional maps correspond to a different set of parameters (α, β). The left figure (parameters: blue point on the stability diagram, first return map: blue curve) is the case of a stable fixed point corresponding to the $1:1$ locking. In the second example (middle figure, parameters: green point on the stability diagram, first return map: green curve), fixed points corresponding to $\phi^* = f(\phi^*)$ still exist but they are all unstable. In the last case (right figure, parameters: magenta point on the stability diagram, first return map: magenta curve), no fixed points of the form $\phi^* = f(\phi^*)$ exists.

Case $\sigma = \mathbf{p/q}$: For other values of $\sigma = p/q$, fixed points of the function $f^q_{\alpha,\beta} = f_{\alpha,\beta} \circ f_{\alpha,\beta} \circ \cdots \circ f_{\alpha,\beta}$ have to be found. For example, for the values of parameter $(\alpha = 0.345, \beta = 0.8)$ which was our example of a case without $1:1$ frequency locking (right figure, magenta color), the function $f \circ f \circ f$ has 3 stable fixed points, as can be shown by plotting ϕ_{n+3} as a function of ϕ_n instead of ϕ_{n+1} as a function of ϕ_n:

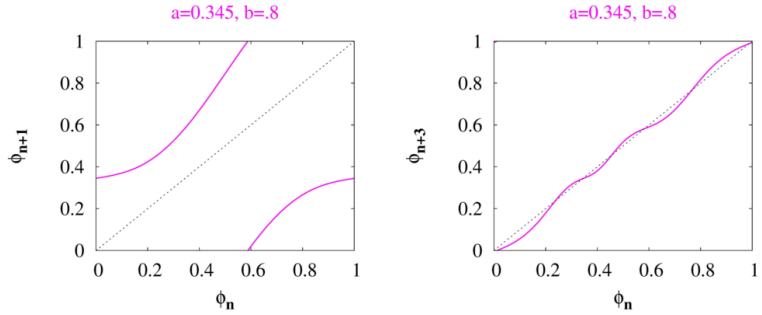

The domain of existence of this 3−cycle can be studied. For a given value of β we can search for the interval of the values of α for which the fixed points exist and are stable:

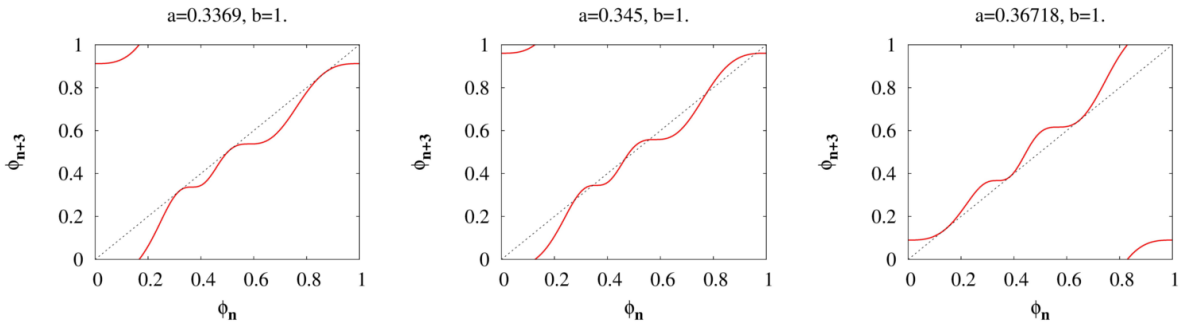

Studying systematically $f^3_{\alpha,\beta}$, we obtain then a new set of "tongues" that we can add to the stability diagram.

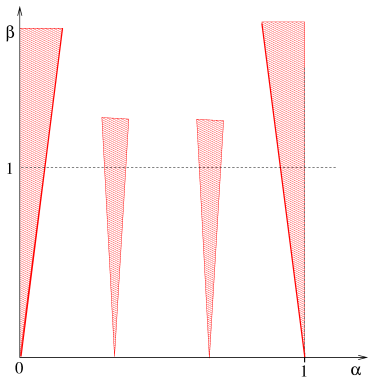

Repeating this study we obtain domains of frequency locking, called *"Arnold's tongues"*, that we can gather on a diagram. For a given $0 < \beta < 1$, we have intervals of frequency locking separated by domains of quasi-periodicity.

4.4.2.b Transition to chaos

When $\beta > 1$, the tongues corresponding to frequency locking in the (α, β) plane overlap. If we go back to the study of the one-dimensional map of a quasi-periodic regime, we observe that the map is not any more inversible for $\beta > 1$:

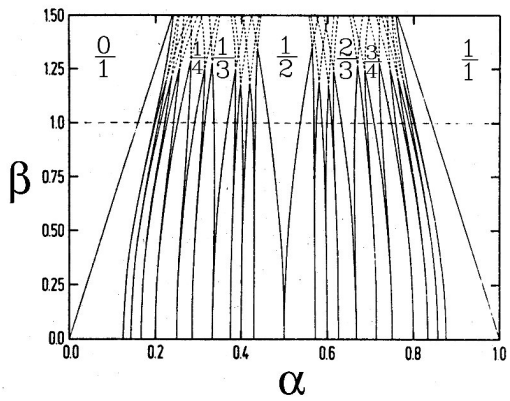

Figure 4.1: Figure from V. Croquette course `http://www.lps.ens.fr/~vincent/`.

If we represent the winding number σ as a function of α, the graph obtained looks like a staircase, called a *devil's staircase*, formed by horizontal plateaus corresponding to the locking domains.

When β increases, the width of the stairs widened and the locking domains are wider and wider. At $\beta = 1$, the tongues are intersecting each other and the unlocked domains of quasi-periodicity form a set of points almost empty. The staircase is said to be *complete*, the sum of the width of all the stairs is equal to 1.

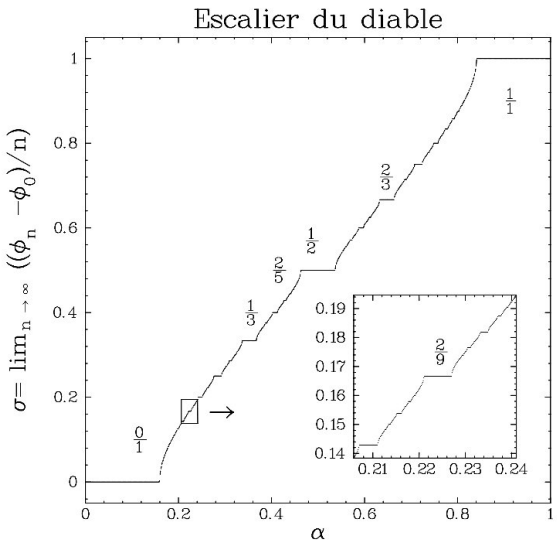

Figure 4.2: Arnold's tongues, figure from V. Croquette course `http://www.lps.ens.fr/~vincent/`.

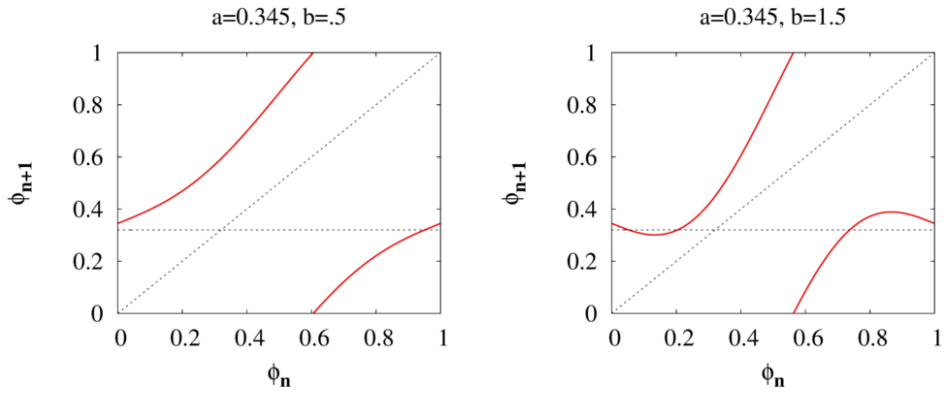

The non-inversibility is the fact that the same ϕ_{n+1} can have different antecedents. It happens when the curve is not monotoneous anymore. As $f'_{\alpha,\beta}(\phi) = 1 - \beta\cos(2\pi\phi)$, the non-inversibility appears when the derivative can change sign, i.e. only if $\beta > 1$. From the Poincaré section point of view it corresponds to a folding of the closed curve, which is an indication of the destruction of the torus.

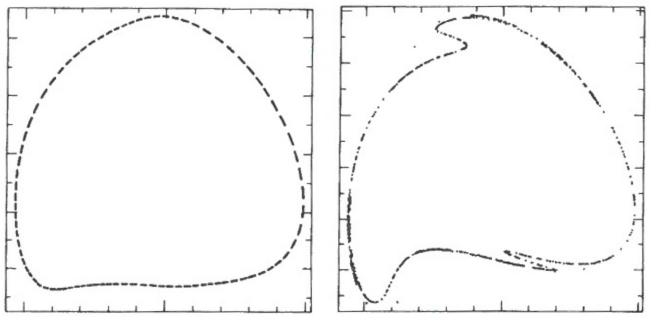

Figure 105: Break-up of a torus as described by the dissipative circle map

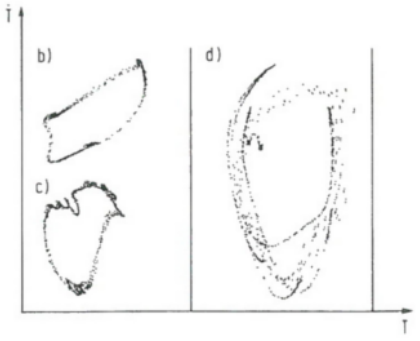

Figure 101: Poincaré sections for the Bénard experiment: a) Schematic section through torus; b)–d) experiments showing with increasing Rayleigh number a transition form quasiperiodic motion (b) to substructures indication the destruction of the torus (c) and then to a strange attractor (d). (After Dubois, Berge and Croquett, 1982.)

Figures from the book *Deterministic Chaos*, W.G Schuster and W. Just.

In the domain $\beta > 1$, we can then observe chaos when the torus is destroyed. Still, some regions of locking persist for some values of the parameters, but outside those regions we observe chaos. Their is a close imbrication of chaotic domains and periodic domains in the parameter space.

As for the other studied routes towards chaos, the main features of the transitions does not depend of the precise form of the considered map but of some generic properties of the first return map.

Conclusion

In this chapter we studied very briefly some roads towards chaos. What is important to note is that all those transitions depend only on a few general properties of the function describing the dynamics of the system. When a first-return map is closed to one of the model maps that have been presented in this chapter, the transition to chaos will be of the type of the corresponding model. This universality explain why those routes have been observed in very different systems.

Much more transitions to chaos exist and most of them are far from being understood as well as the ones described here.

Bibliography

- In English:
  - **Deterministic Chaos, An Introduction**, H. G. Schuster and W. Just
- In French:
  - **L'ordre dans le chaos**, P. Bergé, Y. Pomeau, C. Vidal
  - **Cours DEA** de V. Croquette, `http://www.phys.ens.fr/cours/notes-de-cours/croquette/index.html`